Heat Storage and Management with Phase Change Material in CubeSats

Determining the feasibility and predictability of Phase Change Material as a passive Thermal Storage Device in CubeSats

S.E. Sawyer

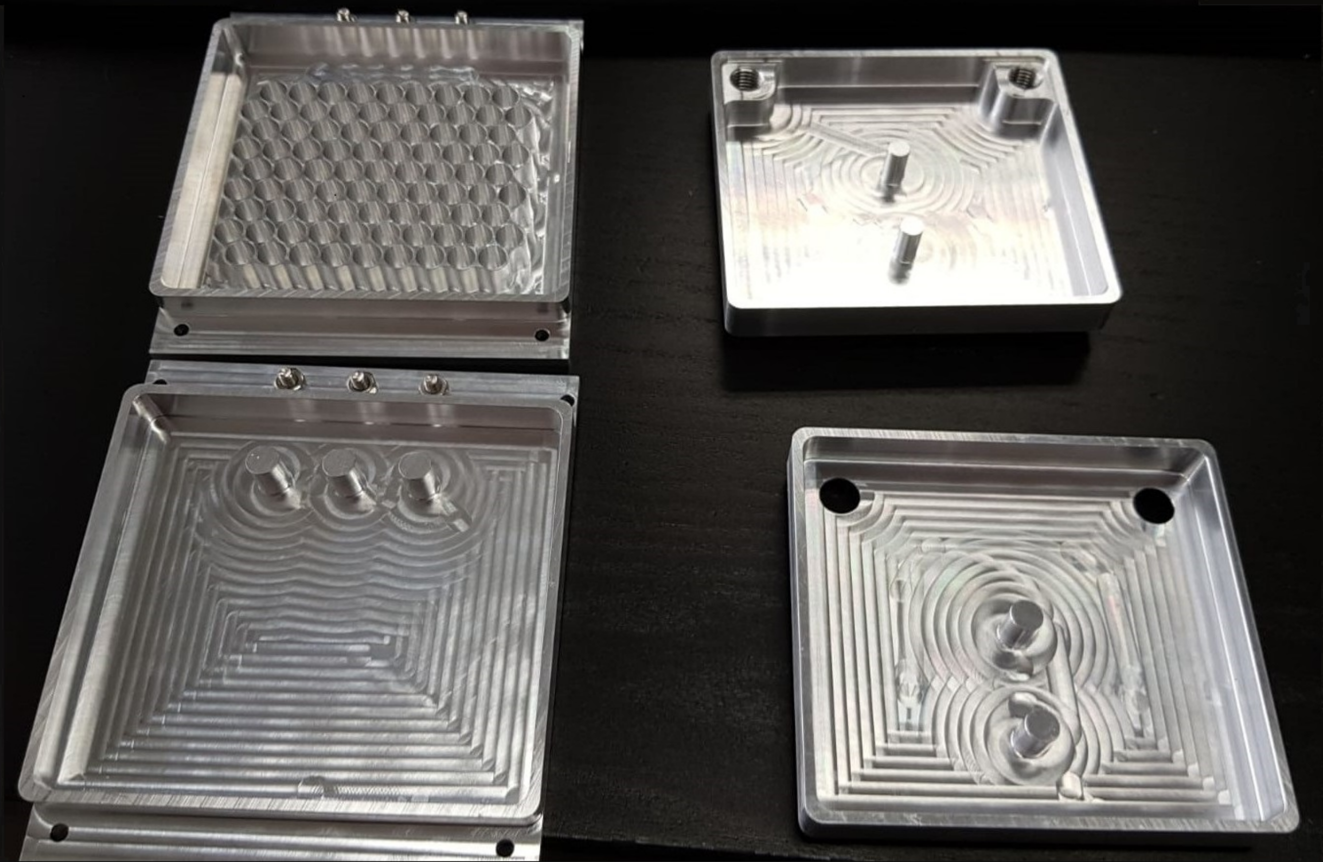

Heat Storage and Management with Phase Change Material in CubeSats

Determining the feasibility and predictability of Phase Change Material as a passive Thermal Storage Device in CubeSats

by

S.E. Sawyer

to obtain the degree of Master of Science
at the Delft University of Technology,
to be defended publicly on Tuesday June 30, 2020 at 9:30 AM.

Student number:	4293231	
Project duration:	May 24, 2019 – June 30, 2020	
Thesis committee:	Assistant Prof. dr. ir. A. Cervone,	TU Delft, Supervisor
	Ir. H. S. B. Brouwer,	Innovative Solutions in Space - ISIS, Supervisor
	Ir. A. K. Te Nijenhuis,	Netherlands Aerospace Centre - NLR, Supervisor
	Prof. dr. ir. B. J. Boersma,	TU Delft, External
	Dr. J. Guo,	TU Delft, Chair

Preface

This thesis is a research project that was done in order to obtain a Masters degree in Aerospace Engineering at the Delft University of Technology (TUD). My thesis advisor, Angelo Cervone, suggested I research phase change materials for use in CubeSats. I had not heard of this subject before and found it intriguing. This thesis was coupled to internships at Innovative Solutions In Space (ISIS) and the Royal Netherlands Aerospace Research Centre (NLR), splitting my time between the two. I worked primarily at ISIS as it was based in Delft where I live, and travelled once a month to the NLR, when it came time to do the experimental part of the project I worked full time at the NLR in Marknesse. The project lasted slightly longer than initially expected, nonetheless I have enjoyed the time I spent on this project.

I would like to express my sincerest gratitude to all of the people who helped me with and contributed to the project. I would like to thank Hugo Brouwer and Arne te Nijenhuis who spent many hours guiding me through my thesis and helping me with and carefully reviewing my work throughout the project. I would also like to thank Angelo Cervone, Henk-Jan van Gerner and Zeger de Groot for setting up this research project and giving me the opportunity to work on it; for helping me plan my thesis, and holding me accountable for the work that I did. With special thanks to Angelo Cervone who let me follow the path the research took me and let me pursue what I found most interesting. I also appreciated his support in allowing me to work at my own pace throughout the project given my personal circumstances.

I would also like to thank Adry van Vliet who spent many hours with me in the laboratory helping me with the tests, thinking through possible test setups and doing a lot of setup work before hand to allow me to easily and quickly go through all the experiments. I would also like to thank Aswin Pauw for also helping me with the early conceptual project design phase, his support in the lab and making sure the work was done correctly and was of high quality while simultaneously maintaining it a fun and cheerful working environment. I would also like to thank Ralph Slootweg and Stefan Brouwer for helping me with the mechanical design of the casing, and Hans van Olst for building the first one. I would like to thank Michiel van den Ouden for helping me order the materials and manufacturing of the test-pieces and making the experience as easy for me as possible. I would also like to extend my gratitude to the staff at ISIS and NLR for making it such a pleasant and interesting working environment. It was great getting to know everyone.

Finally, I would like to thank my friends and family who helped make my time in Delft an enjoyable experience. I would like to thank, Kelly Rigg, Steve Sawyer and Layla Sawyer especially for helping me by proofreading my thesis for me and also for supporting me and helping me my entire life, through my studies and especially through this last period. I could not have done it without you.

S.E. Sawyer
Delft, June 2020

Dedicated to the loving memory of Steve Sawyer

Nomenclature

Acronyms

AU	Astronomical Unit
CAD	Computer Aided Design
CNC	Computer Numerical Control
FDM	Finite Difference Method
FEM	Finite Element Method
IR	Infra-Red
ISIS	Innovative Solutions In Space
ISS	International Space Station
LEO	Low Earth Orbit
NLR	Royal Dutch Aerospace Research Centre
OBC	On Board Computer
PCB	Printed Circuit Board
PCM	Phase Change Material
PEEK	Polyether Ether Ketone
RF	Radio Frequency
SSPO	Sun Synchronous Polar Orbit
TC	Thermocouple
TCS	Thermal Control System
TEC	Thermo-Electric Cooler
TES	Thermal Energy Storage
TSD	Thermal Storage Device
TUD	Delft University of Technology
VCHP	Variable Conductivity Heat Pipe

Symbols

α	Absorptivity
α_{FMH}	Accommodation coefficient of free molecular heating
ΔQ	Change in energy
ΔT	Change in temperature
$\dot{Q}$	Net energy flow of the system
$\dot{Q}_{in}$	Flow of energy into the system

$\dot{Q}_{out}$	Flow of energy out of the system
ϵ	Emissivity
ϵ_m	Mass fraction
$\frac{dT}{dx}$	Differential change of the temperature in direction x
ρ	Atmospheric density
σ	Stefan Boltzmann constant
A	Surface area
c_p	Specific heat coefficient at constant pressure
c_{pl}	Specific heat coefficient at constant pressure of liquid phase
c_{ps}	Specific heat coefficient at constant pressure of solid phase
h_c	Convective heat transfer coefficient
k	Coefficient of thermal conductivity
k_{tot}	Total coefficient of thermal conductivity
l	Latent heat
m	Mass
q	Heat flux
q_s	Convective heat flux coefficient
q_{FMH}	Heat flow from free molecular heating
Q_{in}	Energy entering the system
Q_{out}	Energy leaving the system
RF	Radio Frequency
T	Temperature
T_m	Melting temperature
T_{max}	Maximum temperature
T_{min}	Minimum temperature
V	Relative velocity between spacecraft and the atmosphere
V	Volume

Abstract

As the CubeSats have been getting more energy dense over the years, a greater need has come for thermal control on CubeSats. Phase Change Materials (PCMs) are researched in this thesis as an energy dense passive Thermal Storage Device (TSD). This energy density comes from the melting of the PCM. To determine the feasibility of this TSD. The thermal storage device needed to be able to keep certain components from overheating while keeping other components from getting too cold. This thesis successfully tested that the PCM was able to store heat from a radio and use that heat to keep a CubeSat battery warm. The TSD is meant to stabilize the temperature of all components connected to it by maintaining a temperature around the melting temperature of the PCM. Prototypes were made using eicosane wax, it is a paraffin wax with a melting temperature of $36.7°C$. This PCM was chosen due to its safe and predictable properties, and because of its previous use in the space industry. Two different casings where tested with two different filler materials and casing sealing methods. Although the filler materials had a relatively small effect on the thermal response of the casing at the heat fluxes tested. The fin filler material used less mass and was simpler to manufacture than the honeycomb filler. There was a large difference in the sealing method of the casing that was glued together sealed better than the one laser welded together, the casing which had fill ports that were clamped with a thread with a rubber filament O-ring between them sealed better than the one that was glued on. Although the degree to which this could be tested was limited and is therefore difficult to draw definitive conclusions over. The tests proved that the TSD was much more effective than traditional heat sinks at storing heat. This will allow energy dense CubeSats with large intermittent heat-loads to be designed for their average temperatures and not for extreme peaks and valleys. The complexity this casing adds to the CubeSat is more than traditional heat sinks but much less complex than active thermal control systems. The casing thermal response could be predicted within a $5°C$ accuracy using a simple Finite Element Method (FEM) model using the built-in conduction and Phase Change Material modules in Comsol. The remaining obstacle with this research project is that more work needs to be done to be able to prove that the casing is completely hermetically sealed and will not contaminate other hardware while in operational.

List of Figures

List of Tables

Contents

1 Introduction

This thesis researches the feasibility of using a phase change material based thermal storage device for a CubeSat. This introduction will show what CubeSats are and why they would need this type of device. After that the research questions, aims and objectives will be laid out to so it is clear what was researched. The introduction will end with the research methodology to explain how these questions are meant to be answered.

1.1. Introduction to the Problem

The CubeSat satellite concept was originally developed for easy access to space for research institutions. According to the CubeSat standard: “a CubeSat is a 10 cm cube with a mass of up to 1.33 kg” [2], although multiple satellite volumes can be stacked together to create larger satellites. This allows for standardised parts and shared knowledge between CubeSat developers. These are key factors in lowering the costs and difficulty of entering the satellite market, and increases the speed of development in satellite technology. Eventually these satellites became useful as technology demonstrators, where satellites could fly at low cost and demonstrate new technologies, increasing the rate of innovation in satellite technology [3]. CubeSats steadily started to become more capable due to development of miniaturized electronics in other technologies like cell phones. In 2013 NASA even flew some demonstration missions called PhoneSat, showing how smartphones could be used as avionics in CubeSats [4]. Eventually CubeSats became capable enough with their on-orbit capabilities that they became useful platforms for many science, communications and observation missions. After multiple CubeSat demonstration missions, companies started to notice the potential for commercial CubeSats, for instance the DOVE-3 CubeSat by PlanetLabs [5], which

Figure 1.1: A picture of a pair of Planet Labs DOVE CubeSats deployed from the ISS [1]

were launched in 2013. Figure 1.1 shows a pair of Planet Labs DOVE CubeSats being deployed from the International Space Station (ISS). Due to increased capabilities and lowered development and launch costs, these satellites have potential in constellation, swarm and distributed satellite technologies (where a large amount of smaller satellites fly together to accomplish a common mission). This increases the robustness and capabilities of satellite infrastructure.

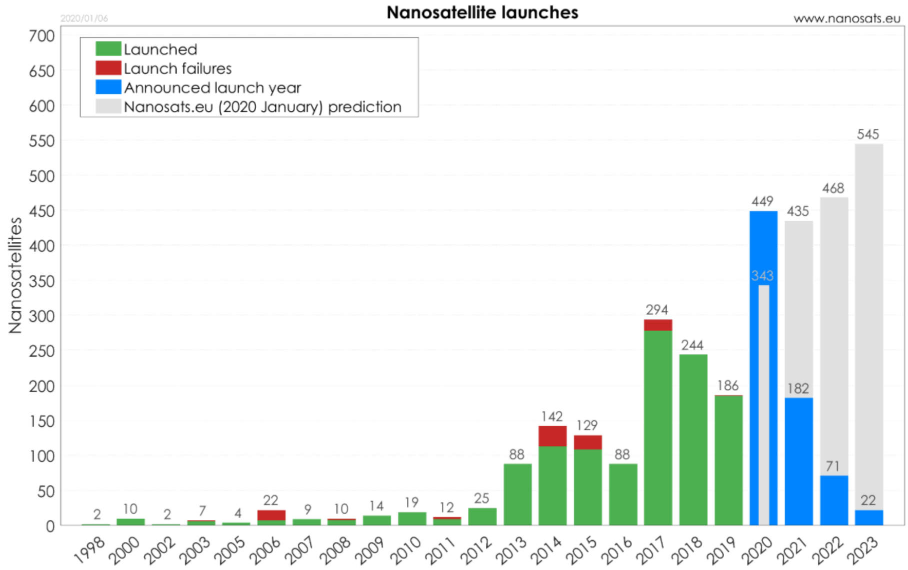

Figure 1.2: Growth and projections in nanosattelite launches since 1998 [6]

The CubeSat market has grown immensely over the last couple of decades as can be seen in figure 1.2. Evidenced by the number of CubeSats that are launched per year. This is both the cause and result of the rapid innovation of CubeSat technology and increase in on-orbit capabilities. The next generation of CubeSats will be able to have even more on-orbit capabilities than the current ones. As satellite launch cost scales with the mass of the satellite, increasing capabilities without increasing the mass, provides more return on money invested. Especially with the use of deployable solar panels much larger power production can be obtained than with traditional body mounted solar panels. 3U CubeSats will easily be able to reach 20 to 30 Watts of peak power production using deployable solar panels [7]. overheating issues will be more likely to occur on relatively large power production for such small spacecraft. More specifically, high power subsystems will create extreme temperatures and temperature gradients within a satellite in the absence of an adequate thermal management system. Especially if this high heat source is intermittent, for instance high power radio transmitters, it can cause large temperature swings and thermal gradients within the CubeSat.

There are multiple strategies to control the temperature on CubeSats, and different technologies that use these strategies. These strategies include removing, transporting and storing heat in the satellite. The topic of this thesis focuses on heat storage by using PCMs (Phase Change Materials) as a TSD (Thermal Storage Device) for a CubeSat. PCMs are materials that change their state of matter (solid-liquid) to absorb or release energy. PCMs are generally used in the food and transportation industries to keep goods at the proper temperature while being transported. PCMs are also often considered in architectural designs to passively control the temperature in buildings. PCMs also where used on the lunar rovers on the historic Apollo missions.

This report will focus on the possible application of PCMs for CubeSat missions. The following usecase will be explored in this report: If a CubeSat component is at risk of overheating, the PCM will melt, absorbing a large amount of energy and keeping the component from overheating. The absorbed heat can slowly be released again over a longer period so that the satellite has time to deal with the excess energy without overheating. An even better situation would be for the heat to be stored until the satellite runs the risk of under cooling, then the material can solidify again and supply the heat required to keep the satellite from under cooling. Essentially it would work as a heat storage buffer for the whole satellite, storing heat from components that need cooling and releasing them to the components in need of heating.

This thesis will research the feasibility of use case. Solutions to the foreseen engineering issues will also be discussed and developed. The properties that a PCM device would have will be catalogued and compared to those of current thermal control techniques. If the advantages in performance of a PCM device outweigh the cost and the risk added to a CubeSat mission they should be considered to fly on CubeSats allowing for high performance missions.

1.2. Research Question, Aims and Objectives

Research Question: Can a Phase Change Material Thermal Storage Device be used as a reliable thermal control system for a CubeSat?

- Can a CubeSat benefit from a PCM TSD?
  - What subsystems would benefit from having a PCM TSD?
  - How could the PCM TSD be implemented?
- What are the design requirements for a CubeSat thermal control system?
  - What are the mass, volume and cost budgets for CubeSats in relation to the thermal control system?
  - What are heat loads a CubeSat can experience that would require thermal control from a TSD?
  - What temperatures need to be maintained by the CubeSat thermal control system for it to be successful?
  - What other requirements does a CubeSat have for a thermal control system and can all these requirements be met by a PCM TSD?
- How does a PCM system need to be designed to control the heat load?
  - What PCM should be used?
  - How much PCM is required to absorb the heat load?
  - How should the PCM casing be designed?
  - Where should the PCM system be placed and to which components should it be thermally coupled?
  - How can this system be sized to fit inside a CubeSat?
  - How can the TSD be made sufficiently reliable so that it can work properly for the entire duration of a CubeSat mission?
- Can the performance of the PCM TSD be predicted accurately, using thermal theory and numerical models?
  - What properties need to be modelled for an accurate model numerically?
  - How can these models be validated so that their results can be relied on?

Research Aim: To design a feasible PCM TSD for use on a CubeSat and to build a tool that can accurately predict the thermal response of that system.

Research Objectives:

- To design a CubeSat thermal control system using a PCM TSD.
    - Size the PCM system to handle the thermal loads.
        - ⋄ Identify the type of thermal loads that need to be controlled by the Thermal Control System (TCS).
        - ⋄ Identify the PCM design parameters by studying the literature.
        - ⋄ Optimize the system for use on CubeSats by making trade-offs based on analytic equations and results of numerical models.
    - Design the rest of the TCS as required for a CubeSat.
- To accurately predict the thermal response of the thermal control system(s).
    - Build a model of the CubeSat and the thermal control system(s) by identifying and applying the best practices in literature and advise from experts.
    - Validate the numerical model by measuring the thermal response of the system in an experiment and comparing the results to the numerical model.

1.3. Methodology

The first objective of the project is to make a basic TCS design. Thermal loads can be estimated by comparing representative examples of previously flown missions. Estimations of the thermal response of the system depend on the thermal properties of the CubeSat and the PCM. Basic sizing of this system can be done by using heat transfer theory.

A more detailed design can be made using a numerical model. This design can be iterated and optimized for use on CubeSats and one or multiple ideal test prototypes can be designed. A numerical model was built in collaboration with NLR which has experience in thermal models and PCMs. Effective thermal modelling techniques can also be determined from previous research. From these models the critical aspects that need to be measured to validate the design will be identified.

One or multiple prototypes of the PCM system will be made to verify the model's performance by measuring the thermal response of the prototypes. The prototypes can then be integrated into a CubeSat representative prototype to measure the thermal response of the assembly.

If successful, and the designs pass all CubeSat requirements, this would validate the design of the PCM based TCS. If not successful, then it does not mean that this concept is not feasible, just the design brought forward in this thesis. The same is true for the modelling techniques. If the model is capable of predicting the thermal response of the TSD, then the model is validated and the design of the TSD is predictable. If not, it means that the model is not valid, but it does not mean that a different model using more detail or different equations or different modelling techniques wouldn't be able to predict the results.

This project was carried out in collaboration with the following three institutions:

- Delft University of Technology (TU Delft)
- Innovative Solutions In Space (ISIS)
- Royal Netherlands Aerospace Centre (NLR)

Most of the research and design was done at ISIS, where there was a great deal of knowledge and expertise about CubeSat design. Most of the manufacturing was outsourced to third parties, manufactured internally at ISIS or in the student workshop at the TU Delft. Much of the hardware used was also designed by ISIS CubeSat. The TSD and CubeSat final assembly and testing were done at the NLR where there is much experience in high tech testing and qualification. All the tests where done using NLR hardware. The research was conducted with close oversight and supervision from each institute.

2

CubeSat Thermal Control System

This chapter discusses the thermal theory and properties of CubeSats in a space environment. Understanding the basic theory of heat transfer is needed for designing TCSs on CubeSats because it can predict the temperature of satellites in specific, idealised environments. Controlling spacecraft temperatures can be challenging as they cant be cooled through convection due to the lack of air in space and are therefore mostly dependent on radiative cooling. Therefore it is important to consider the thermal environment and its interfaces with the satellite to make sure every subsystem stays within its operational temperature. This chapter, the heat fluxes experienced by the satellite in its environment will be considered.

2.1. Thermal Environment

Most CubeSats fly in a Low Earth Orbit (LEO) environment. The heat flux experienced by the satellite is dependent on solar radiation, albedo, Infrared (IR) radiation from the earth, free molecular heating and charged particle heating. The orbital period in LEO is not long enough for a satellite to reach its steady state temperature, around 90 minutes. Because of the short orbital periods and therefore short eclipse periods the thermal inertia of satellites is often enough to keep the satellite within operating temperatures from these sources alone. Due to the low mass of the CubeSat compared to traditional satellites the temperature variations are larger with similar power inputs, and therefore have a higher risk of exceeding their allowable temperature range. The different periods during the orbit do have different heating characteristics making it important to understand during which part of an orbit certain heating occurs to be able to determine the potential worst case scenarios.

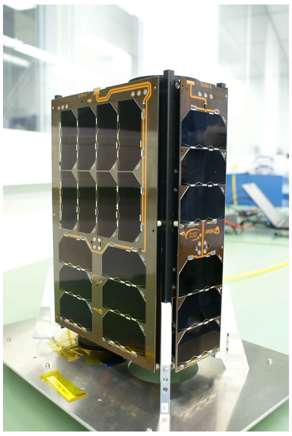

Figure 2.1: Hiber CubeSat [8]

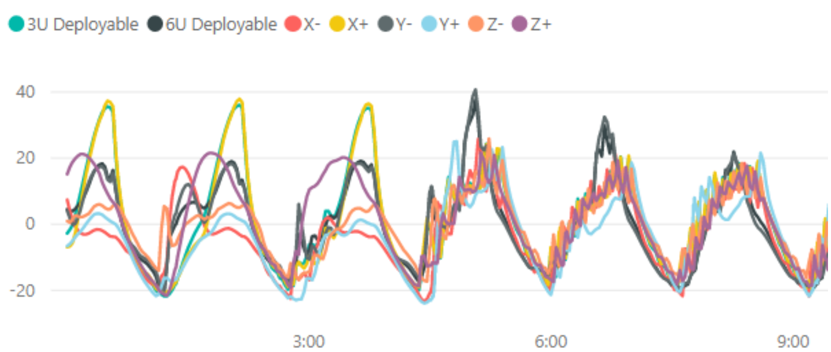

Figure 2.2: Hiber temperature plots, degree C on y-axis, by ISIS [8] the first three cycles have A controlled attitude, during the second three it is tumbling

Many CubeSats operate in a Sun Synchronous Polar Orbit (SSPO). These orbits have uniquely consistent thermal profiles due to the fact that the orbital plane follows the path of the Sun, thereby keeping the same relationship towards to the Sun. These orbits are chosen so that heating and power cycles during an orbit are more predictable and therefore CubeSat designs can be made lighter, cheaper and more efficient. An example of CubeSats with this type of orbit are the Hiber satellites, the specs of which are shown in table 2.1, and the orbital parameters of the satellites are shown in the table 2.2). The Hiber satellite, developed by ISIS, can be seen in figure 2.1. Temperature data from the Hiber satellite in this orbit can be seen in figure 2.2. A phased average plot of the temperature of the 6u deployable panel can be found in figure 2.3.

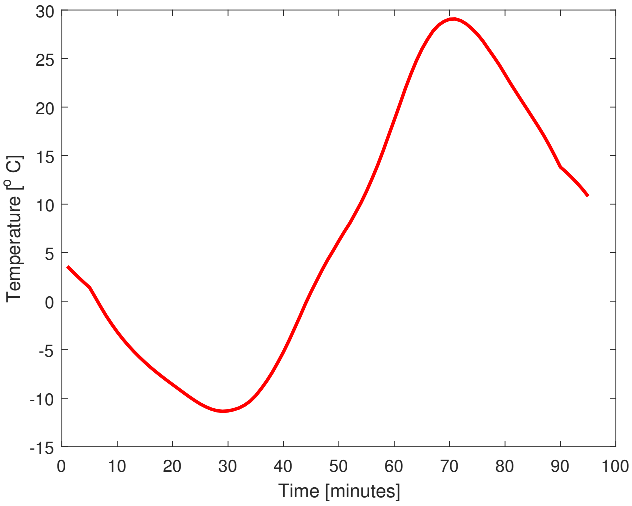

Figure 2.3: Phase averaged 6U deployable Hiber panel temperature plot

These short orbital periods cause repetitive thermal cycling. Due to the short orbital period the CubeSat will heat up and cool down frequently over its lifetime. These thermal cycles can cause material fatigue and degradation of chemical processes which can shorten the lifetime of the satellite.

Table 2.1: Hiber satellite specifications [9]

Requirement	Value	Driver
Peak power	45W	Antenna deployment
Orbit avg power	13W	Payload duty-cycle
Max pointing error	3°	RF coverage and gain
Downlink capacity	0.5GB/day	Payload data
Availability	>95%	Data Service
Lifetime	>1 year	Data service

Table 2.2: Hiber orbit parameters [10]

Satellite	Apogee $[km]$	Perigee $[km]$	Orbital inclination	orbital period $[minutes]$
Hiber 1	476	500	97.48°	94.22
Hiber 2	575	591	97.77°	96.19

2.1.1. Solar Radiation

The solar flux is dependent on the distance of the satellite from the sun. The eleven year solar cycle does not significantly affect the solar radiation from the sun. The distance of the earth from the sun can change by more than 10000 km. Therefore during different times during the year varying amounts of radiation reach LEO. This value is between 1414 $\frac{W}{m^2}$ and 1322 $\frac{W}{m^2}$; the value taken at 1 Astronomical Unit (AU) is 1367 $\frac{W}{m^2}$ and is often used as a representative average. These variations are large enough that they need to be taken into account during thermal modelling. This radiation is only present when the satellite is not in the shadow of the earth, and it only heats the area facing the Sun [11].

Solar flux is inherently intermittent in LEO as the satellite passes through Earth's shadow, unless the orbit is in a SSPO facing the sun. If the orbit is sun synchronous but not facing the sun then the solar flux will still be intermittent but it will be periodical; other orbits will shift the flux timing and duration throughout the year. The intermittency of the heating is dependent on the height, eccentricity, the angle, ascending node of the orbit and the time of year.

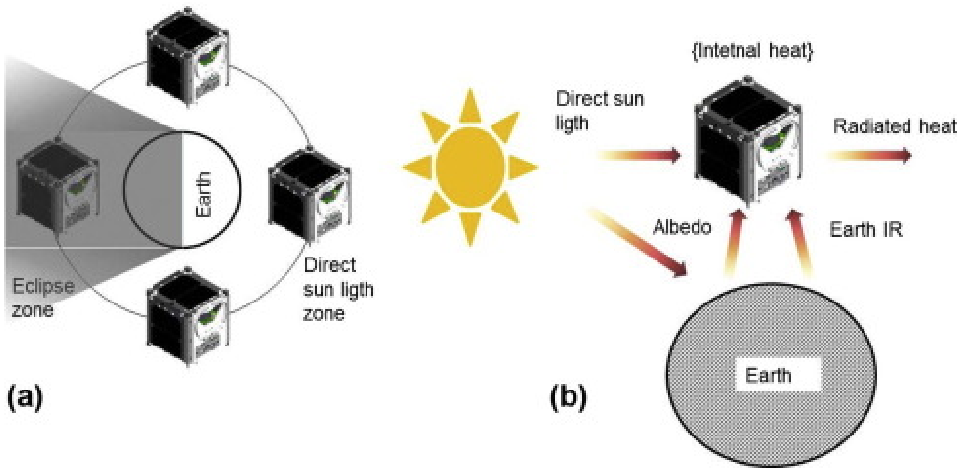

Figure 2.4: Thermal environment in space [12]

2.1.2. Earth Albedo

The albedo is the reflection of the solar flux off the Earth, in this case onto the satellite. Albedo is different at different places on the earth and is also affected by clouds. So the intensity of the albedo depends on the position of the satellite in the orbit. The albedo can be as low as 6% and as high as 50% of the solar flux [11]. For simple calculations the albedo can be assumed to be 30% of the solar flux while the satellite is not in eclipse. This is a fairly accurate estimate of an average albedo heating during an orbit of 90 minutes. Again only the panels that are in view of the Earth are heated in this way.

2.1.3. Earth Infra-Red Radiation

Infra-Red (IR) radiation from earth is also a significant contributor to the total heat flux experienced by the satellite. The earth is much cooler than the sun but it is also a lot closer to the satellites in LEO. For higher orbits this affect is smaller than for lower orbits because of the inverse squared law. Generally for LEO IR radiation is between 227 and 249 $\frac{W}{m^2}$. For simple analysis it is often taken at 238$\frac{W}{m^2}$ as an average for a 90 minute orbit [11].

2.1.4. Other Heat Fluxes in LEO

Free molecular heating (FMH) is caused by free particles from the upper atmosphere colliding with the satellite. This effect is larger when the satellite is at a lower altitude, and is generally the largest when the satellite is being inserted into its orbit right after the fairings are deployed. In the regular operating life of the satellite this effect will be much smaller than the previous heat sources discussed. The equation for free molecular heating is dependent on the density of the atmosphere and the velocity of the spacecraft with regard to the atmosphere. This effect can be calculated with equation 2.1:

$$q_{FMH} = 0.5 \cdot \alpha_{FMH} \rho V^3 \tag{2.1}$$

In this equation q_{FMH} is the free molecular heat flux in $\frac{W}{m^2}$. α_{FMH} is an accommodation coefficient, which is a dimensionless number that characterizes how much heat is transferred from the particles as they collide with a particular surface. ρ is the atmospheric density in $\frac{kg}{m^3}$ and V is the relative velocity between the spacecraft and the atmosphere in $\frac{m}{s}$.

This effect only becomes significant when the satellite is flying at relatively low altitudes at high speeds. According to the Thermal Control Handbook [11], this heating only becomes significant if the satellite perigee drops below $180km$. Using equation 2.1 at a circular $400km$ orbit, a relative velocity of $7667\frac{m}{s}$, an atmospheric density of $2.75 * 10^{-12}\frac{kg}{m^3}$ and a conservative accommodation coefficient of 1 the FMH flux is equal to $0.62\frac{W}{m^2}$. This is more than three orders of magnitude less than the previous heat sources.

Charged particle heating generally has a minimal effect in LEO and is usually ignored because of its small effect compared to the other heating sources. Only at cryogenic temperatures will this effect become significant [11]. But if a CubeSat is placed into an orbit with a large radiation band then there might be some heating, for instance in the Van Allen radiation belts. Also if the satellite is placed into an interplanetary mission the particle bombardment might have a significant heating affect.

There can be other sources of heat fluxes in LEO but in general these are too small to be of any affect just like the charged particle heating. The most relevant heat fluxes to this thesis, more precise values can be found above, listed in order from most to least intense are:

- Solar flux
- Earth albedo
- Earth IR radiation

The above heat fluxes are on the order of $10^3 - 10^4\frac{W}{m^2}$. With a threshold for relevant heat fluxes set to >1 Watt, the heat fluxes that are not as relevant for spacecraft thermal control analysis in LEO are:

- Free molecular heating
- Charged particle heating
- Other potential heat fluxes in LEO

2.2. CubeSat Thermal Properties

CubeSat Thermal Control Systems (TCS) tend to be almost completely passive. “A passive control is applied to most of the nano-satellites because of the simplicity, cost reliability, mass, and power” as quoted in [13]. Passive solutions may be insufficient given the increased power usage of higher performance satellites. It can be difficult to keep temperatures within an acceptable range if the temperature control systems are completely passive. If higher performance is required in transportation, storage and dissipation of heat, the satellite will need an active system.

2.2.1. Passive Thermal Control Systems

Passive thermal control systems are the systems that don't require control input from the On-Board Computer (OBC) or power input. Passive thermal control systems control the satellite temperature with their inherent conductive and radiative properties. In designing a thermal control system, existing components can have their material or surface properties adjusted to control the satellite temperature. If this is not enough, dedicated thermal control hardware can be implemented.

Passively removing heat from a system in space occurs through radiation to space. Every surface on a satellite radiates to space and receives radiation from other sources. Adjusting the existing surface with paints, tapes and coatings can change the radiative properties of a satellite enough to control the energy entering and leaving the system. Figure 2.5 shows different thermo-optic properties of different surfaces. Dedicated hardware can be employed, for instance by using radiator panels [14] [15].

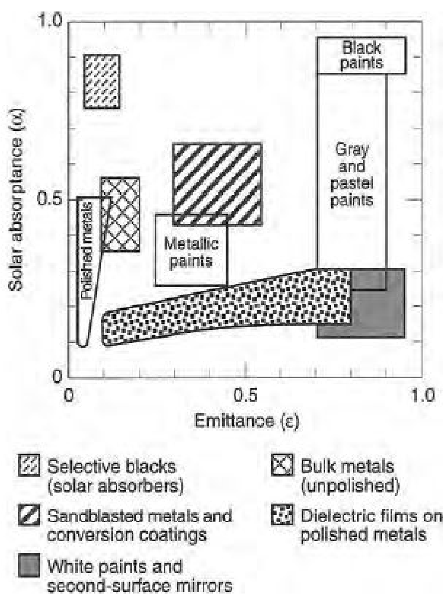

Figure 2.5: Thermo-optical properties of surface finishes [11]

Transportation of heat through the satellite happens through conduction and radiation. Radiative heat transfer between components utilize similar strategies as radiation in removing heat from systems. Paints, tapes and coatings can go a long way. For conductive heat transfer material properties and shape play an important role. If a lot of heat needs to be transferred from the system, metal connections are made with materials like aluminium and copper. Also large surface area contacts are created to transfer large amounts of heat. To insulate components, steel with low surface area or plastics are used with little contact surface area to hinder heat transfer between components. For instance cryogenic subsystems need to be insulated so their temperature does not rise too high or the satellite temperature too low. Dedicated hardware can be used to increase and control the heat transfer between components. Flexible straps of highly conductive material are sometimes added to increase thermal conduction between components [16] [17]. This allows there to be a thermal connection between subsystems while still allowing them to thermally expand and vibrate independently

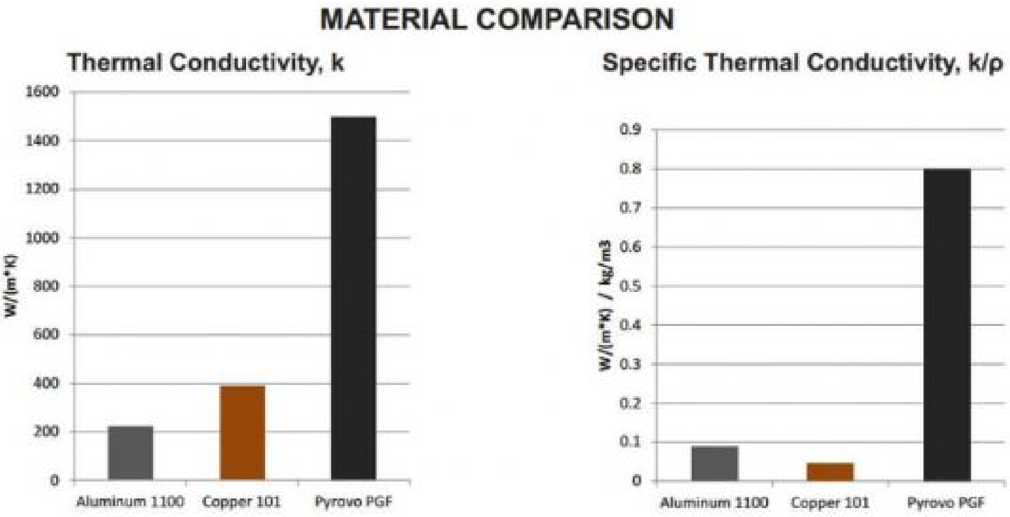

Figure 2.6: Performances of thermal straps made from different materials [18]

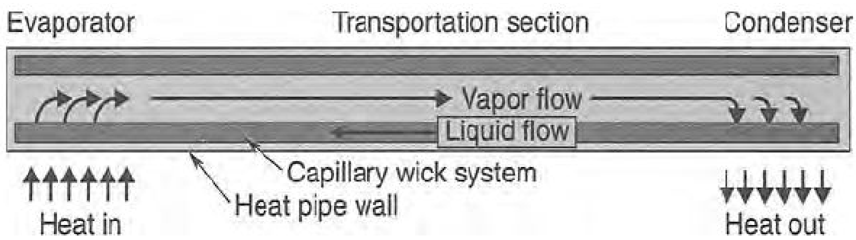

Figure 2.7: Working principle heat pipe [11]

from each other. The difference in performance of various materials are shown in figure 2.6.

For larger non-flexible heat transfer subsystems, heat pipes can be used [19] [20]. These are copper pipes containing a liquid and gas vapor. liquid evaporates from the hot end of a heat pipe and condenses at the cold end of the pipe. The liquid is pumped back to the hot end using a capillary effect in a wick structure along the edge of the pipe. This allows for relatively large heat transfer between components, and are often used in smaller high performance electronics like mobile phones and laptops. A figure of the working principle of a heat pipe can be seen in figure 2.7.

Another type of heat transportation control system is the heat switch. The heat switch uses thermal contact pressure to control the heat flow between two components. It uses thermal expansion of materials to change the pressure between two conducting plates. In extreme cases the conduction can be completely removed, totally isolating the component. Generally this is done by using differential thermal expansion of materials or by using expansion caused by phase change of a material.

Temporary storage of heat is generally done in the specific heat of the mass of the satellite materials. The heat generated or received by the system is used to increase the temperature of the satellite and subsystems. This is fine for large systems with a lot of mass as long as the energy received does not increase the temperature too much. For smaller components that have large power inputs, like electronics, hot-spots often occur. The solution for this is to add a large metal mass to the component that absorbs and spreads the heat so that it is easier to removed later. This is called a heat sink. As discussed in section 1.1, to increase

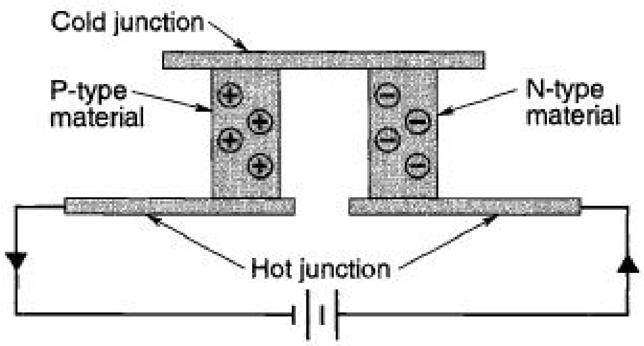

Figure 2.8: Peltier junction [11]

the storage capacity of the heat sink a material can be added that changes its material phase to absorb extra energy. This PCM temporarily stores heat from a system in the form of its latent heat of fusion, and releases it at a later point in time. The main advantages of this system are a low mass thermal control solution for removing thermal peaks in the satellite and its high power, thermally sensitive subsystems. This system will be discussed more later in this chapter.

2.2.2. Active Thermal Control Systems

Active thermal control systems require an input signal and power. Active control systems will generally have more precise temperature control and will be able to handle higher heat loads than passive systems. They tend to be more complex and have a higher risk of failure than passive systems. These systems also tend to cost more than passive systems.

If a system requires high performance and variable thermal control, a pumped fluid loop is generally used to control the temperature [21]. These systems historically have required large amounts of power to run which is often unavailable on CubeSat. Low power pumped fluid loops are currently being researched [18] and therefore could become an interesting option for CubeSats. Pumped fluid loops can reliably transport large amounts of heat over large distances. Also the amount of heat that can be transported can easily be adjusted by varying the pump speed and valves. The main drawbacks in using this system for space systems are that such a system is usually large, heavy and has many complicated moving parts in a pump that can easily develop problems that can not be fixed remotely.

TECs (Thermo-Electric Coolers) are active cooling systems that employ the Peltier effect to electrically cool a device. The Peltier effect uses a voltage differential between two separated metals on a hot junction. This will cause heated electrons and thereby thermal energy to flow from the cold plate to the hot plate [11]. This system is illustrated in figure 2.8. This process can also be reversed using the Seebeck effect. Here a current is produced by applying the pn-junction to a hot and a cold plate. It is highly reliable because it does not require any moving parts to work. These systems do require power to cool the system, however; this causes the TEC to have a low efficiency. TECs are not equipped to handle a large heat load and are also most efficient with a large heat differential between a hot and a cold plate. Although if the difference is too high the system will suffer from parasitic heat losses and therefore a multistage system is used to make multiple smaller temperature jumps. A figure of the working principle of TECs can be seen in figure 2.8

Variable Conductivity Heat Pipes (VCHP) is a technology currently being researched as can be seen in this reference [22]. These heat pipes are an active TCS. The working principle of the heat pipe has the requirement that the vapor inside the pipe can condense on the cold

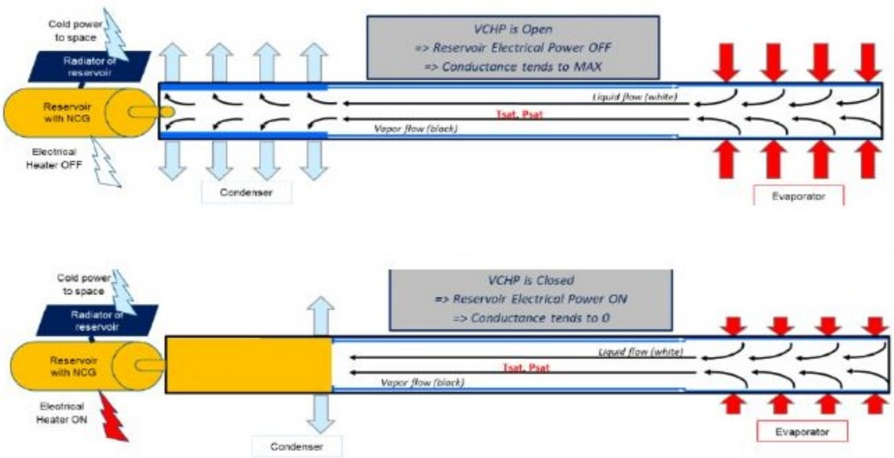

Figure 2.9: An actively controlled variable conductivity heat pipe [22]

surface of the condenser to deliver the heat to the cold side of the pipe. If a non-condensing fluid is present at the condenser then there is no condensing of the fluid and the heat pipe thermal conductivity will drop. In a VCHP a reservoir of non-condensing fluid is placed next to the condenser and if the temperature of the cold end of the heat pipe rises too much the fluid will expand and the pressure will push it into the condenser region thereby reducing the conductivity of the heat pipe. The system can also be actively controlled by adding an electrical current to the non-condensing fluid causing it to heat up and expand into the condenser region. This makes the electrical current the controller of the active TCS. A figure of the working principle of a VCHP can be seen fin figure 2.9

The next strategy is to actively add or remove heat from the system. A method of actively adding heat to the system is by using electrical heaters. Heaters can be turned on when satellite component temperatures drop too low. These heaters generally use electrical resistance through a wire to produce a large amount of waste heat. This system is a very reliable active TCS because it does not use any moving parts to control the temperature. A picture of a resistive heater used to keep a battery warm can be seen in figure 2.11

Louvers are used in space in combination with radiators. The louvers can open and close over the radiator surface, changing its radiative properties. Louvers are moving parts in the system and are therefore less reliable than other TCSs. The louver system also generally has large mass and operating power. Passive louver systems have been flown on CubeSats where the louvers are opened when a certain temperature is reached due to differential expansion in a bi-metallic spring. This is shown in figure 2.10.

2.2.3. CubeSat Thermal Control System

According to [23], the space environment can cause component temperatures to swing from 100 $^{\circ}C$ to -130$^{\circ}C$ in the order of tens of seconds or minutes. Therefore having a proper TCS for spacecraft is extremely critical. High power subsystems that fire intermittently can help to balance these temperatures out, but ideally these subsystems should be used for their intended purpose and not as an improvised TCS. Also these systems could possibly exacerbate the problems if used at the wrong times. This thesis will focus on how to use and spread out the thermal load of these intermittent high power subsystems. CubeSats have traditionally relied on very low power and continuous subsystems and have therefore not had these issues. The next section will discuss the current CubeSat TCS and how it avoids these large temperature swings.

Figure 2.10: Passive louver developed by Goddard Space Flight Center [18]

CubeSat TCSs tend to be almost completely passive, except for the occasional heating element. The only exceptions to this are payloads that require a dedicated thermal control element (like a cryocooler) if its performance is dependent on temperature. CubeSats are designed this way for multiple reasons, first reason is to keep the complexity of the satellite as low as possible. The higher the complexity of the satellite the higher the risk of failure for the simple reason that there are more parts that fail. To keep the mission safe from failure more testing and qualification will be required for the satellite, this will in turn drive up the price of the satellite dramatically. Lowering cost of the satellites is one of the main goals of CubeSat manufacturers, therefore using active TCSs are generally avoided. Another reason to avoid using active TCSs is the high power requirements of the CubeSats, which already have low power budgets. But as satellites move to more deployable solar panels, more power will be available for the CubeSats and this becomes less of an issue. The mass budget for passive thermal control subsystems on CubeSats tends to be around 2-5% of the dry mass according to [24]. For active TCSs larger mass budgets of around 10% are allocated to the TCS according to [23] (although this budget is used for traditional satellites and not for CubeSats and are therefore only a design guideline). With a CubeSat weight of 1.33kg per U, this leaves 26.6-66.5g of mass per U for a passive TCS and 133g per U for an active TCS. Because most TCSs in CubeSats tend to be coatings and paints, this leaves a lot of mass for dedicated TCSs. The challenge tends to be fitting the volume of these TCSs into the CubeSat.

CubeSats tend not to have dedicated radiator panels. The surface area is generally reserved for solar panels to produce power. CubeSats tend to just radiate the heat away through the surface panels. Because of the small distances between satellite components the thermal gradient between components is usually small unless it is specifically thermally isolated from the rest of the CubeSat. Also due to the low mass of the satellite, its temperature is highly sensitive to energy input. Where a large satellite can absorb a lot of heat in sensible heat without increasing a lot in temperature, in CubeSats the temperature would increase dramatically with the same power output.

The temperature of a CubeSat is dependent on the amount of heat entering and leaving the system. this is done mainly through radiation. If there is more heat entering than leaving, including the heat generated from within, then the temperature will rise, and the opposite as well. If we assume an even temperature distribution throughout the CubeSat then equation 2.2 describes this relationship.

$$\Delta T = \frac{\Delta Q}{c_p \cdot m} \tag{2.2}$$

In this equation ΔT is the change in temperature in the CubeSat in K, c_p is its average specific heat $\frac{J}{kg \cdot K}$, m is its mass and ΔQ is the change in the amount of heat energy in the CubeSat in J.

If there is a large heat input from a high performance subsystem, the heat output will have to be equally large for the satellite temperature to remain constant. If this power source is intermittent but the output of heat is equal, like on passively controlled satellites, then large temperature swings will occur due to the mismatch in input and output powers. If these oscillations become too large then the peak temperatures can exceed the operating temperatures on the satellite which can cause damage to the satellite components. one current solution, is to add mass to the satellite for more thermal stability. Ideally this added mass can serve other purposes, like a support structure. Heat storage in these components is limited, therefore dedicated hardware may be desirable, traditionally heat sinks are used for this. This is where the use of PCMs have the potential to reduce mass and/or increase energy storage of the heat sink and therefore the satellite.

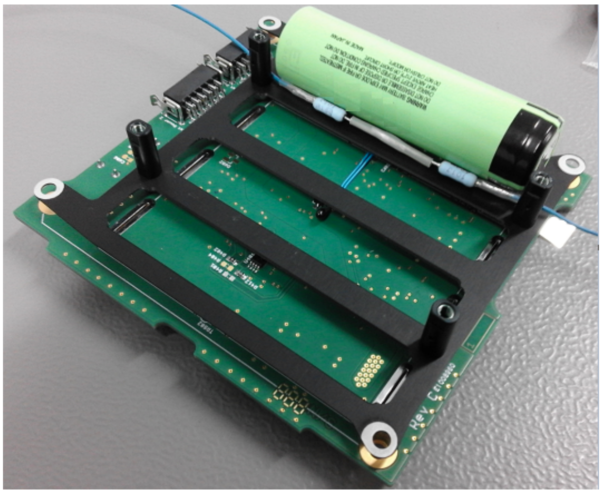

Figure 2.11: An earlier prototype of an ISIS battery pack [8]

Thermal control for spacecraft involves keeping the spacecraft and all its subsystems within their respective operating temperatures. The components with the largest operational temperature ranges tend to be the solar panels and the structure of the CubeSat. Solar panels for CubeSats sold by ISIS have a temperature range of -40 to 125°C [25]. Components that typically have stringent temperature requirements are be the batteries. The chemical reactions of the battery pack are affected by the temperature and therefore have specific temperature operating ranges to prolong the life of the battery. For instance the Panasonic NCR18650A lithium-ion batteries that are often used for CubeSats have an operating temperature range of 0 to 45°C while charging and -20 to 60°C while discharging [26]. Although to increase the lifetime of the batteries it would be better to keep them above 10 °C. In figure 2.11 a picture of a battery stack for CubeSats can be seen with a heating element mounted inside. In orbit data of CubeSat battery temperatures of the Hiber satellite can be seen in figure 2.12. In this figure it can be seen that the batteries stay within their operating range in this particular configuration although they do drop below 10 °C.

In orbit measured temperature ranges from other subsystems of the Hiber missions can also be found in figure 2.12 underneath the operating temperature range of their subsystems. For many CubeSats the payload will be driving the temperature requirements on the satellite and therefore will require stringent thermal control [27], especially for optical devices that measure low energy electromagnetic radiation. The requirements can be an operating temperature range, or for instance a maximum thermal gradient over the component or stability in the temperature over long periods of time.

The average temperature of the satellite and its subsystems can be adjusted by varying its surface properties. The CubeSat will be heated up while in the sun, and cooled dramatically when in the shadow. Even though the full steady states probably will not be reached, the

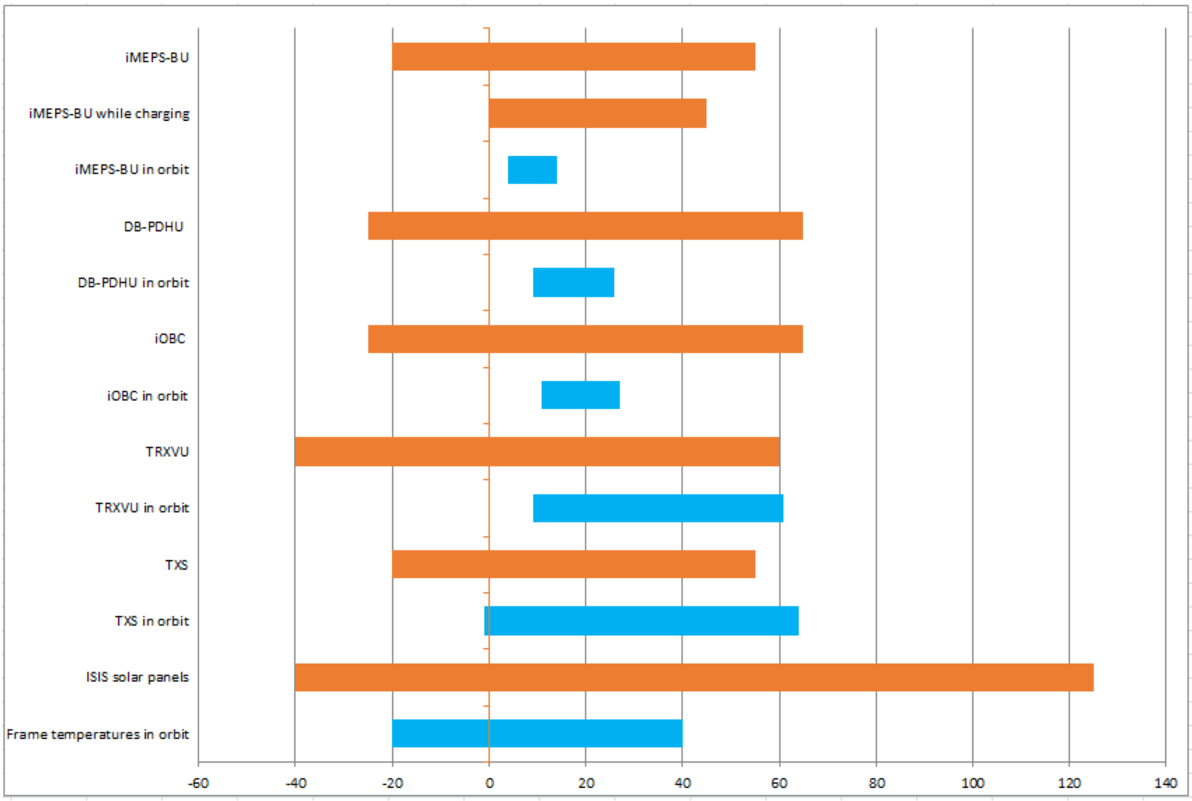

Figure 2.12: Subsystem temperature ranges and measured temperature ranges of Hiber CubeSats [8]
Orange = component operating temperature,
Blue = Measured in-orbit temperature range

smaller the satellite the quicker the satellite is capable of reaching its steady state temperature. This is because the energy satellites receive is proportional to the surface area, and the heat capacity of the satellite is dependent on the mass which scales with the volume. Because surface area scales with the size of the satellite squared and the volume scales cubed, the satellite temperature becomes more sensitive to the radiation as it get smaller. The exact equations describing these values is discussed in section 5.1

The other place a satellite can gain thermal energy is from inefficiencies in high energy subsystems. Any electronics that are used dissipate their energy into waste heat. If Radio Frequency (RF) antennas are used then a fraction of the energy is released in the form of RF waves but most of the energy is still released as heat. And finally for thruster systems all the energy that is generated but is not imparted into the fuel before firing also enters the satellite as waste heat. It is possible to time these components to keep the satellite within its operational temperature range. But ideally it is better that the operations of a satellite are not governed by thermal requirements but by mission requirements. Therefore it would be better if a more robust TCS could be developed so that these systems can work in the most extreme possible use cases. Ideally the TCS would vary its power to accommodate these different thermal fluxes in a thermal control loop. To do this with a passive system is much more difficult.

In current CubeSat designs regulating the heat that enters, leaves and is transported through the system can already be achieved for most applications. The main area where CubeSat temperature control lacks performance is heat storage. This is due to the constant push to miniaturize systems and minimize the mass of the CubeSat. This mass that would usually dampen the temperature swings in a CubeSat is missing. Therefore this paper is researching light weight energy storage in the form of PCMs, as this allows for a larger thermal inertia of

CubeSats while keeping the trend of low mass and simplicity in its design.

2.3. CubeSat Radio Heat Source

This thesis will focus on a specific heat source as an example, in order to size and design a TSD prototype. This is done so that the design can be built and tested to verify that it works as intended. The ISIS TXS S-band radio transmitter, as seen in figure 2.13, was chosen for this application. This is a printed circuit board that is attached to an antenna. A lot of power goes through a power amplifier used to amplify the radio signal. The current design of this radio has a large copper heat sink attached to the Printed Circuit Board (PCB) where it is most needed. This transceiver runs at relatively high power compared to other subsystems on a CubeSat. This power is only used when the CubeSat has data that needs to be transmitted to antennas on the ground, and when it is flying over ground stations so it is actually capable of doing it. Low flying satellites have short visit periods where they can be viewed from a ground station. Therefore if a lot of information needs to be transmitted, either the data-rate of the information transfer needs to be increased or the satellite has to visit more ground-stations to transmit all of the data. A higher data-rate can increase the power demands of the antenna, and multiple ground-stations require it to transmit for longer.

Figure 2.13: TXS High data rate S-band transmitter [28]

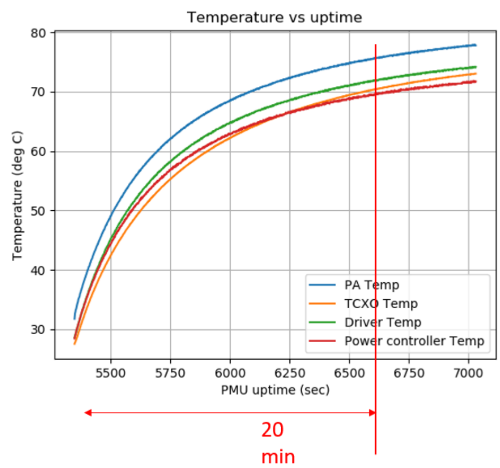

Figure 2.14: TXS heat response experiment [8]

The current TXS setup of the antenna allows for 8 Watts of power to be used for 15 to 20 minutes before overheating. This can clearly be seen in tests done in ambient temperature starting at above room temperature, the results of which can be seen in figure 2.14. Here the temperature went from around $30°C$ to $75°C$ in 20 minutes. Figure 2.12 shows that the maximum operating temperature of the TXS as being $55°C$, this is the operational temperature of the subsystem. The power amplifier on the PCM which is being measured in 2.14 can reach about $80°C$ before failing. $55°C$ is recommended because prolonged periods of elevated temperatures will reduce the lifespan of these devices. In orbit tests have been conducted as well, the results of which can be seen in figure 2.15. These temperatures have a lower starting point, which allows the TXS to stay within an acceptable temperature range over the 20 minute transmission period.

To increase the performance of the TXS, its copper heat sink is clamped to the CubeSat frame. This allows for heat to be transferred from the heat sink to the frame, which has a relatively large thermal mass. This does require the TXS to be placed at either the top or the bottom of a CubeSat stack. The TXS can transmit data for 20 minutes at 8 Watts if the satellite starts at a lower temperature and with the large heat sink attached to the PCB. The

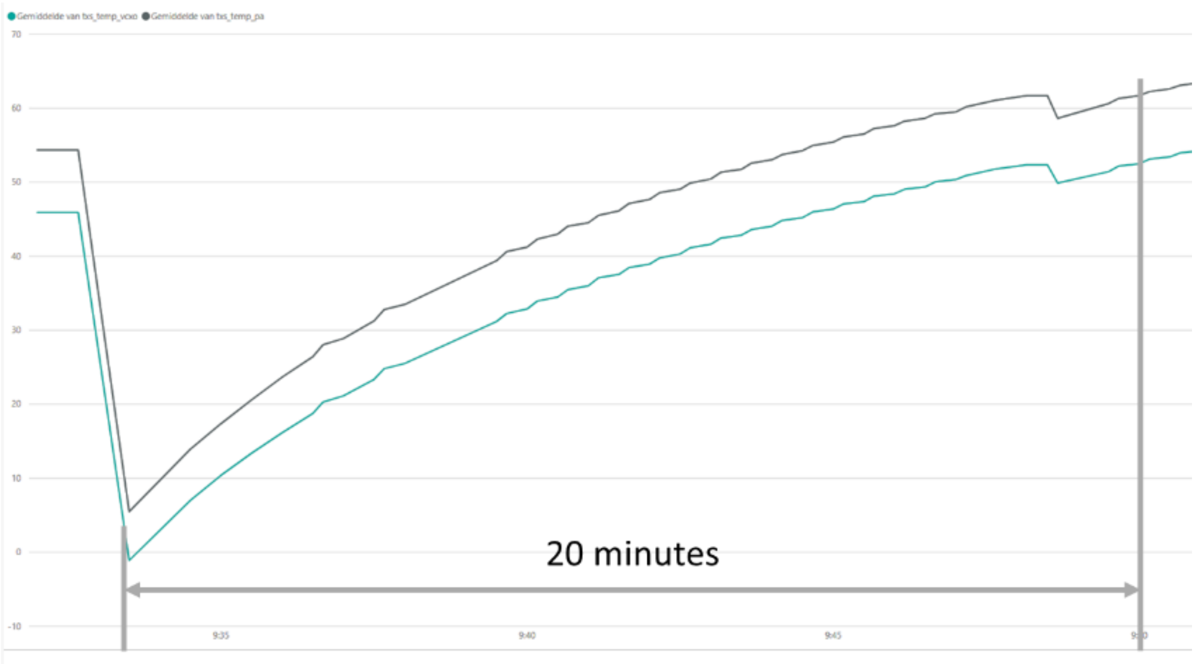

Figure 2.15: TXS on orbit temperature response [8],
the x-axis shows the local time the measurements where done and the y-axis shows temperature in $^{\circ}C$

PCM TSD would allow for the energy to be absorbed by the PCM instead of the heat sink or the frame. The following TSD requirements can be derived from the information in this section:

- To keep the power amplifier in the TXS below 80 $^{\circ}C$ as at this temperature it will fail
- To keep the entire TXS temperature below 55 $^{\circ}C$ as taken from figure 2.12.
- To keep these lower temperatures while extending the transmission period of the TXS.
- To have the ability to store this heat and later release it to subsystems that require extra heat, in this case the battery pack.
- To achieve these goals with less mass than a traditional heatsink system.

2.4. PCM Thermal Storage Device

PCMs inherently able to increase the thermal inertia of a satellite with less mass than a regular heat sink. This is due to the fact that it stores heat as sensible heat as well as in latent heat. This is shown in the equations and examples shown in section 3. This increased heat storage density reduces the satellite's temperature sensitivity to the energy received from high power systems. Because PCMs have a very specific melting point and a latent heat of fusion, they are very good at maintaining a constant subsystem temperature. If the allowable temperature range is very narrow then PCMs have a unique advantage in absorbing a large amount of energy within a narrow temperature range. If the allowable temperature range is larger, then at a certain point it might become more useful to just use a heat sink to absorb the energy using sensible heat.

Specific components on CubeSats can have intermittent power usages. This will cause the temperature in the satellite to change: to rise when the power is turned on, and fall when the power is turned off. When this is done periodically over a certain amount of time they are called thermal cycles. This effect is large if this is a high power, low mass component. Examples of these types of components are propulsion systems and power amplifiers for RF-antennas. The example that is used in this thesis is the use of a TSD, which in this situation

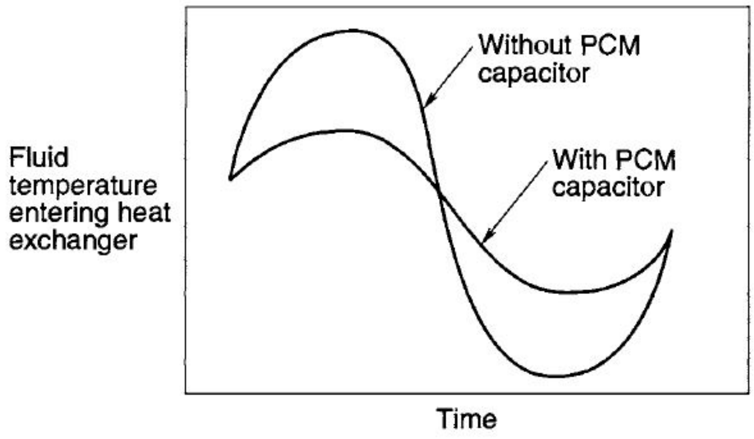

Figure 2.16: Temperature variation during thermal cycle with and without PCM [11]. (Expected temperature plateaus are not reached in these graphs due to the thermal gradient caused by the already melted PCM)

would remove the peaks and valleys of a thermal cycle. Ideally a PCM would have a melting temperature at the average temperature between the highest and lowest temperature in the thermal cycle. The amount of energy leaving the system in the low temperature phase should be equal to the amount of energy entering the system during the high temperature period. In this case the temperature will balance out over continuous thermal cycles. The amount of PCM used can be tailored to how much the peaks and valleys of the thermal cycle need to be dampened out. An example of this working principle can be seen in figure 2.16.

A TSD on a CubeSat would ideally act as a temporary storage of heat for all the high power satellite components. These are distributed around the CubeSat. A thermal storage device could be used on each individual component, or it could be centrally located. The advantage to having the TSD centrally located is that all the components could share the heat load so that the peak heat load of the entire CubeSat is averaged out over all of the components. It would also reduce, the extra weight of having multiple separate PCMs, casings and fasteners. The disadvantage is that all the excess heat would have to be transported to the TSD. As CubeSats use simple passive methods of transporting heat, this will be through conduction. Luckily the distances within CubeSats are not that large so heat transportation through conduction can still be done relatively efficiently. If the heat has to travel farther than ideal, a good simple passive solution would be to use a heat pipe or a flex strap. An example of this system can be seen in figure 2.17. These thermal transportation methods are driven by the difference in heat as can be seen by equation 2.3.

$$q = -k \cdot \frac{dT}{dx} \tag{2.3}$$

In this equation q is the heat flow in $\frac{W}{m^2}$, k is the thermal conductivity in $\frac{W}{m \cdot K}$, T is the temperature in K and x is a distance in m.

PCMs have a distinct advantage over regular heat sinks. During phase transition of the PCM the temperature of the TSD is kept steady thereby not reducing the TSDs effectivity during that time. In contrast a heat sinks temperature would slowly increase requiring the heat source's temperature to rise along with it to transport the same heat flux.

After the heat has been stored in the TSD it can be an ideal way to keep the batteries warm during eclipse of the satellite behind the earth. As discussed previously the time when the

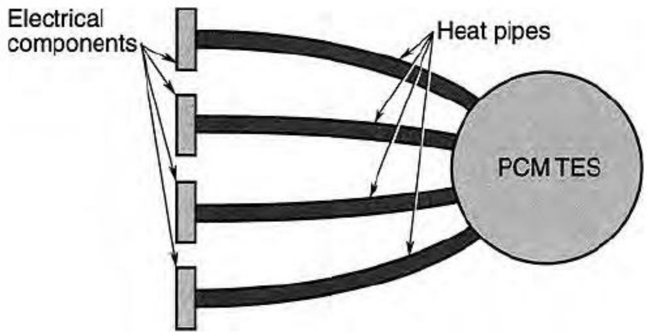

Figure 2.17: PCM and heat pipe thermal control system [11]

temperature of the batteries is most sensitive is during charging. But the time when the satellite is at its coldest is also when the batteries are in the most need of charging, right after eclipse when the satellite cools down because it is not exposed to the intense radiation of the sun. All this time it has also been running on stored battery power because it has not been able to use its solar panels. Once the satellite comes out of eclipse, it should start charging its batteries again to be able to sustain the power for the next eclipse. But if the batteries are too cold at this moment they can be damaged, causing them to degrade prematurely. This makes the batteries the ideal candidate to reuse the heat previously stored in the TSD.

For the specific use case of the TXS the following design and performance options are possible:

- It would allow for TXS placement anywhere in the CubeSat, preferably close to the TSD.
- The duration of the transmission can be extended allowing for more data to be transmitted over multiple ground stations.
- The heat sink on the TXS could be made smaller, thereby reducing the overall mass (assuming the TSD is energy denser than the heat sink).
- The waste heat expended by the TXS can be absorbed by the PCM and later reused to keep other subsystems warm, for instance the batteries.
- Eventually it would allow for an even more powerful radio to be used on a CubeSat instead of the TXS.

3

Phase Change Materials

The previous chapters have discussed the value of PCMs are for CubeSats. This section will focus on the properties of the PCMs themselves. The PCM selected to be the focus of this thesis is paraffin wax. The choice and properties of paraffin wax will also be discussed in this chapter.

3.1. Use of Phase Change Materials

PCMs change their material phase (solid, liquid, gas) thereby absorbing or releasing a large amount of energy. A PCM device is a TSD that has more energy storage capacity than a regular heat sink. PCMs have historically been used to store materials at cool temperatures. The most well known and common use of a PCM is when ice is used to keep something cool, like putting ice in a drink. While the ice is melting it absorbs heat without changing temperature, because the phase change of the material requires the energy. When material absorbs heat by increasing in temperature it is referred to as sensible heat storage. When material adsorbs heat by changing phase, which it does at specific temperatures and pressures, it is called latent heat storage. At small temperature changes this phase change reaction absorbs orders of magnitude more energy than sensible heat. Examples of this can be seen in table 3.1.

The expansion of a solid to liquid phase change is an order of magnitude less than the liquid to gas phase change. To keep the container size reasonable for spacecraft, solid liquid phase change materials are used in a closed system, rather than liquid to gas. The PCM can store energy in the form of latent heat when the PCM reaches its melting temperature and liquefies. This heat is released again when the PCM solidifies. This allows the thermal control system to be sized for the average heat flow of a thermal cycle instead of the peak flows. An example of a PCM TES device for CubeSats can be seen in figure 3.1. This PCM design is similar to the

Table 3.1: Energy storage capabilities of different materials in different temperature ranges

Material	c_p $[\frac{J}{g \cdot K}]$	$\Delta T = 1°K$ $[\frac{J}{g}]$	$\Delta T = 10°K$ $[\frac{J}{g}]$	$\Delta T = 100°K$ $[\frac{J}{g}]$
Steel	0.46	0.46	4.6	46
Aluminium	0.9	0.9	9	90
Copper	0.385	0.385	3.85	38.5
Eicosane	1.926	1.926	19.26	192.6
Water	4.187	4.187	41.87	418.7
Eicosane (with phase change) Latent Heat = 248 $\frac{J}{g}$	$1.926 - 2.4$	> 249.9	> 267	> 440
Water (with phase change) Latent Heat = 334 $\frac{J}{g}$	$2.108 - 4.187$	< 338.187	< 375.87	< 752.7

design developed for this thesis, although this one was developed for thermal management for a specific component to be mounted on a PCB, and not as a central CubeSat heat storage system. If it turns out that a CubeSat only requires a TSD for a particular component then this casing is already in use and can be bought from TMT. On the other hand if a more general CubeSat TSD is required then it would be advantageous to develop the TSD discussed in section 2.4. Another example of a PCM device used on a CubeSat is QBITO [29]. No data was found on the satellites performance.

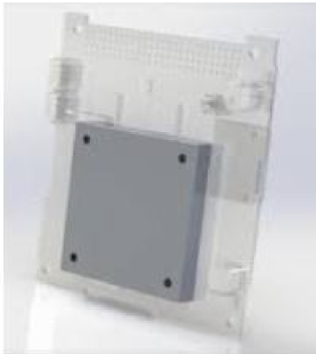

Figure 3.1: PCM device for CubeSats by TMT [18]

3.2. Choice of PCM

Choice of PCM to be used in a TSD is an important step in the design process as this will determine many of the design constraints. This section will briefly show the results of the analysis done in the literature study preceding this thesis. The final choice of using eicosane wax will also be justified and the implications this choice has on the design will be shown.

3.2.1. Type of PCM

The type of PCM influences the material and size of the container. Different materials are compatible with different types of containers and therefore have their own design characteristics. Thermal, mechanical and chemical interactions have to be taken into account. There are a number of different types of PCMs as can be seen in figure 3.2. Each has its own characteristics. A list of the desired attributes according to [30] can be seen in table 3.2. A more detailed review of all the different types and their properties can be found in Appendix A.

These are the reasons the traits in table 3.2 are desirable:

- A high heat of fusion is desired because this directly determines how much energy can be stored. Heat of fusion per weight or per volume is what needs are to be looked at depending on what needs to be optimized for.

- The thermal conductivity will determine how easily it will absorb the heat compared to other materials like the casing and the rest of the surrounding satellite. Also before all the PCM is melted a thermal gradient will have formed through it; the steepness of this gradient is determined by the heat flux and the thermal conductivity.

- A high specific heat also determines how much heat it can absorb without going through its phase change. Even though this is usually orders of magnitude below the latent heat, having a high specific heat over a large temperature range can have a major effect on heat storage capabilities.

- A high density is optimal for reducing the volume required.

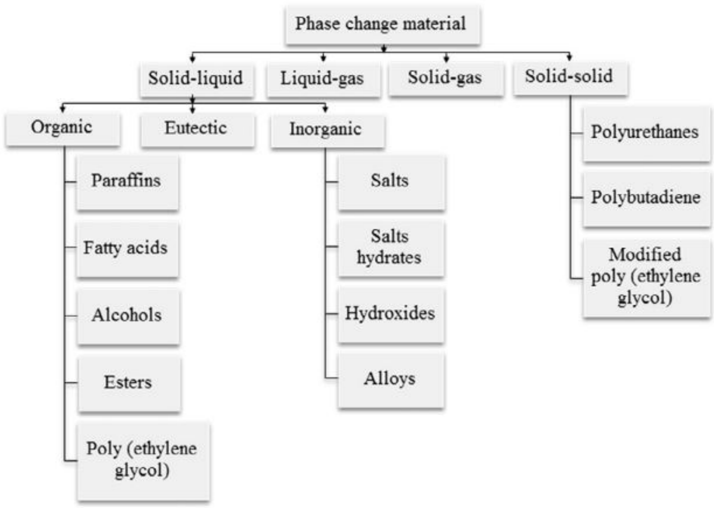

Figure 3.2: types of PCM [31]

- A low volume change during melting is desirable because the volume change causes large stresses on the casing. Therefore the lower the volume change the smaller and lighter the casing can be.
- A low vapor pressure is desirable because a higher vapor pressure can cause a low pressure inside the casing to become pressurised again (for instance when it is solid). This can cause higher pressure spikes when it expands to become liquid again. This would require a stronger, or larger casing.
- The melting behaviour needs to be dependable and reversible. This is the case because if a TCS is designed around a PCM device then the satellite relies on its effects. If these where to become unreliable then the times when they fail the satellite could cause thermal issues for the satellite.
- High availability is part of its manufacturability. If it is very difficult to obtain then either large orders have to be placed long beforehand and stored if necessary, or risk long waiting periods that may cause delays in manufacturing the PCM devices.
- A low cost is obviously desirable to keep the CubeSat affordable. A major cost for CubeSats is the launch cost. This is thousands of dollars per kilogram to LEO. The main cost-goal would be to have cost increase of the PCM be less than the cost savings due to a lighter satellite.
- Compatibility: if the PCM is not compatible with the container then the container can fail and cause the PCM to leak out. This can cause it to stop working and can contaminate and corrode the satellite or other satellites in the vicinity.
- A low toxicity is advantageous as this reduces the risk for humans when handling it. If it were toxic then many handling and disposal procedures would increase difficulty and cost in manufacturing and testing the TSD.
- Hazardous characteristics are disadvantageous for similar reasons as toxicity. It would require all sorts of safety precautions which complicate and increase the cost of manufacturing and testing,
- Property data should be readily available and well documented because this allows for a properly designed TSD that will behave predictably.
- A high flash point means it will not suddenly combust at low temperatures, which would be a fire hazard requiring all sorts of safety precautions.

Table 3.2: Ideal spacecraft PCM properties [30]

Property or Characteristic	Desirable Value or Tendency
Heat of fusion	High
Thermal conductivity	High
Specific heat	High
Density	High
Volume change during melting	Low
Vapour pressure	Low
Melting and freezing behaviour	Dependable and reversible
Availability	Readily available
Cost	Low
Compatibility	Compatible with container and filler materials
Reversible Solid-to-Liquid Transition	High
Long Term Reliability During Repeated Cycling	High
Toxicity	Nontoxic
Hazardous behaviour	Not exhibited
Property data	Readily available and well documented
Flash Point	High
Coefficient of thermal expansion	Low
Surface tension	Low

- A low coefficient of thermal expansion is desirable for the same reason as low volume change during melting.
- A low surface tension is also desirable as this reduces the cavity size within a casing which can cause the PCM to behave unpredictably. The cavity size is reduced by having smaller bubbles form and allowing it to creep into smaller crevices. This also has a direct influence on the capillary effect of the material.

An overview of all the different types of PCMs and their properties relative to each other was made in the literature study preceding this thesis. The results of this can be seen in table 3.3. There are many specific designs of compatible PCMs and casings that would have advantageous properties for CubeSats. The eventual choice of paraffin wax was driven by its inherent chemical inertness, non-hazardousness, and wide choice of melting temperatures. From this table it seems that other PCMs like poly ethelyne glycol or water, but although their melting temperatures are within reasonable ranges for use on spacecraft, they are not good melting temperatures for the use case with a TXS radio and a batter pack as defined in section 2. Most importantly the goal was to keep the development costs low and paraffins are already proven to work. There are certain PCMs that perform better than paraffins in certain respects, but it is risky to develop completely new technologies for CubeSats due to the likelihood of unforeseen technical issues. It would be a better strategy to develop safe paraffin PCM systems and see if their performance is good enough for CubeSat applications. Only if performance is unsatisfactory should more complex solutions be developed. This will keep research and development costs low on these types of systems.

Commercially available PCMs will often be cheaper and more readily available than pure chemicals of a certain type. CubeSats have a general philosophy to use COTS (Commercial Off The Shelf) products. This is because all of the research and development costs have already been borne by companies that have had a long development time and a large budget and therefore will have a well tested product. On the other hand most commercially available PCMs are developed for the food or transportation industry or in architecture and not for spaceflight applications. So the commercially available PCMs might have an optimal ratio of specific materials that would make them ideal PCMs. But for safety and predictability of

Table 3.3: Trade off table PCM types (relative values green=high, yellow=medial, red=low, white=unknown)

PCM	Melting temp	Latent heat	Specific heat	Thermal conductivity	Density	Cost	Vapor pressure	Super cooling	Chemical stability	corrosive	Flammable	Toxicity	Volume Change
Paraffin	green	yellow	yellow	red	red	green	green	green	green	green	yellow	green	yellow
Fatty acids	green	yellow	yellow	red	red	yellow	yellow	green	green	yellow	red	green	yellow
Sugar alcohols	red	yellow	yellow	yellow	yellow	green	white	yellow	yellow	green	red	red	yellow
Esters	green	yellow	yellow	red	red	green	yellow	green	green	green	red	red	white
Poly (Ethelyne glycol)	yellow	red	yellow	red	red	green	green	green	green	green	green	green	white
Ionic liquids	green	green	green	green	green	red	green	white	green	red	white	yellow	green
Salt Hydrates	green	green	yellow	yellow	yellow	green	white	red	red *	red	white	yellow	green
Metallics	yellow	red	red	green	green	yellow	yellow	red	green	red	yellow	yellow	green
Water	red	green	green	yellow	red	green	red	yellow	green	green	green	green	red
Eutectic	green	green	white	white	yellow	white	white	white	red **	red	white	white	white

*Stratification

**Highly influenced by moisture

a system a pure chemical PCM was chosen.

Paraffin waxes are generally used for space applications, for instance the Apollo lunar rovers [32]. They have also been extensively tested by NASA for the Constellation program which can be seen in the following reference [33]. There are other PCMs that would have more favorable properties but have never been applied to spaceflight or have other attributes that make them more risky for space missions. But the fact that CubeSats are a niche market might explain why these PCMs might be useful even though they have not been used on other satellites before. Therefore if paraffins under-performs as a PCM TSD then it will be good to look at these alternatives.

Although the choice of paraffin as the CubeSat PCM has been made it is still useful to consider alternatives as certain applications might require a specific performance that paraffin PCMs are not capable of achieving. There are a number interesting possibilities, for instance a gallium PCM with a titanium casing. The gallium and titanium are chemically compatible, while other casing materials like aluminium or copper would slowly dissolve into the gallium [34]. The poorly conducting casing is a small price to pay for the large conductivity of the gallium. The added advantage of this is that the casing can have a very simple design as no extra filler material is required to increase the PCM conductivity as is required for most PCMs. The melting point ($29.76\ ^{\circ}C$) is excellent for most CubeSat applications. It has a relatively low latent heat of fusion, $\approx 80\frac{J}{g}$ which is about a quarter that of paraffin, but the advantage is that it has a high density, $\approx 5.9\frac{g}{cm^3}$ which is about 6.5 times larger than that of paraffin and the energy storage per volume is relatively high. Most CubeSat components are more volume constrained than weight constrained.

Other systems with custom designed PCMs, like ionic liquids or eutectics, can have superior properties to all other PCMs. In the literature study the large list of ionic liquids and eutectics were not researched for all their attributes (besides latent heat storage) as this could have been the subject of an entire research project on its own. But even then, these materials also tend to be corrosive and if leaked pose a risk to other subsystems and satellites in the vicinity. If these materials become mainstream in TSD for high tech components, then they would start to look very attractive for CubeSat applications.

3.2.2. Paraffin

Paraffin wax, also known as candle wax, was selected as the best choice for a PCM device on a CubeSat in the literature study preceding this thesis [35]. This is mainly due to its high latent heat capacity and its general non-hazardousness. Paraffins consist of hydrocarbon chains in the form of C_nH_{2n+2}. These different hydrocarbon lengths have different properties and melting points. While in most applications a mix of these hydrocarbons would be sufficient for the use case. The PCM device, which requires a narrow melting region, needs to use a specific chain length which has an optimal melting point for the specific CubeSat application.

The main advantages of paraffins over the other materials taken from the following references [34], [36], [31] and [32] are:

- they are not flammable at moderate temperatures ($< 100°C$)
- they are non-corrosive to metal, which is advantageous because metal has a high thermal conductivity and can easily transport the heat into the PCM.
- they are not expensive, depending on the purity but even the extremely pure ones are still affordable.
- They do not exhibit supercooling, so they have a predictable melting point.
- They have a wide range of melting temperatures, so a paraffin can be chosen that perfectly fits a specific application.
- They have a relatively small to medium phase change expansion.
- They have a low vapor pressure.
- They have a high wetting ability which makes them attach well to surfaces. This is advantageous as cavities won't form on the casing wall or filler materials.
- They are readily available.

The main disadvantages of paraffins over other materials are:

- They have low density and therefore require a relatively large volume.
- They have lower latent heat properties than other PCMs.
- They tend to chemically decompose at higher temperatures, which changes their properties when heated up too much.
- They have low thermal conductivity. (Although most PCMs have this problem).

A selection of other PCM types is shown in appendix A. These PCMs can be examined further if paraffins turn out to be insufficient for CubeSat applications. These choices will each come with its own unique properties and engineering difficulties to overcome.

3.2.3. Type of Paraffin

Another important choice for the design is which paraffin to use. The most important characteristic of the PCM for this application is its melting point. This characteristic will have a large influence on how the system will respond. As can be seen in figure 2.2 the temperature range of the Hiber CubeSat frame in orbit stays within $0 - 40°C$. This is fairly typical and is chosen as a reference temperature for CubeSat missions. Choosing the right temperature for the melting point can be tricky; it should not be too high or too low. If the goal of the PCM is to keep a certain subsystem below a maximum temperature, for instance $80°C$, the

Table 3.4: Paraffin family properties [36]

No. of carbon atoms	Melting point (°C)	Latent heat of fusion (kJ/kg)
14	5.5	228
15	10	205
16	16.7	237.1
17	21.7	213
18	28.0	244
19	32.0	222
20	36.7	246
21	40.2	200
22	44.0	249
23	47.5	232
24	50.6	255
25	49.4	238
26	56.3	256
27	58.8	236
28	61.6	253
29	63.4	240
30	65.4	251
31	68.0	242
32	69.5	170
33	73.9	268
34	75.9	269

PCM should not already be partially melted during regular operation of the satellite or the advantage of the latent heat could be largely lost due to the satellite's regular steady state temperature. Therefore a PCM should be selected with a melting temperature above around $35 - 40°C$. According to table 3.4 this includes every paraffin with equal or more than 20 carbon atoms. To maximize the cooling effect the lowest possible melting point should be taken. This is because the lower the melting temperature the more PCM can be melted before the subsystem overheats. This is due to the thermal resistance through the interface and the melted PCM itself. Ideally all of it will be melted before the subsystem overheats. To properly design a PCM system the energy absorbed above the melting temperature should be the same amount of energy released below the melting temperature. This is necessary because if a net amount of energy is added every thermal cycle then it will not completely solidify after every cycle therefore leaving less meltable material for the next cycle until the TSD has lost its latent heat storage capability. When looking at the subsystem temperature ranges in figure 2.12, the subsystems that are in most need of temperature control are the TXS and TRXVU radios. Eicosane ($C_{20}H_{42}$) with a melting temperature of 36.7 is the best fit for these subsystems, as this temperature is in the middle between the maximum and minimum temperatures. This is also a paraffin with a relatively high latent heat of fusion as can be seen in table 3.4. Other thermal properties of eicosane can be seen in table 3.5

The satellite frame also is subject to large temperature swings that could be controlled if needed. This would make hexadecane ($C_{16}H_{34}$) with a melting temperature of 16.7 $°C$ a good candidate. This would require a fairly large heat sink to absorb all the energy of the satellite; this is also not necessary as these temperature ranges are still within the operating temperature of the subsystem. This would also be a good PCM to use for a combined TSD for multiple subsystems. In this case the TXS radio and the batteries. This melting temperature would take energy from the TXS and transfer it to the batteries. Shifting the average temperature of the TXS down and the average temperature of the batteries up. Although this setup is more complex than just a single subsystem thermal control system and is therefore not the focus of this thesis. This thesis focuses on eicosane PCM to control the TXS temperature. If this is successful then this type of system would be a good follow-up research topic.

Table 3.5: Properties of eicosane [36]

	Solid (25 °C)	Liquid (50 °C)
Density ρ (kg/m^3)	910	769
Thermal conductivity k (W/m K)	0.423	0.146
Specific heat c_p (J/kg K)	1926	2400
Thermal expansion coefficient β (1/K)	N/A	8.161×10^{-4}
Reference temperature T_{ref} (°C)	N/A	36.4
Melting point T_m (°C)	36.4	
Latent heat L (kJ/kg)	248	

3.3. Properties of PCMs

In this section the properties of PCMs that are applicable for paraffins will be described. A more detailed description of different properties and engineering issues associated with a wide variety of PCMs can be found in the literature study [35].

3.3.1. Thermal Properties

The thermal properties of a PCM system have to do with how heat interacts with the PCM. Specifically, how much heat is absorbed and how easily heat travels through it. These properties determine how much is needed to absorb heat and how quickly this heat can be absorbed. It is important for a heat sink material to have a high sensible heat so that the material can absorb a large amount of heat without increasing its temperature excessively.

Because the purpose of the PCM is to absorb heat it is important to look at precisely how much heat it can actually absorb. This is the function of the mass of the PCM, the latent heat and the sensible heat multiplied by the operating temperature range of the system, as shown in equation 3.1:

$$\Delta Q = m \cdot (l + c_p \cdot \Delta T) \tag{3.1}$$

In this equation ΔQ is the change in energy in J, m is the mass of the PCM in kg, l is the latent heat of fusion in $\frac{J}{kg}$, c_p is the specific heat in $\frac{J}{kg \cdot K}$ and ΔT is the change in temperature in K.

In most cases the specific heat of the liquid and the solid phase are different. The total heat absorbed becomes as shown in equation 3.2:

$$\Delta Q = m \cdot (l + c_{ps} \cdot (T_m - T_{min}) + c_{pl} \cdot (T_{max} - T_m)) \tag{3.2}$$

In this equation ΔQ is the change in energy in J, m is the mass in kg, l is the latent heat of fusion in $\frac{J}{kg \cdot K}$, c_{ps} is the specific heat of the solid in $\frac{J}{kg \cdot K}$, c_{pl} is the specific heat of the liquid in $\frac{J}{kg \cdot K}$, T_m is the melting temperature of the PCM in K, T_{min} is the lower temperature in the temperature difference in K and T_{max} is the maximum temperature in the temperature difference in K.

In reality the specific heat of a material is also temperature dependent. This would complicate the equation as the specific heat would need to be expressed as a function of the temperature and then integrated over the temperature. The amount of energy absorbed by eicosane was measured in reference [37] and the results are shown in figure 3.3. In this figure the latent heat of fusion can clearly be seen.

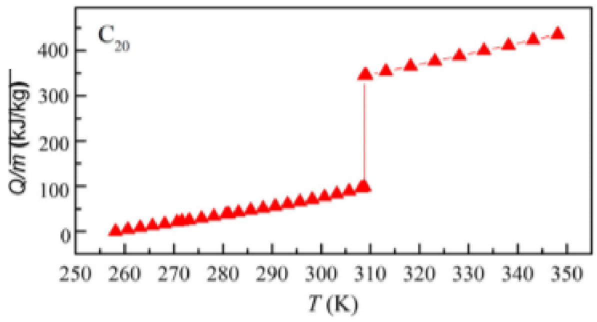

Figure 3.3: Total energy storage eicosane paraffin [37]

It is also important for the material to have a good thermal conductivity because if it is heated up quickly the material closest to the heat source will start to heat up more which can still cause the component to overheat without utilizing the full storage capacity of the heat sink. This is because when the PCM first heats up the outer layer will melt and insulate the rest of the PCM making it difficult to utilise all of the PCM. This causes a temperature overshoot over the melting temperature before all of it has melted. This overshoot will increase with input power and will decrease with thermal conductivity of the system. The steady state of a thermal gradient of the material through a system can be calculated with equation 3.3.

$$\frac{dT}{dx} = \frac{q}{-k\cdot} \tag{3.3}$$

In this equation q is the heat flow in $\frac{W}{m^2}$, k is the thermal conductivity in $\frac{W}{m\cdot K}$, T is the temperature in K and x is a distance in m.

The thermal conductivity is usually also temperature dependent. In figure 3.4 the measured temperature dependent thermal conductivity of eicosane can be seen. A large drop in thermal conductivity can be seen after the phase change of the material. This is a poor quality to have for a PCM if it needs to keep something from overheating. For this reason other materials that conduct better are often added to the PCM. Paraffins have a terrible thermal conductivity similar to insulators. Therefore they are often paired with metallic fins to increase the heat absorption speed.

3.3.2. Physical Properties

The physical properties of the PCM effect the mechanical design of the container. These determine the size of the casing and the amount of pressure it needs to be able to withstand.

For a regular heat sink the thermal expansion will be relatively small. If the system is attached to the satellite correctly this should not cause any mechanical issues to the system. The expansion of the phase change is relatively large. Depending on the temperature range of the PCM the regular thermal expansion can be significant.

The density is also an important factor in how useful a PCM is on a CubeSat. A CubeSat has very limited volume and therefore has limited room for a large heat sink. The volume of material that is required to store a certain amount of energy must be able to fit into the CubeSat while allowing space for other subsystems. Also, the required amount cannot be too heavy because of the weight limitations of a CubeSat. There is only a specific amount of weight budgeted for the TCS of a CubeSat. As shown in section 2.2.3 this is between 26.6-

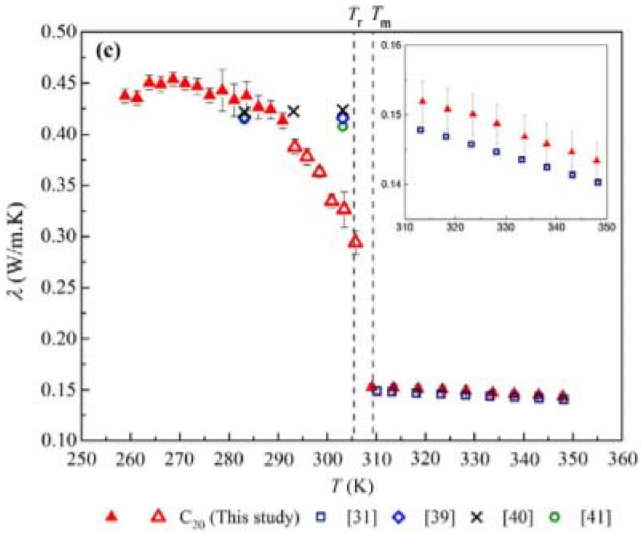

Figure 3.4: Thermal conductivity eicosane [37]

66.5 grams per CubeSat unit.

Paraffins are a low density PCM, but should be sufficient for most CubeSat applications depending on how much space is available. Back of the envelope calculations can be done using equation 3.4 with the properties of eicosane. If 10% of the volume of a CubeSat stack is used for eicosane then the amount of energy that can be stored is $0.1 \cdot \frac{1}{1000} \cdot 248000 * 769 \approx 19kJ$. This is double of what is required for the TXS use case.

$$\Delta Q = V \cdot l \cdot \rho \tag{3.4}$$

In this equation ΔQ is the change in energy in J, l is the latent heat of fusion of the PCM $\frac{J}{kg \cdot K}$, ρ is the density of the PCM in $\frac{kg}{m^3}$ and V is the volume of space available for the PCM in m^3.

The density of a material is also temperature dependent. The measured density of eicosane with respect to temperature was measured in reference [37] and the results are shown in figure 3.5. Also, the phase change of most PCMs causes a volumetric expansion. For eicosane the expansion can be determined from table 3.5, it increases 18.34% in volume between 25 $^\circ C$ and 50 $^\circ C$. This expansion is quite large for PCMs and consideration of this will have to be taken into account when designing a container for this PCM.

Another important attribute is the vapor pressure. A PCM in a solid or liquid state within a closed system will have an equilibrium vapor pressure. This pressure will be exerted onto the container of the system. To be able to contain the PCM the container needs to be able to withstand this pressure, or the container will leak or deform. PCMs with a higher vapor pressure will need a stronger and therefore heavier container. So it's best to choose a PCM with a low vapor pressure. The vapor pressure of eicosane at low temperatures is almost negligible about $6.16 \cdot 10^{-4} Pa$, which is extremely low. As the temperature increases the vapor pressure increases but it is still very low in the temperature ranges expected in the CubeSat use case. Once the temperature reaches 70.85 $^\circ C$ the vapor pressure reaches 0.407 Pa [38].

3.3.3. Chemical Properties

Another important attribute is the chemical stability of the PCM, due to heat changes and stresses or other external factors. Its chemical properties can change and thereby alter the storage capability or the phase change temperature. Paraffins are stable to up to 500 $^\circ C$

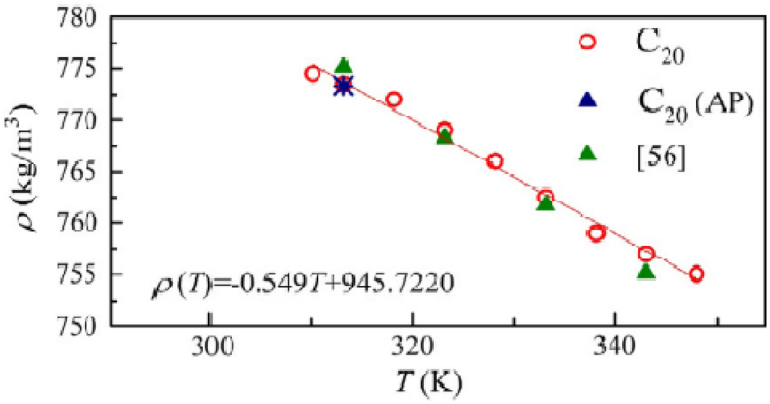

Figure 3.5: Density of eicosane with respect to temperature [37]

according to reference [36].

The material needs to be compatible with the casing and maybe even the rest of the satellite in case of leakage. Paraffins have a softening affect on plastics but they are chemically inert to metals according to reference [36].

Other factors to consider are the toxicity and combustibility of the material. If this is hazardous to people then the PCM might be difficult to handle thus driving up the cost. Although paraffins are generally considered non-toxic, it is considered dangerous if it enters the airways, and if ingested it can be fatal. [39]

Paraffins have a high flash point (>110 °C)[40] so if it is heated up to 110 $^{\circ}C$ it will be flammable in air. If there is a fire it will ignite in the presence of oxygen. This temperature is high enough that under normal circumstances this should not occur.

3.3.4. Kinetic Properties

The kinetic behaviour can also play an important role in the choice of PCM. The effects of super cooling for instance can be a nuisance. This is where materials exceed their phase change temperature without changing phase. This is because an energy gap to start the phase change reaction is required. If this initial energy gap is not bridged the material can keep on cooling and not change phase at all, thereby decreasing the amount of heat that can be absorbed. The initial energy gap is the energy that is required to form an initial nucleus. The surface of this nucleus has a potential energy and if this energy is not bridged, it will not form. Once the initial nucleus is created the crystal can easily grow and change the phase of the entire material. This is an advantage of using paraffins as they do not exhibit supercooling behaviours. [36]

For kinetic properties he range of the melting temperature is important. A small melting range has the advantage of utilizing the full latent heat storage potential over a small temperature range. If the temperature range is too large then some of the latent heat storage potential will fall outside of the operating temperature of the satellite. This is very sharp when materials have a crystal structure and are made up of only one material. If a PCM is an alloy made up of multiple materials it hill have a less precise melting temperature, or it can even have multiple melting temperatures. Amorphous structures also often have a larger melting range [34]. The melting point of eicosane is considered to be 36.7 $^{\circ}C$, but a melting range is taken around this temperature, these ranges are usually around 3$^{\circ}K$ [37].

3.3.5. Economic Properties

Finally there are economic considerations for the satellite. Is the material abundant and readily available? If the material is particularly difficult to acquire it may not be a viable solution. The difficulty can increase the delivery time and increase the cost of the system due to the delay.

How much does it cost? The added value of the PCM is that it can simplify the whole satellite system and thereby lower the cost. But if the material is too expensive it might be cheaper to use an alternative TCS. The launch costs are also an important factor a CubeSat mission. The difference between a 3U and a 6U CubeSat launch price can be around \$250,000, which amounts to a price of \$83.33 per gram. Therefore the price of the PCM would be justified if it is below the mass increase costs of using a heat sink. With an estimated mass of around 30 grams for the TXS use case, also taking into account that an equivalent storage capacity aluminium heat sink over a temperature range of $20°C$ would weigh about 415 grams, the cost saved by using a PCM would be in the range of \$32,000. Of course these are just estimated and idealized costs and would be different in reality. But it shows the general trend of how PCMs can be very cost beneficial. To stay at the low end of this range the price limit should be about $€1,000$. CubeSat components prices tend to be in the range of about $€1,000 - €100,000$. grams of PCM this puts the maximum price of the PCM at $\approx \frac{€3{,}333}{kg}$

Technical grade paraffins have very low cost compared to the laboratory grade. Technical paraffins are less pure and therefore have less latent heat capacity than more pure paraffins of ≈ 99%. For instance 6106 is a technical grade paraffin which has a melting point of 42-$44°C$ and a latent heat of 189 $\frac{j}{g}$ [36], whereas laboratory grade paraffins of that melting range all have latent heat of $> 230\frac{j}{g}$ as can be seen in 3.4. Using technical grade paraffins therefore would only increase the required PCM mass for the TXS use case by about 10 grams. This is very advantageous when large amounts of PCM are required, but for CubeSats the extra cost of having a high purity paraffin is relatively low compared to the price limit of the TSD. The exact price depends on the vendors and the bulk in which the material is bought. The eicosane used in this thesis costs $\approx \frac{\$600}{kg}$. If this turns out to be difficult to acquire or if it turns out to be a major cost point then it would be worth switching to a technical grade paraffin as this would decrease the cost.

4

PCM TSD design considerations

Once the right PCM has been chosen, the rest of the system must be designed accordingly. Every PCM has a unique combination of advantages and disadvantages. This section is tailored to the attributes of paraffin wax as a PCM. The design could be used with different PCMs but special considerations will have to be taken into account for this particular PCM. Figure 4.1 shows the working principles of a PCM system. The specific heat loads and design requirements for a system greatly depend on the specific use case. This section will show the different system requirements and design choices to make an effective TSD for a general CubeSat application. The major design choices for this system are:

- The attachment and interface of the TSD to the CubeSat
- The TSD casing material
- the TSD manufacturing method
- The means to fill and properly seal the PCM into the casing
- How to effectively transfer the heat from the heat source into the PCM

4.1. CubeSat TSD Interface

A CubeSat is designed from modular cubes. This means that the different frames of the CubeSats will have similar attachment points. To make the design as versatile as possible, as many configurations and attachment points as possible should be built into the design. The cube frame consists of an aluminium frame and ribs; running through the frame are

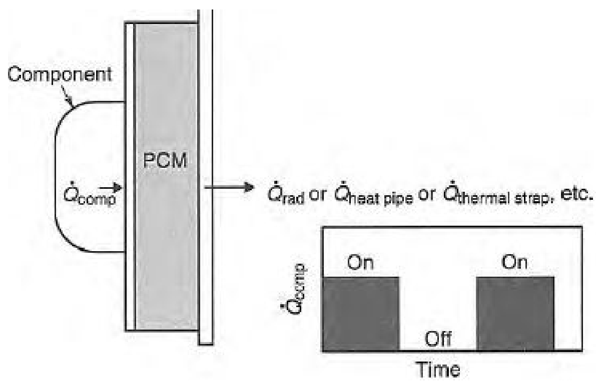

Figure 4.1: PCM TES Working principle

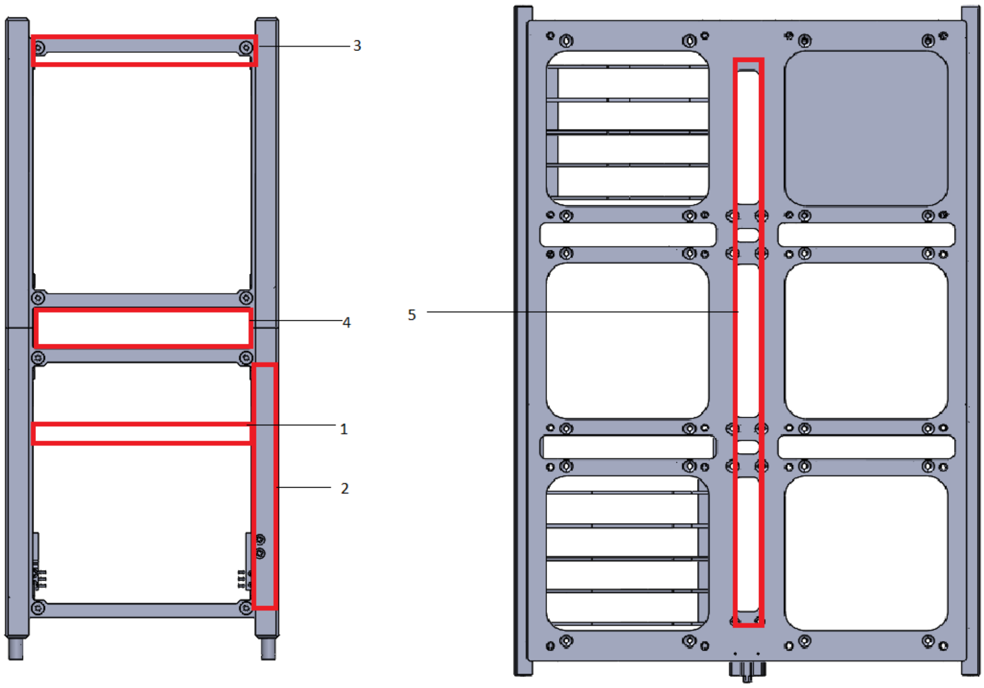

Figure 4.2: Possible locations for the PCM TSD on a 2U and 6U ISIS CubeSat frames [41]

steel rods to which the PCBs are attached. Also attached to the aluminium frame are aluminium panels that cover the satellite, the solar panels are often attached to these panels.

The TSD would ideally be able to be attached to any CubeSat in multiple different configurations. All CubeSats frames have the steel central rods and are therefore a perfect attachment for the TSD. Also the frame of the 1U, 2U and 3U CubeSats are similar and have similar attachment points on the sides, top and bottom where the device could be attached instead of panels. The 6U has a different frame design so either separate attachment methods have to be designed for the 6u CubeSat. Although the steel rods int he centre can still be used on this frame.

The TSD should try to use as much volume as possible (to maximize energy storage capabilities) without using space that would be required for other subsystems. This will give the TSD a the square shape of the CubeSat. There are multiple spaces where the TSD could be placed. These places are listed below and correlate to the places highlighted in figure 4.2

- (1) In the area between the PCBs.
- (2) In the area between the side panels and the PCBs. Or instead of a side panel.
- (3) At the top or bottom of the CubeSat.
- (4) In the area between stacks.
- (5) For 6u CubeSats there is an even larger inter-stack space between the 2 3u stacks.

Low density paraffins take up larger amount of CubeSat volume then a higher density PCM would. It is difficult to set constraints on volumes as they are mission dependent. The larger the CubeSat the more volume is available for these paraffins. Although reasonable limits should be set, section 3.3.2 calculated a storage volume of 10% of a 1U CubeSat. This estimate is oversized for the use case of the TXS which would only require around 30 grams of

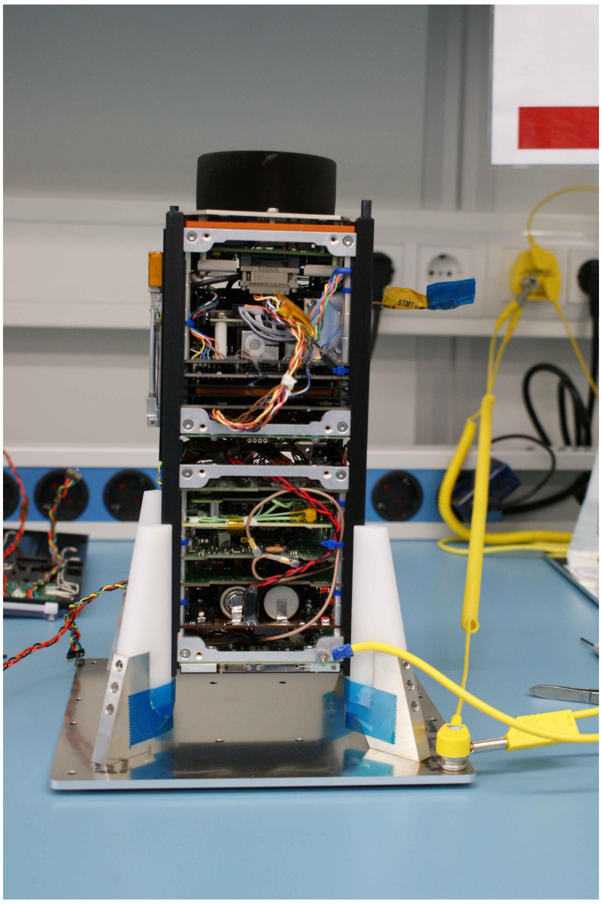

Figure 4.3: Precursor to the QB50 satellites by ISIS [8], with harnessing exposed

eicosane (although if higher storage capabilities are needed then these larger volumes could be required). This does not take into account the volume that the casing adds. The casing is usually about half the mass of the TSD, although it is also usually made of metals which are dense. Therefore 10% volume capacity for the TSD per unit of a CubeSat seems like a reasonable upper limit to set for the TSD.

In order to attach to the steel rods, the TSD would have holes for the steel rods to pass through. Spacers (usually aluminium) would be used to keep the TSD positioned correctly along the rods. If the device is attached to the frame then the attachment points that the frame uses for the side panels could be used. This would alleviate the need for extra separate attachment points on the CubeSat frame.

Placement in the area between the panels and the PCBs would not be ideal. There is very little space as the PCBs generally already come very close to the side panels, and this space is usually used for the routing harness as well. This can clearly be seen in figure 4.3. The figure also shows just how completely filled a CubeSat is and how its precious volume is maximally utilized. The possibilities would be to keep the device very thin, to cut a chunk out of the PCBs to leave space for the device, or to machine grooves into the device to allow space for the PCBs. This would greatly complicate the entire TSD design. Given the multiple alternatives this does not seem to be the best solution, and it is recommended this configuration be avoided.

For the area between the stacks (number 4 & 5) there are larger spaces that could be effectively utilized by this device. Current CubeSat designs often use this space for a variety of needs such as wiring or other subsystems. But relatively small design changes could free up

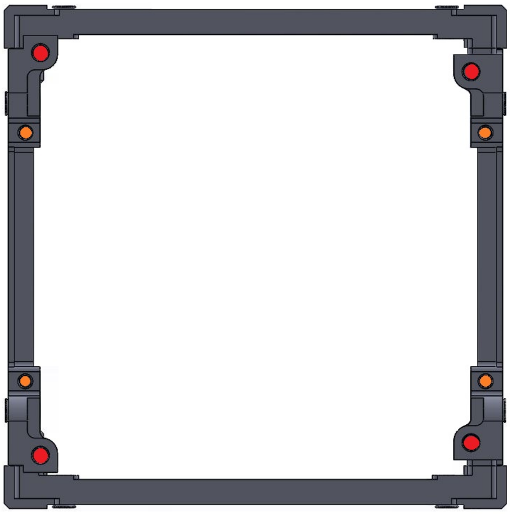

Figure 4.4: Connector holes, red = steel rod connector holes, orange = top frame connector holes

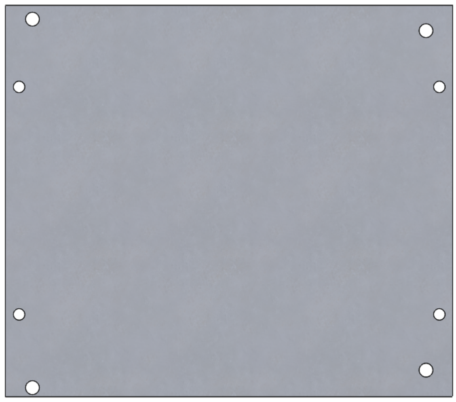

Figure 4.5: Casing connector holes

these large spaces for the PCM device.

The CubeSat frame experiences large temperature swings due to large heat fluxes, but the frame has a large operating temperature range and therefore is not in much need of extra thermal control. To avoid using all the latent heat storage capabilities of the TSD in regulating the temperature of the frame and everything attached to it, leaving nothing for the more critical components, the casing should be thermally connected to the components that have the most need thermal control. This favours the centre steel rod attachments as they do not conduct heat as well as the aluminium frame. The threaded profile of the steel rods also further reduces the possible contact area to the TSD. The main way heat will transfer is through the highly conductive aluminium spacers that are in contact with the TSD around the steel rods. Also Polyether Ether Ketone (PEEK) spacers or nuts can be used to make sure the TSD is thermally isolated from the aluminium spacers. If the TSD is attached to the frame then in theory PEEK washers could be used to thermally isolate it.

Ideally the first design of the prototype would be as versatile as possible and have it capable of attaching in multiple configurations as this would allow the TSD to be feasible for a wider range of CubeSat missions. Ignoring the side panels and the 6U location for the TSD, leaves two mounting hole schemes for three possible configurations. These configurations are 1, 3 and 4 from figure 4.2. The mounting hole locations are shown in figure 4.4.

4.2. Casing

The first design choice is the casing, which needs to be chemically compatible with the PCM so that it does not erode and allow the PCM to leak out. For paraffins this excludes plastic casings as discussed in in reference [42]. The casing also needs to be able to accommodate the expansion of the PCM. This can be done by leaving extra room in the casing for the PCM, or by letting the casing flex along with the expanding PCM. Of course the casing also needs to be able to transport the heat from the outside of the casing to the PCM/filler material. The material selection plays an important role in how well this works.

4.2.1. Pressure Vessel

The casing is basically a pressure vessel. It needs to be able to withstand the pressure difference between the inside and the outside of the casing while at atmospheric pressure or in a vacuum. The pressure on the inside of the casing once filled will always be at least the vapor pressure of the PCM because of out-gassing of the PCM. The vapor pressure of solid eicosane

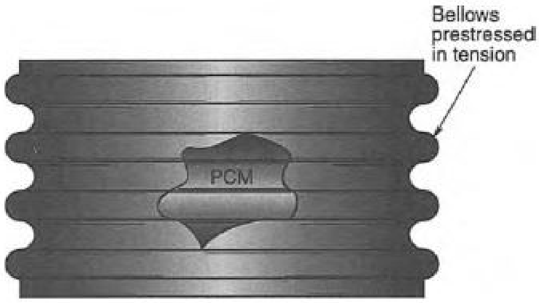

Figure 4.6: Schematic of a bellow design [11]

this is negligible as mentioned in section 3, when liquid at higher temperatures this becomes slightly more relevant (Eicosane at 70 $°C$ has a vapor pressure of 244 Pa). To avoid pockets of air inside the casing a vacuum could be created in the casing before filling it, then it would need to be able to withstand one atmospheric pressure while on the ground. There is also the expansion of the material due to its phase change reaction, this expansion causes the liquid to expand the pressure vessel which can create extremely high pressures due to the poor compressibility of most liquids. This expansion could also cause vapor bubbles inside the casing to be compressed, this can also cause pressure spikes in the casing and should therefore considered when designing the casing. The easiest design would be to make a stiff casing that is strong enough to withstand the change in pressure within, while leaving some space inside to allow for the expansion of the PCM. One solution to minimize mass and reduce the stresses on the casing would be to make it flexible. This could just be the flexing of the walls or could be done with the use of bellows. An example of a bellow can be seen in figure 4.6. These solutions would create less stress on the casing and can therefore be more lightweight. For a design with a bellow, a bellow with the correct dimensions for a CubeSat would need to be found or would need to be custom made. Also the large expansion would be difficult in the relatively short and wide design required for a CubeSat. The bellows would need to be very small for enough of them to fit next to each other such a short distance. Attaching a thin walled bellow to a heat transfer plate while keeping the casing sealed would be difficult. Therefore if the mass budget of the CubeSat allows a stiff casing, this would be the safer and easier choice.

For a stiff design the casing needs to be able to withstand the atmospheric pressure and a vacuum before it is put in orbit. There are also cyclical stresses the casing will experience caused by the phase change reaction and accompanying expansion and contraction cycles which can cause fatigue in the casing. The casing needs to be able to withstand the cyclical pressure cycles for the duration of the CubeSat mission. Aluminium for instance is known to experience high cycle fatigue. If the satellite has an expansion cycle once every orbit with a 90 minute orbit, the satellite will make 5844 thermal cycles a year. If the satellite is in service for 3 years, then the maximum stress experienced should be below the fatigue stress calculated at 17488 cycles (order of magnitude of $2 \cdot 10^4$). This can be mitigated, as is often done for the CubeSat frame itself, by using work hardened high strength aluminium or by decreasing the stresses experienced by the aluminium through a properly designed structure.

Often for extra safety and redundancy the casing is designed to withstand larger pressures. According to reference [11], common practice is to assume that air at atmospheric pressure is trapped in the casing while the PCM is in a solid state. This would cause the pressure within the casing to be even larger when the PCM expands. Therefore it is also prudent to leave extra space in case this happens.

4.2.2. Materials

A summary of different material choices and their properties can be seen in table 4.1. The materials with the best thermal conductivity are copper and aluminium; these will spread the heat properly throughout the system. Heat can travel easily through the casing and also act as a heat spreader to reduce hotspots. If the casing is made out of the same material as the filler then this choice will also determine how well the material disperses the heat throughout the paraffin.

Table 4.1: Casing material properties [43]

Material	Thermal conductivity $\frac{W}{m \cdot K}$	Density $\frac{g}{cm^3}$	fatigue strength resistance	Price $\frac{euro}{kg}$	Strength to weight ratio $\frac{kN \cdot m}{kg}$
Aluminium	205	2.7	+-	1.8-2.18	115
Stainless steel	14.4	7.85	+	0.63-0.68	63.1
Copper	385	8.96	+	4.8-5.8	24.7
Titanium	17	4.5	++	11-12.5	260
Carbon fibre	up to 180 in direction of fibres	1.27-1.29	+-	6.9-7.72	4300

Building the casing in a strong shape makes it possible to create a strong and stiff design without making it too heavy. It is good practice to keep components as light as possible. The design should be stiff because the phase change reaction will cause the casing to bulge outward, and these elastic deformations can create difficulties for alignments within the CubeSat. The main problem with large elastic deformations is that they occur every thermal cycle and can therefore lead to high cycle fatigue. Therefore the ideal casing strength-wise would be a casing with a high strength to weight ratio while also having a high fatigue strength resistance. Combining these two criteria, titanium seems like the best choice although it's low thermal conductivity makes it less ideal. Carbon fibre has the best strength to weight ratio but can become brittle at low temperatures and can therefore easily experience fatigue. Aluminium also is known for failing due to fatigue, and while its strength to weight ratio is good it is not as good as titanium or carbon fibre. This is mostly because aluminium is very light and therefore a lot of material can be used for the same mass. Copper experiences less fatigue then aluminium but the strength to weight ratio is much lower. Higher strength and stiffness copper alloys can be used but these alloys have lower thermal conductivity which makes them less attractive than aluminium. Cold forged copper is stiffer and harder than aluminium, but is still dense and expensive.

Carbon fibre and titanium are prohibitively expensive, and also difficult to manufacture. Carbon fibre requires moulds to be made and needs to be vacuum packed and baked in an oven. This is often very labour intensive and can drive up the cost. Titanium and copper are usually considered difficult to machine as well and both require specialised tools and craftsmanship. Being able to seal off the casing is an important choice in manufacturing difficulty as well. The best seals are usually done by welding brazing or soldering. Steel and titanium are the simplest to weld. Copper is difficult because of its high thermal conductivity causes the heat to spread quickly throughout the material. Aluminium is difficult to weld because of its high conductivity and low melting temperature. A copper or aluminium casing could still be soldered or brazed. Although the welding, brazing and soldering could possibly be avoided all together by using bolted connection with rubber O-ring filaments to seal the casing.

Cost definitely favours aluminium and steel, and these are also the most common metals to machine making them the go-to choice for most projects. Combining all these attributes for this casing high strength aluminium was chosen. This is because the relatively high thermal conductivity and strength to weight ratio. The high strength aluminium increases the fatigue strength of the material and allows for less aluminium to be used. The higher strength does increase the cost however. A material that has good thermal conductivity, high strength to weight ratio and a high cycle endurance is high strength aluminium. 6082 T6 Aluminium is a high strength aluminium alloy. Its properties are:

- Yield Strength: 240-280 MPa
- Thermal Conductivity: 169-175 $\frac{W}{m \cdot K}$
- Density: 2670-2730: $\frac{kg}{m^3}$ [43]
- its fatigue strength is about 150 MPa [43] (60 MPa for 6063 0 at $2 \cdot 10^4$ cycles).

4.2.3. Manufacturing

This section will focus on how the casing prototype and eventual design will be manufactured. The easiest solution would be to modify a commercial off the shelf casing. Although off the shelf casings are unlikely to have the right dimensions or properties for use on a CubeSat. These off the shelf casings could be modified to be used on a CubeSat, but if the casing requires too much modification it is necessary to manufacture it from scratch.

The casing needs to be completely sealed, therefore the casing should be made out of one solid piece where possible, with a cavity to contain the PCM left inside. The main manufacturing methods for creating a part out of a single piece of aluminium are: machining it out of a single block of aluminium; or printing the casing out with a 3D metal printer. Another simple way to produce a casing of this shape is by cutting aluminium plate and assembling the casing out of multiple parts, which would require the casing to be welded, soldered, brazed, or clamped together with a gasket in between. These plates can be laser- or water-cut to cheaply create complex shapes. A casing made out of multiple pieces can become complicated designs that could leave multiple possible locations where leaks could occur. Therefore it would be better to make the casing out of as few parts as possible. A property of the 6082 T6 aluminium is that it is work hardened to increase its strength. If the aluminium is heated up too much it will lose its strength from work-hardening. This makes welding, printing and laser-cutting less attractive a solution for this application, because more material/mass will be required to create a casing of the same strength.

3D metal printing has many advantages. The casing can easily be made in any shape, with any type of filler material directly connected to the base plate. Printed metal is basically one large weld and therefore does not have the T6 work-hardening property. Complex shapes can be printed and therefore the printed casing could possibly still be lighter with weaker metal by having a stronger shape. Printed metals often have poor surface finishes with respect to smoothness, this often requires an extra treatment after it's printed. Smooth surface finishes are required for making well fitting pieces in order to be able to assemble the casing. A smooth surface finish is also required for a good thermal contact between components, which is required for efficiently transporting the heat through the casing. A rough surface finish is an advantage for the inside of the casing by increasing the contact area and therefore the heat transfer between the casing and the PCM.

For this project it was chosen to machine the casing out of a single piece of aluminium, a simple method that keeps the material strength properties and does not require any extra treatments. This method is not capable of creating a lid on top of the casing in one piece, so this piece was manufactured separately and attached to be sealed. This design is explained in section 4.3.2. If the heat transfer to the PCM is not high enough then a 3D printed part is the next obvious choice.

4.3. Sealing the PCM

The need for contamination prevention is discussed in projects where paraffins are introduced to vacuum systems. An example of this can be seen in reference [44]. The PCM needs to be enclosed inside a sealed casing or when it melts it will deform and creep away from its

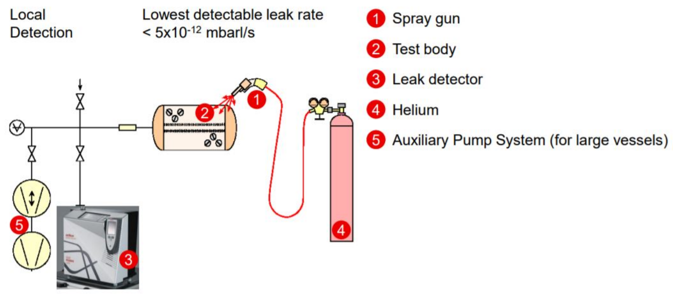

Figure 4.7: Vacuum helium leak test schematic [45]

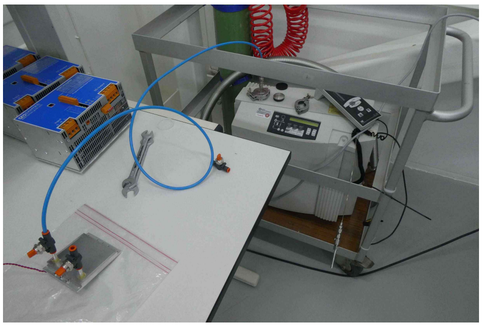

Figure 4.8: Vacuum helium leak test setup at the NLR

intended location. Also if it is not hermetically sealed then the PCM will out-gas and possibly contaminate other parts of the satellite. This section will describe how the casing needs to be filled and sealed.

4.3.1. Contamination

It is important that the casing is air tight because otherwise paraffin wax vapor will leak out. This would cause the satellite to lose a thermally stabilising component with which it was designed and could start overheating. The paraffin vapor could also condense onto and contaminate the rest of the satellite, for instance a lens in the main payload. Moreover during testing of the satellite all the highly sensitive testing facilities could be contaminated with wax, making it a very expensive test. Therefore it is a good idea to perform leak-tests to minimize the chance of the casing contaminating sensitive and expensive components.

Before the casing is filled there is an opportunity to test the seal of the casing. Afterwards it becomes difficult because putting paraffin into a vacuum without properly sealing it would contaminate the vacuum equipment. Therefore it is prudent to first prove that the casing will not leak paraffin when put into a vacuum environment. A helium leak-test is set up at the NLR to be able to test if the casing leaks helium. A schematic representation of the setup is shown in figure 4.7. This setup consists of a helium detector that is connected to a vacuum pump. The casing is pumped to a low pressure and helium is released around the casing. If the casing is helium airtight it will not detect any extra helium atoms. If a spike in helium is measured then the casing is not sealed hermetically for helium. Paraffin molecules are much smaller than helium molecules. Therefore if the casing is not helium airtight it does not necessarily mean that the casing is not paraffin air tight. But if it is helium airtight then we can assume the casing will also also not leak paraffin either. Other larger atoms could potentially be tested as well but this was the test we had available at the NLR facility. A picture of the NLR helium leak test setup with one of the prototypes can be seen in figure 4.8. The results of the casings had varying degrees of hermetic seals but none of them where considered to meet the threshold of helium airtight. This is considered by the lab-technicians to be about $10^{-8}\frac{mBar \cdot L}{s}$.

During heat cycle tests the mass of the casing can be monitored to determine if paraffin vapor has escaped the test setup during operation of the satellite. Either by inspecting the casing or by weighing it, it might be able to be determined if a leak has sprung. Finally with a more refined prototype more sensitive tests can be done with the paraffin wax in the casing.

4.3.2. Sealing off the Casing

A sealing lid is critical to the design of the PCM device. A schematic of the cross-section of the casing with a sealing lid is shown in figure 4.9. Critical structural points can be found

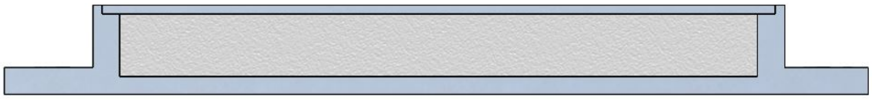

Figure 4.9: PCM casing

using simulation tools. The most likely structurally critical locations are along the lid of the device at the wall. Here the largest stresses and material deformations will occur. This is also where the lid needs to connect to the casing.

Cutting the lid out of an aluminium plate is the simplest way to manufacture the lid as it can be water- or laser-cut instead of having to be machined out like the casing. This was also done for the first prototype. After this proved to be difficult to seal the casing, it was later machined out so that a larger contact surface could be created to attach to the lid for this proved to hermetically seal the casing well enough as was later tested at the leak test setup described above.

There were multiple choices for how to seal the lid to the casing, the most obvious ones being:

- Glue
- Clamp with gasket
- Weld
- Braze

Gluing would appear to be the easiest and most obvious choice. However the surface area is very small and gluing works best with sheer stresses, and not the normal stresses that would occur sealing it this way. Also multiple heat cycles could damage the glue; especially at elevated temperatures glues are known to break down.

Clamping the lid on with a rubber gasket would work very well and would not be prone to fatigue. Difficulty in manufacturing would be to make a custom sized gasket that has the correct shape of the casing. Also the added grooves for the gasket and bolt holes for clamping would need to be machined into the casing and lid. This is all extra unnecessarily complex and can be avoided using other methods.

Welding and brazing should create very good seals. The main downside is that these are heated treatments that would heat up the casing to a high temperature. This could reduce the work hardening on the material, weakening the casing. Although new laser welding techniques can weld very small surface areas very quickly thereby minimizing the heat spreading out through the casing. The main disadvantage is that the weld would have to be at the most structurally critical locations.

Due to the heated cycles of the casing it was chosen for the first prototype to laser weld the lid onto the casing. This was thought to give the best seal for the flat plate lid design. When this design turned out not to be airtight enough the lid was machined out. This was required to be done with a Computer Numerical Control (CNC) milling machine to get tight tolerances and the rounded corners required for the design. The best way to seal this casing was by gluing, because the glued interface was not at the structural weak-point anymore. Also the glue has sheer stress instead of normal stress and is therefore a good choice for this sealing technique. These three different options are shown in figure 4.10.

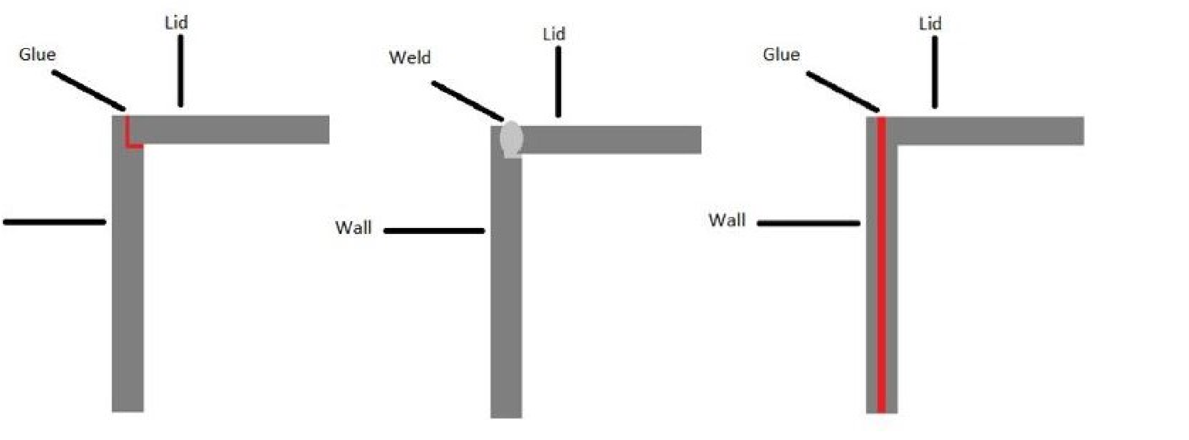

Figure 4.10: Different lid sealing techniques

Figure 4.11: Metalworks valves [46]

4.3.3. Filling the Casing with PCM

The filling method the container and having it be airtight afterwards is critical for the design. Careful consideration needs to be taken for how much PCM should be put into the container, how to avoid air pockets and how to seal it off afterwards. The easiest method of filling the casing would be to place the solid PCM inside of the casing and then seal it off, air getting trapped inside of the casing. Then when the PCM expands the trapped air will cause a pressure spike in the casing, which is exacerbated when the casing is placed in a vacuum.

The next obvious solution is to fill the casing while the PCM is melted. If the casing is completely filled and then sealed, the PCM will shrink when it solidifies and create a low pressure cavity inside the casing. This low pressure will equalise when the casing is placed into a vacuum again. The problem with this is that it may be difficult to seal the casing of an open container with a liquid inside, depending on the sealing method. The second problem is that because the casing is filled in an atmospheric environment, there could be bubbles in the PCM due to trapped air in the casing or filler material. These bubbles can create high pressure situations inside the casing, and can prevent the proper amount of PCM coming into the casing.

To solve these issues Metalworks valves and fill ports can be connected to a pump to create a vacuum in the casing. The Metalworks materials can be seen in figure 4.11. The valves can be attached to the tubes connected to the casing. These tubes can be attached to the lid either through welding, soldering or gluing. Because this is not a thermal or structurally

Figure 4.12: fill ports glued on, cross-section view

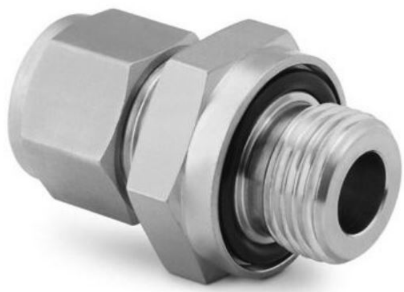

Figure 4.13: Threaded tube adapter with O-ring seal by Swagelok [47]

critical component gluing was first thought to be the easiest solution. A model showing how this was attached can be seen in figure 4.12. After testing however, this turned out to be a weak spot due to the large moment arms these fill ports create on the attachment interface. These could be strengthened by a welding instead of gluing.

For the second prototype it was chosen to use a thread and an O-ring. The O-ring is clamped around the periphery of the casing lid. The Swagelok component used for this fill port is shown in figure 4.13. This allows for a flexible joint at the weak spot at the base of the fill port. For the best seal the fill ports would be milled out of the same block of aluminium as the casing. But this would make for a relatively expensive casing lid compared to the Swagelok component which is relatively cheap, and was therefore the preferred option.

Given that the liquid PCM out-gasses and could contaminate the vacuum pump and Metalworks valves and tubing, given that it would be best to have two filling ports in the casing. The first one would be attached to the vacuum pump and be able to create a low pressure in the casing. The second would be used to fill the casing with liquid PCM. The vacuum on the inside would avoid air pockets being trapped inside the casing. The amount of PCM that enters the casing can be controlled by controlling the temperature of the PCM as it enters the casing. The casing is filled to the brim and shrinks when it solidifies. As an additional safety factor the PCM should be filled at a higher temperature than it would experience in space.

A schematic view of the filling setup can be seen in figure 4.14. Here is a step by step guide to the filling process:

- Heat up the casing, PCM and setup
- Open the vacuum pump valve
- Turn on the vacuum pump
- Close the vacuum pump valve
- Turn off the vacuum pump
- Fill a funnel with PCM connected to the closed valve
- Open the PCM valve
- Wait for the casing to fill up
- Close the PCM valve
- Pour leftover PCM out of the funnel

- Remove funnel from the PCM valve
- Let the setup cool down

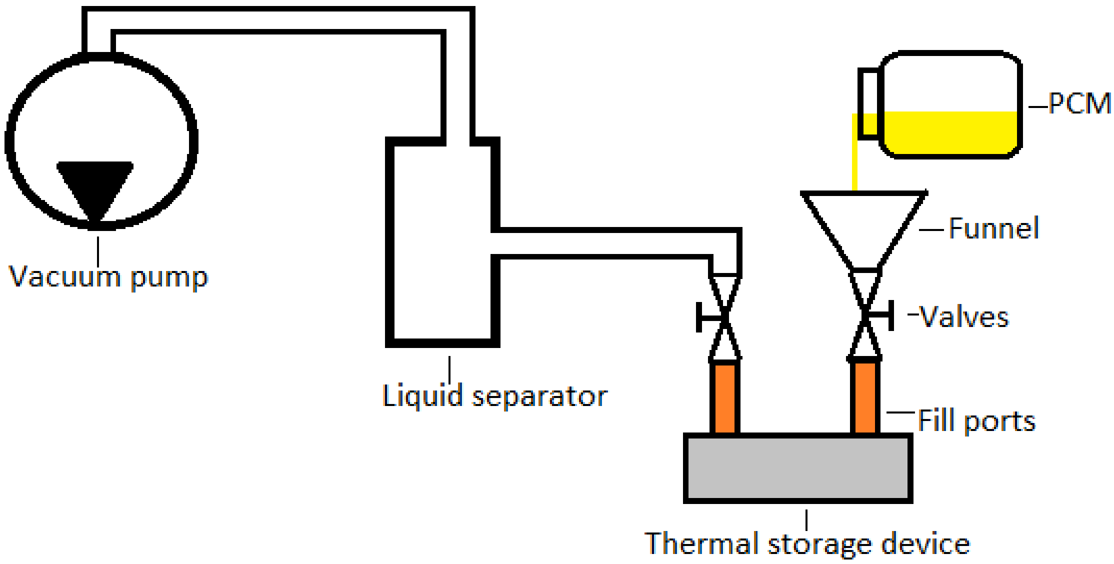

Figure 4.14: Schematic overview of the filling setup

During the filling process all of the Eicosane needs to kept liquid. All of the PCM, the casing and the tubing is warmed up in a thermal chamber. Hot air can be blown onto the casing and tubing to keep the entire system above a certain temperature throughout the filling process. (This was not done during this thesis project as the paraffin was at little risk of cooling off significantly in the time it takes to fill.)

After the casing is filled it needs to be sealed off. For the experiments the Metalworks valves can be left on the casing. For flight hardware the tubes would have to be cut short and sealed off, without losing the vacuum inside the casing. This can be done using a pinch sealing method, with the pinch enhanced by welding, brazing, soldering or gluing the end. An example of this can be seen in figure 4.15. The advantage of this is that the casing is not exposed to ambient air pressure. The main issue is that paraffin wax will still be on the inside of the tube. It is not clear whether this will actually seal the tube. If the tube is welded afterwards it will also be contaminated by the wax. A solution to this would be screw a plug into the thread in the lid, a gasket can be added to seal the plug. An example of this type of setup can be seen in figure 4.16. This temporarily exposes the casing to ambient pressures and can trap air inside the casing which could have problematic effects. Although this can be minimized by letting wax solidify near the openings, thereby using the wax to seal off most of the casing while the fill ports are removed. These plugs also have the advantage that they take up very little space in the height of the casing and thereby minimize the space the TSD takes up in the height of the CubeSat. This makes it easier to place other subsystems in this area. The fill ports stick out to a relatively large degree, but this could also be minimized by bending the fill ports down as flat as possible. This would have to be done with care as to not create new leaks in the casing.

Figure 4.15: Pinch and weld sealing

Figure 4.16: Example of plug with an o-ring seal [48]

4.3.4. Leak-Test Results

Leak-tests were done on the prototypes using the helium leak-tester shown in figure 4.8. The first prototype had the laser-cut and laser-welded lid. This casing wasn't very air tight. Using the vacuum pump the casing could be pumped down to 0.7 $mBar$. This pressure is too high to do any meaningful leak tests with the helium setup. It is not clear if this was due to the glued-on fill port or the laser-welded lid. After use it turned out to probably both be the case as wax residue was found both along the weld and along the base of the fill-port. The glued on fill port probably did not have a complete seal due to the small gluing area, or the seal could have come loose due to moments created on the fill port. Because of the relatively large moment arm these could have caused damage to the glued interface. The weld did not create a seal; this was because of some manufacturing issues when machining out the casing. Due to some mistakes in the milling the lid had to be ground down to fit inside the casing. These could have been slightly misaligned and could have caused the leak in the casing.

The second set of casings were also tested using the same setup. When testing the Swagelok valves they could be pumped down to $5 \cdot 10^{-3} mBar$. Next the casing itself was attached to the leak-test. After a thermal vacuum bake-out this casing could also be pumped down to $5 \cdot 10^{-3} mBar$. This implies that the casing can seal at least as well as the Swagelok components. The helium leak-rate was measured to be around $10^{-5} \frac{mBar \cdot L}{s}$. As mentioned in section true helium seal is considered to be $10^{-8} \frac{mBar \cdot L}{s}$. The casing therefore has a helium leak-rate 3 orders of magnitude more than that of a helium seal. This might be because of the at the fill-port or the glue of the lid. It could not be determined with this setup but it also does not matter as the casing does not need to be helium airtight but paraffin airtight. Therefore this test does not sufficiently prove that the casing is airtight enough to be flown. But it is airtight enough for a representative test prototype. A separate test needs to be developed to test if the casing would be paraffin airtight. Otherwise a helium airtight casing would need to be developed in future work. For final qualification a test should also be carried out after the casing has been filled and placed in a vacuum environment after multiple heat cycles. A test of this type will need to be done before the casing is ever used in sensitive vacuum chambers or before actual flight.

4.4. Heat Transfer

An important point to take into account while designing a thermal storage system is the need to reduce the thermal resistance between the heat source and the PCM. This section will describe the strategies that are used to maximize the effectiveness of the TSD by minimizing the thermal resistance to it. Thermal resistance through conductive heat transfer is created by conductive resistance through components and contact resistance between components.

4.4.1. Thermal Transportation

As shown in section 2.4 heat is transported to the PCM through conductive heat transfer. Steady state conductive heat transfer can be calculated using equation 4.1.

$$\dot{Q} = -\frac{\Delta T \cdot A \cdot k}{L} \tag{4.1}$$

In this equation $\dot{Q}$ is the heat transfer in $[W]$, ΔT is the temperature difference over the length of the component in $[K]$, A is the correctional area of the component (assumed to be consistent) in $[m^2]$, k is the thermal conductivity in $[\frac{W}{m \cdot K}]$ and L is the length of the components in $[m]$.

To minimize heat loss through conduction the cross-sectional area should be maximized and the heat transfer length should be minimized. Also material with a good thermal conduction should be used. Ideally the PCM device can be clamped directly onto the heat source. This minimizes the thermal path between the component and the PCM, and only leaves the thermal resistance through the heat source and TSD themselves. If this is not possible or if the TSD is used for multiple heat sources, then separate thermal transportation devices can be used such as the ones described in section 4.4.1. Obviously the longer the distance the longer the connecting piece and the higher the thermal resistance will be and and the less efficiently the PCM will work. Over short distances stiff connector pieces or thermal straps can be used. Over long distances it might be advantageous to use a heat pipe. An example of a heat pipe connector piece that can be made for a TSD in a CubeSat is shown in figure 4.17.

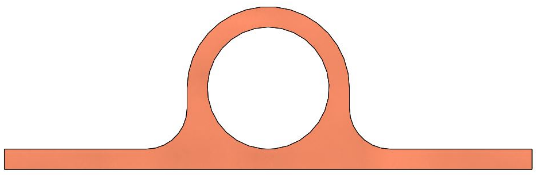

Figure 4.17: Heat-pipe connector piece, front view

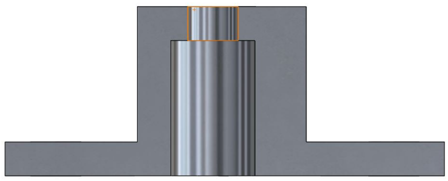

Figure 4.18: Connector piece cross-section view

The advantage of using a flex strap on a CubeSat is because if the thermal connection becomes a rigid connection, and the TSD is also connected to the CubeSat frame, then extra stresses can be introduced into the frame. This can make the frame vulnerable to the vibration loads experienced during launch, or to extra stresses due to differential thermal expansion. For prototypes in this thesis a stiff rod was sufficient given its simpler design and since these prototypes will not be rated on vibrations. These connecting pieces should be designed for bolting onto the TSD and the heat source. This can be done by adding flanges to the connector rods as on the heat-pipe connector piece in figure 4.17. Bolt holes can be drilled through these flanges. A cross-section view of the connector piece used for this project can be seen in figure 4.18.

As seen in section 2.2.1 the best material to use to transfer the heat is graphite. For simple cheap designs aluminium or copper would work fine. Calculations can be made using equation 4.1, on the temperature drops through thermal transportation devices. Estimations of the thermal loads and transportation distances experienced in CubeSats with an aluminium connector piece is good enough. If these thermal loads and therefore temperature drops become too large, then either thicker materials or more conductive materials can be used.

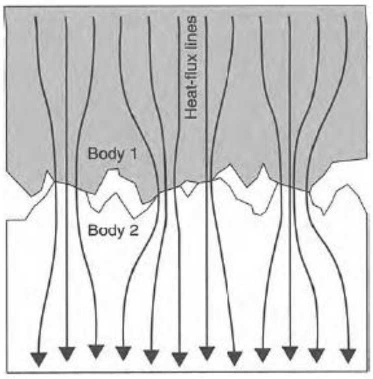

Figure 4.19: Microscopic contact resistance [11]

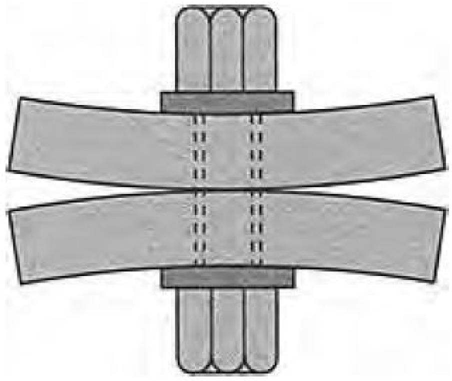

Figure 4.20: Bolted interface deformation [11]

4.4.2. Contact Resistance

The casing is very thin and made of highly conductive material, therefore the majority of the thermal resistance will come from contact resistance between components instead of through the material. Therefore aluminium would work fine and be simpler to manufacture. From experience at ISIS on CubeSat temperature control, the temperature drop through the material will be on the order of 1 K and between contact interfaces it can quickly become on the order of 10 K, contact resistance being a major determining factor in the performance of a PCM device as determined in reference [30]. The equation used for calculating the thermal contact resistance over an interface is shown in equation 4.2:

$$R = \frac{\Delta T}{q \cdot A} \tag{4.2}$$

A large part of the thermal resistance is created by there not being a continuous contact but rather having only microscopic contact points between components. This narrows the effective contact area and thereby increases the thermal resistance as shown in equation 4.2. A schematic representation of how this looks can be seen in figure 4.19. There are multiple strategies that can be used to minimise this effect. The first is to apply a force to the components so they are pressed together, causing microscopic plastic and elastic deformations on the surface imperfections and thereby increasing the contact area. Increasing the macroscopic contact area is also good because this increases the surface area and decreases the heat flux. This force is often applied using bolts to clamp plates together. This means the design will either be required to have a threaded hole so that a bolt can clamp the components together, or the components need to be clamped externally. Applying a clamping force for larger plates creates a good local contact area but can cause other parts of a plate to deform away from each other. A representation of this is shown in figure 4.20. Therefore it is imperative to apply the correct amount of torque to the specific bolted interfaces, but also to use multiple bolts spread out over the contact surface area to minimize thermal resistance between interfaces.

Another method of decreasing thermal resistance is to introduce a thermally conductive material between the components. This material should be soft enough to fill in the microscopic imperfections when clamped together thereby creating a continuous contact interface for the heat to travel through. The filling material can also be a liquid or a gel. It can also be an adhesive that hardens out and perfectly forms the materials together. The best solutions tend to be those where there is a continuous metal body through which the heat can conduct. This happens when the interfaces are welded, brazed or soldered. It is not always possible to weld, braze or solder and liquids or gels can become messy when components are assembled

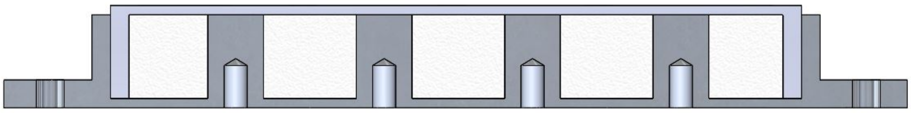

Figure 4.21: Cross section view of casing design with fin filler and threaded holes for bolted connections

and disassembled multiple times.

The solution used for this thesis is a thin graphite layer (Sigraflex) that is placed in between plates and are clamped together. The soft graphite deforms to the microscopic imperfections and the highly conductive graphite conveys the heat with very little thermal resistance over the contact area. One of the main issues with this is that the thin walled PCM casing is not suitable for having threaded holes inside of it. Therefore the casing will have to either have relatively thick walls to allow for threaded holes, or will have to have flanges that bolted connections can run through. Both of these have their disadvantages. The thick walled box increases thermal losses through the casing while adding a lot of mass to the TSD. The flanges clamp the heat source to the casing but not at locations close to the PCM. A solution to this problem was designed into the casing for this project by locally thickening the base plate to allow for threaded holes for bolted connections, they could be machined out, acting as fins to spread the heat throughout the PCM. A cross-section of this design is shown in figure 4.21.

4.5. Filler Material

Paraffins have a very low coefficient of thermal conductivity, comparable to the best insulators. This causes large thermal gradients in the TSD. If the heat flux is high enough, the heat source will overheat before the all the PCM has melted. The thermal gradient that will go through the casing can be calculated using equation 3.3. The area over which the heat can be spread is dictated by the shape of the CubeSat as shown in section 4.1. This allows for a surface area of 85x79 mm for the base plate of the TSD. As an example a power of 8 Watts is taken as representative heat load. Equation 4.3 shows how the heat flux can be calculated.

$$\frac{\dot{Q}}{A} = q \tag{4.3}$$

In this equation $\dot{Q}$ is the heat flow through a system in W, A is the surface area of the system in m^2 and q is the heat flux in $\frac{W}{m^2}$.

If the heat is spread out evenly and all goes into the PCM, by using equation 4.3 a heat flux of $1.191 \cdot 10^3 \frac{W}{m^2}$ is calculated. If we assume that the TSD is 10 mm thick we can calculate the temperature at the base plate before all the PCM has melted. Figure 4.22 shows a schematic of this setup of this calculation. This can be calculated by taking the thermal conductivity of liquid eicosane, $0.146 \frac{W}{m \cdot K}$, as seen in table 3.5. If these properties are filled into equation 3.3 the thermal gradient can be calculated: $\Delta T = -\frac{1.191 \cdot 10^3 \cdot 0.01}{0.146} = 81.6°C$. This thermal gradient is extremely high and it is therefore likely the component will have overheated before all the PCM has melted. If we assume that the PCM is heated from both sides, which is not unreasonable as the heat will travel through the casing to the other side, then the surface area has doubled thereby halving the heat flux also the distance through the PCM is halved. Using the same calculations as before this results in a thermal gradient of four times less $20.4°K$. Using eicosane wax this causes the hotplate to be 57.1 $°C$, after adding the contact resistance between the heat source and the TSD this will cause the TXS to have overheated before all the PCM has melted. Figure 4.23 shows the results of these calculations. This thermal gradient does still improve by adding the surface area of the sides of the casing and filler materials into the calculations. These equations quickly become complicated when cal-

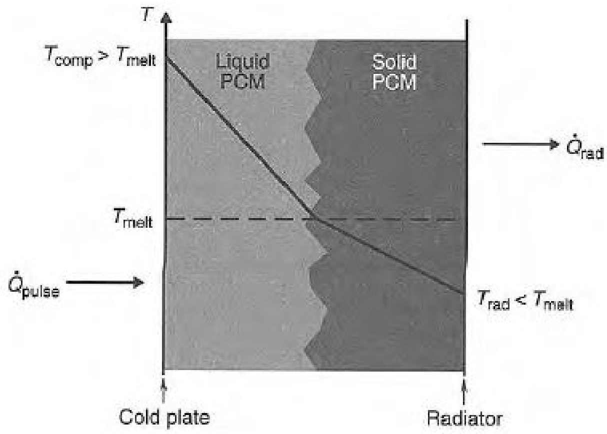

Figure 4.22: Schematic representation of thermal gradient through melting PCM [11]

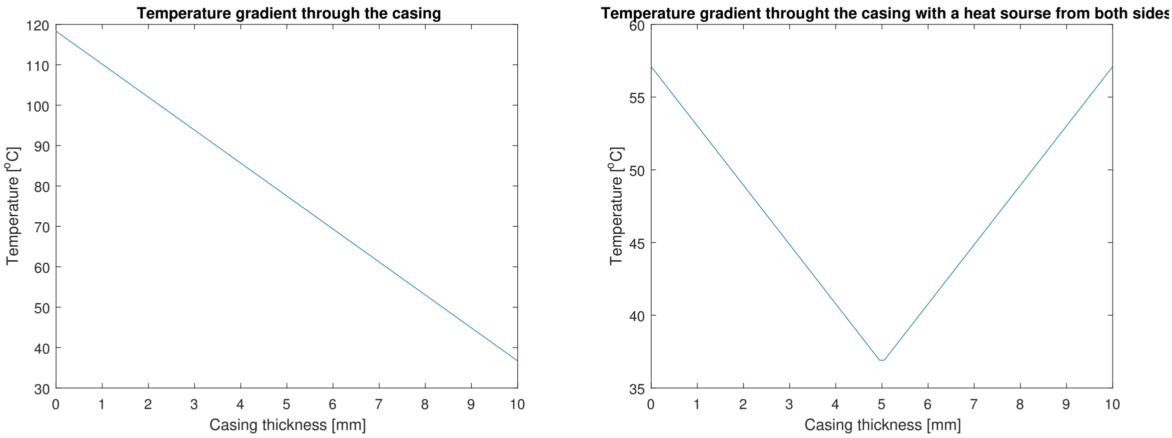

Figure 4.23: Temperature gradient through casing thickness with heat source from one side (Left), and from both sides (Right)

culating in multiple dimensions and can therefore more easily be done in numerical models. These models will be discussed in section 5.

The values calculated above are only valid for the power-source and casing dimensions taken in that example, but they offer an approximation of the gradients that are expected. To get the most performance from the PCM TSD filler material is added to the casing. Filler material is extra material is placed inside of the casing to distribute the heat throughout the PCM. This filler material will take up volume that could have been used for PCM thereby increasing the size and the weight of a TSD with the same storage capacity. There are multiple options for the shape and type of filler material. Here is a list of possible solutions that are explored in this thesis:

- Mixing
- Fins
- Lattices
- Honeycombs
- Foams
- Heat pipes

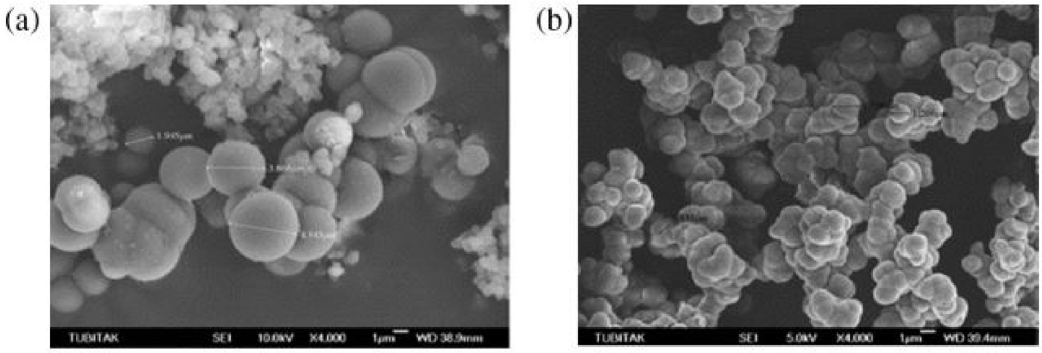

Figure 4.24: micro-encapsulated PCM [31] used in textile fabrication

The main goal of the filler material is to optimize the heat-flow from the heat source connected to the casing into the PCM. An important aspect in how well a filler material will work is to maximize the surface area to volume ratio of the interface between the filler and the PCM. Because of the insulating properties of paraffins, large pockets of PCM without any filler material should be avoided as much as possible because the heat will have difficulty penetrating to the centre leaving the pocket unused. Therefore it is also important for the PCM to spread out throughout the casing minimizing the sizes of these pockets. Also the thermal resistance through the filler should be kept to a minimum as this will decrease the amount of heat that can enter the PCM.

A large determining factor of how well a filler material will perform is the thermal resistance between the casing and the filler [34]. This is largely dependent on the type of materials used and how they are attached to the PCM casing. This is a similar case with similar solutions to the contact resistance problem discussed in section 4.4.2. The solutions with the least contact resistance is to have the filler material should be one continuous piece of conducting material that is either machined out of one piece or welded, brazed or soldered together.

4.5.1. Mixing

One of the more obvious solutions to the low thermal conductivity is to mix a material into the paraffin that has a better thermal conductivity. This can increase the thermal conductivity of the material but reduces the latent heat storage of the PCM. Mixing in highly conductive materials, for instance metal powders, does not work that well because the thermal path through the conductive material is not continuous as it is broken up by the paraffin. This makes the paraffin the dominant factor in the conductivity. This was determined in experiments where metal particles were added to paraffins as mentioned in reference [34]. Mixing is effectively used in alloyed metals and eutectic salt mixtures. Here the goal of mixing is not necessarily only to improve thermal conductance of the material but also to control other parameters like avoiding supercooling. Due to the difference in density of these mixed materials they can separate and lose their advantageous effect. In some applications micro-encapsulated paraffins are added to a more conductive medium. This allows for a continuous heat flow through the medium [36]. Figure 4.24 shows microscopic pictures of micro-encapsulated PCMs used for textile fabrics. This is the main use case for this technology in the current market but could be an interesting field for further development.

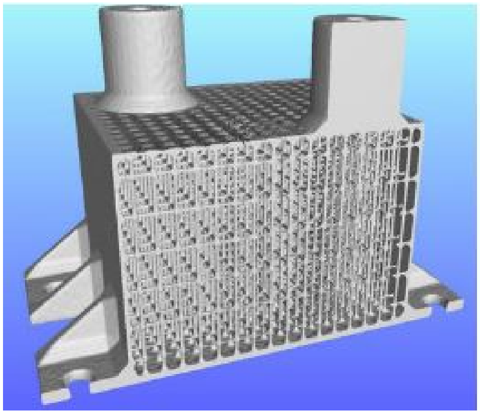

Figure 4.25: Example of a 3D printed lattice filler for a PCM device [50]

4.5.2. Fins

Metal fins are often used to cool heat sinks, the main use case being for microchips in computers. It is assumed that the Russian Venus modules had a PCM device that used aluminium fins as filler material. Metal fins are often the easiest choice for filler material as they are easier to connect to a base plate than for instance honeycomb [32]. This is because fins are easily welded or soldered to a container, minimizing the contact resistance between the container and the fins. To maximize the surface to volume ratio of a finned system the fins need to be thin and spaced closely together. The limits of this are usually determined by the manufacturing process. With new manufacturing methods like micro-machining and additive manufacturing much smaller and more efficient fin placings are possible [49]. With added manufacturing techniques many new, different optimized filler shapes are possible. An example of a finned system can be seen in figure 4.21.

4.5.3. Lattices and Honeycombs

Lattices and honeycombs have a large heritage in space due to their high strength to mass ratio. They display a similar heating behaviour as fins. Examples of these types of filler materials are shown in figures 4.25 and 4.26. But due to the difficulty of efficiently connecting the lattice to a base plate, fins are often chosen. With additive manufacturing methods lattice and honeycombs become interesting filler material options. The added advantage of lattices over fins is their increased structural integrity as they have more of a box shape than fins. Fins are usually only connected at one side which makes them easy to manufacture, but also vulnerable. Due to the shape of the lattice it is much stiffer in all directions. This could increase the durability of the filler material due to the expanding and contracting fluid within the PCM system. It could also have a secondary advantage to provide stability and stiffness to the casing.

4.5.4. Foams

Metallic foams can be added as a filler material for paraffins. This was researched in the following reference [52]. The results of the improved performance using a copper foam with a paraffin can be seen in figure 4.27. In theory foams have an extremely high surface area to volume ratio. Also the foam shape is highly interconnected within itself, and therefore creates short thermal paths through the material. This makes these materials a very interesting choice for filler materials in a TSD. Foam has the added advantage that it has a capillary effect on the PCM thereby pulling it into the foam. Foams can have a large range of porosities. The less porous a foam the more thermally conductive it is, but also the denser it is thereby leaving less room for PCM and decreasing the latent heat storage. Also the number of pores per volume plays a role in how well the heat is transferred from the foam to the PCM. It is also important to note that if the cell size of the foam becomes too small then they can become fragile, especially given the expanding and contracting nature of the PCM. If the cells break apart from each other the foam no longer has a continuous heat path and becomes a less effective heat exchanger.

Again the main difficulty with using foams is the question of how to attach them to a base plate. The best option for reducing contact resistance would be to weld the foam somehow. Friction welding seems like an obvious candidate for this type of material, for this type of thesis project this is prohibitively expensive. Soldering could be attempted but due to the capillary effect of the foam the solder will be absorbed into the foam, which makes it difficult to attach to a plate and reduces the amount of PCM that can be used for storage. The simplest option seems to be to glue it onto the casing base plate. This will increase the contact resistance and therefore decrease its effectiveness as previously mentioned in reference [30]. The degree of thermal resistance through the glue depends on the thickness of the glue layer, this is made as thin as possible but is still an unknown variable. The advantages of the foam might still outweigh other filler materials that have less thermal contact resistance.

A more state of the art solution is the use of expanded graphite as a carbon foam instead of metallic foam. The carbon foam has a very low mass and a high thermal conductivity. This is studied in article [53]. The micro-structure of this expanded graphite can be seen in figure 4.29. The mass fraction of the carbon foam will be low but the volume fraction will be high. The main difficulty with this type of filler material will be the thermal contact between the carbon and the casing. The carbon is also capable of being machined as well. This solution is an acceptable compromise if mass penalties need to be reduced.

4.5.5. Heat-Pipes

Heat-pipes are an excellent solution for achieving high thermal conductivity over long distances. Because of the small scale of the PCM system the increase in performance would be negligible. The difficulty of the heat-pipe is the dispersion into the PCM material. To maximize the performance of a PCM system with a heat-pipe the PCM could be wrapped in a thin film around the heat-pipe, possibly embedded within the heat-pipe wall. This thin layer can again be aided with a filler material to maximize the heat transfer. This is studied in this paper [54].

4.5.6. Conclusions on Filler Materials

From the literature it is not obvious that any specific type of filler material is clearly superior to the others. Some combination of filler materials and additives can be advantageous for

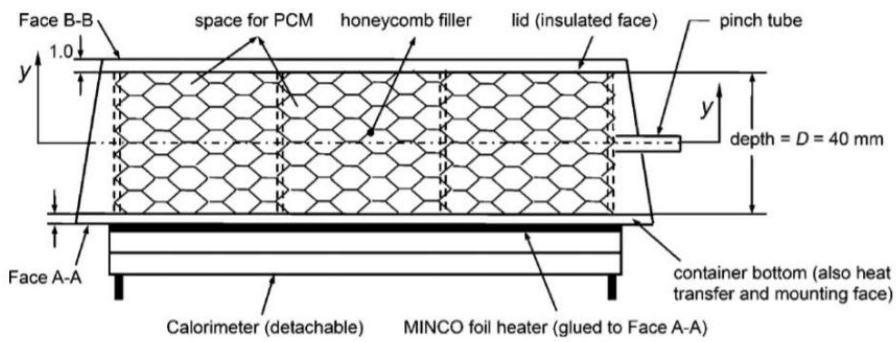

Figure 4.26: Honeycomb filler [51]

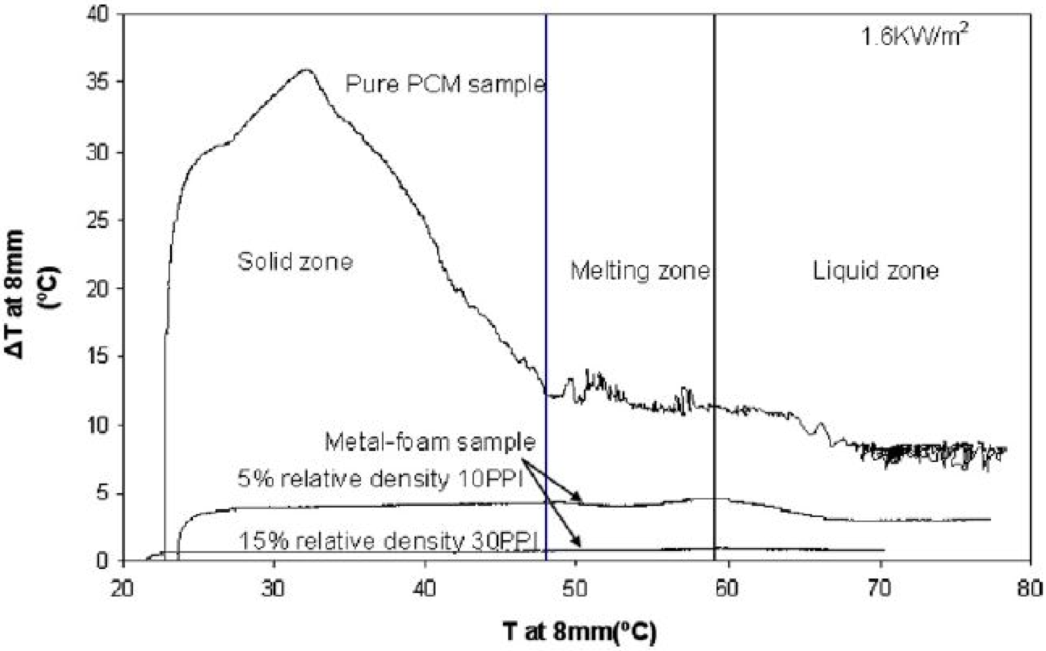

Figure 4.27: Performance of a copper foam with paraffin added and a power source of $1.6[kW/m^2]$ [52]

Figure 4.28: Example of copper foam with PCM [52]

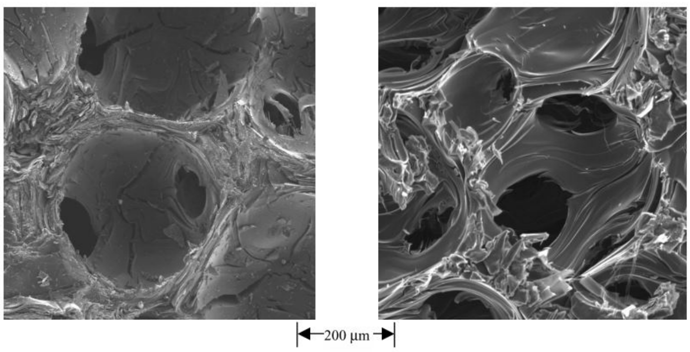

Figure 4.29: Structure of carbon foams [53]

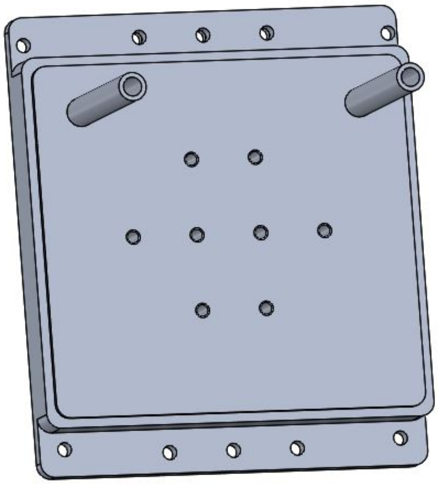

Figure 4.30: General TSD design concept

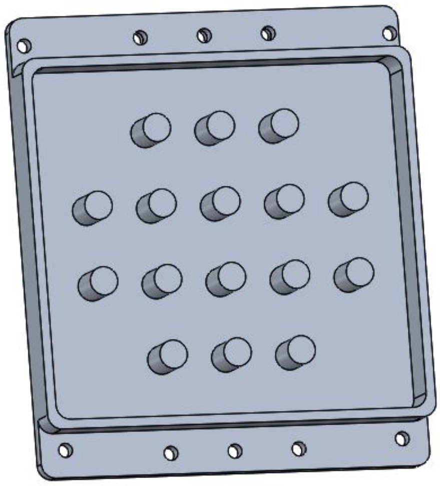

Figure 4.31: General TSD design concept with fin filler

specific design cases. For CubeSats it is not obvious that filler materials are even needed. However, due to the need for threaded holes to be able to clamp a heat source to the casing, fins are used in the casing prototype. As the prototype is to be machined out, filler material can be machined out as well avoiding the need of separately attaching them to the casing. For later designs it was also chosen to machine out a honeycomb prototype. Finally a third casing is made with an aluminium foam as well so that this type of filler material can be explored as well. The foam was chosen to be aluminium as well to avoid the glue breaking due to differential thermal expansion of dissimilar materials. These three different filler materials can be tested and compared. To avoid having to do large studies with large numbers of prototypes these different filler material types can be used to validate simulations to calculate thermal responses of these filler materials, thereby allowing for the correct filler shape and size to be chosen for their specific applications.

4.6. General PCM TDS Design Concept Summary

The TSD is designed to enable its use in different configurations for multiple purposes. The exact size dimensions and attachment points can be changed for specific applications. The TSD is sized to fit within the CubeSat stack, in between stacks or at the top or bottom of the satellite. The casing design is a stiff high strength aluminium box with extra room into which the paraffin can expand. The aluminium casing and filler material are machined out using a milling machine. The fins of the filler material allow for a threaded hole to be made into the casing and also the possibility for increasing the stiffness of the casing by gluing the fins to the lid of the casing. When filler materials are desired that cant be milled out it will have to be attached to the casing. For an aluminium foam filler material this would have to be friction welded or glued.

There are multiple sealing method designs for the lids and the fill ports. Section 6 goes in to more detail on which performed better during the experimental phase. Two different lid designs are used to attach to the casing, the first one is laser cut and welded to the top of the casing. The second design is milled out and glued along the inside wall of the casing.

The first fill port designs are machined out and glued on to the lid. This fill port would then be pinched and welded, soldered or glued shut. The second design is an off the shelf Swagelok component with an attached to seal off the casing. This Swagelok component can be attached with a threaded hole in the lid or by using a nut on the inside to attach the component.

The heat source can be clamped onto the casing directly or through heat transfer devices like flex straps or heat-pipes using the threaded holes machined into the casing. For this thesis these designs are compared by how well the casing responds to heat loads and how well it is capable of sealing the PCM into the casing without leaking. Adding all of these sub-components together results in a general TSD design shown in figures 4.30 and 4.31. This is a generalized model but this specific one was not built for this thesis, although all the prototypes that where built are derivative of this design.

5
Thermal modelling

Thermal models are a valuable tool, once validated, in engineering design. They allow for rapid design of products without having to produce and test intermediate designs. If a model can be produced that can calculate the thermal performance of a system with enough accuracy, these calculations can be relied on to rapidly design multiple prototypes. This is done by designing a prototype calculating the thermal response and iterating the design until the thermal system behaves as is desired. A schematic overview of this can be seen in figure 5.1 The feasibility can be determined much faster and cheaper using thermal models than actual prototypes. Once the product has been designed it must still be tested in real life. This would only be one set of tests though and not the whole testing campaign which could make developing certain products prohibitively expensive for companies. This section will explain the thermal theory used for thermal modelling. Also the thermal models that where built for this thesis and how these models where validated.

5.1. Theory on Heat Transfer

This section will explain the basics in heat transfer theory, the theories and equations used for thermal engineering practice, and how they can be applied to the design of the TSD.

5.1.1. Heat and Energy Balance

The temperature of a an object is dependent on how much energy it contains. A change in the amount of energy in the CubeSat will change its temperature. The temperature change can be calculated with equation 2.2.

The energy added to or lost from a system can cause the temperature to change; this is called sensible heat. Energy can for instance also be stored in its material phase (latent heat) or its chemical composition, (chemical energy). The change in energy of a system depends on the energy entering and the energy leaving the system. This is because a system

Figure 5.1: Schematic of thermal modelling and design process

requires the conservation of energy. This can be expressed in equation 5.1:

$$\Delta Q = Q_{in} - Q_{out} \tag{5.1}$$

In this equation ΔQ is the change in energy in J, Q_{in} is the energy entering the system in J and Q_{out} is the energy leaving the system in J.

The rate of change of the energy in the system is shown in the following equation:

$$\dot{Q} = \dot{Q}_{in} - \dot{Q}_{out} \tag{5.2}$$

In this equation $\dot{Q}$ is the rate of change of energy in W, $\dot{Q}_{in}$ is the rate of energy entering the system in W and $\dot{Q}_{out}$ is the rate of energy leaving the system in W.

It is also possible for energy to be generated or absorbed within a system. This can be given its own term in the energy balance equation or just added to the Q_{in} term. If the $\dot{Q}$ is equal to zero then the system is considered to be in equilibrium and the temperature will remain constant.

Energy can be generated in a CubeSat and can be stored in the batteries. This energy turns into waste heat when it is used to power the electrical systems on board. This energy is usually in the order of only a couple of Watts for a CubeSat. Most of the energy change in a system happens due to radiation entering and exiting the CubeSat. All of the radiative sources are described in section 2.1. These heat sources are usually an order of magnitude larger than the internal power generated, although they depend on the surface properties and environment of the CubeSat. This is determined from calculations shown in section 5.1.3.

5.1.2. Conductive Heat Transfer

Conduction is the way heat travels through a medium by directly transferring energy from molecule to molecule. In space no heat is conducted outside of the system, because in the vacuum of space there is very little material through which heat can actually travel. Within the system this is still an important feature given how heat is spread throughout the space-craft. A one dimensional analysis of heat flowing through a medium is known as Fourier's law of heat conduction which is shown in equation 2.3, expanded to three dimensions the differential equation is shown in equation 5.3.

$$\frac{\delta T}{\delta t} = \alpha \cdot (\frac{\delta^2 T}{\delta x^2} + \frac{\delta^2 T}{\delta y^2} + \frac{\delta^2 T}{\delta z^2}) \tag{5.3}$$

In this equation T is temperature in K, α is the thermal diffusivity in $\frac{m^2}{s}$, t is time in $seconds$ and x, y and z is distance in m.

5.1.3. Radiative Heat Transfer

Radiation is the main element governing the heat transfer to and from the satellite system. Objects radiate electro-magnetic radiation that is proportional to the temperature of the object. This radiation transfers heat to and from the system. According to the Stefan Boltzmann law the power that leaves the system through radiation is:

$$\dot{Q}_{out} = \epsilon \cdot A \cdot \sigma \cdot T^4 \tag{5.4}$$

In this equation $\dot{Q}_{out}$ is the energy leaving the system in W, ϵ is emissivity of the surface, A is the surface area in m^2, σ is the Stefan Boltzmann constant in $\frac{W}{m^2 \cdot K^4}$ and T is the temperature in K.

Electromagnetic radiation when absorbed by a surface turns into heat. The surface properties determines if a wavelength is absorbed, therefore over a certain bandwidth of radiation a surface will have an absorptive coefficient. The main ones used for radiation calculations

Table 5.1: Thermo-optical properties standardized 1U CubeSat of Step Cubelab [55]

Component	Optical property	α	ε	α/ε
Structure	Black anodize	0.88	0.88	1.0
Solar cell	ITO-GaAs	0.92	0.85	1.1
MEMS thruster	Quartz glass	0.90	0.10	0.1
SEC	PMMA	0.04	0.04	1.0
FER	Kapton tape	0.2	0.37	0.54
VER	(La,Sr)MnO_3	0.24	0.28 at −40°C 0.41 at 0°C 0.54 at +40°C	—
MLI	Aluminized Kapton	0.8	0.45	1.78

in space are the visible wavelengths (A in the form of solar radiation) and infra-red radiation (ϵ in the form of black body radiation emitted by surfaces). Energy entering the system from solar radiation is calculated using the following equation:

$$\dot{Q}_{in} = q \cdot \alpha \cdot A \tag{5.5}$$

In this equation $\dot{Q}_{in}$ is the energy entering the system in W, q is the heat flux in $\frac{W}{m^2}$, α is the absorptivity and A is the surface area in m^2.

The final thing that determines the radiative thermal coupling between two objects is the view factor. This refers to the amount of surface area that can be 'viewed' from the emitting surface and what percentage of its view is made up of the receiving face. Satellites have operating temperatures at which they mainly emit IR radiation. This radiation is emitted in all directions by every exposed panel. The radiation between panels on a satellite a can be calculated taking the temperature, surface properties and the view factor into consideration.

A table of standardized thermo-optical properties of a 1U CubeSat by Step Cubelab can be seen in table 5.1. This can be used as an example of the radiative properties a CubeSat can have, although they can be tailored to specific missions to control the heat fluxes. Rough estimations of the actual radiation heat flux values can calculated using these equations and parameters, these are only meant to show the order of magnitude of the heat fluxes. An illustration of what is being calculated can be seen in figure 2.4. A single surface area of a 1U CubeSat has an area of $0.01[m^2]$ and assuming an incoming heat flux of $2015.1[\frac{W}{m^2}]$ (based on section 2.1) and an absorption coefficient of the surface of 0.88, then using equation 5.5 the heat entering the system is 17.3 W. The solar radiation is generally the largest radiation source in LEO. Other heat fluxes would include the earth albedo and IR radiation. For calculating the energy leaving the system of a 1U CubeSat the heat leaves all six sides so the surface area is $6 \cdot 0.01[m^2]$ an emission coefficient of 0.88 and a temperature of $25°C$ are assumed, then using equation 5.4 the total energy lost to the environment is 23.7 W.

Another part of the CubeSat thermal design is the radiative heat transfer between subsystems. Because of the poor thermal conduction between components and relative close proximity this can be an effect on the heat transfer, although conduction is generally still the dominant effect. This is of course dependent on the surface properties, locations and shape of the subsystems. The radiative heat coupling between components can be calculated by using equation 5.6. But seeing as this is very much dependent on the setup of the satellite and subsystems, it will not be used in the thermal models.

$$\dot{Q}_{1,2} = A_1 \cdot F_{1,2} \cdot \epsilon_{eff} \cdot \sigma \cdot (T_2^4 - T_1^4) \tag{5.6}$$

In this equation $\dot{Q}_{1,2}$ is the energy transferred from surface 1 to surface 2 through radiation in $[W]$. $F_{1,2}$ is the view-factor between surface 1 and 2; this is a factor which is the fraction of heat radiated from surface one that reaches surface 2. ϵ_{eff} is the effective thermal emission coefficient of surface one and effective absorptive coefficient of surface 2; they are taken as effective because if radiation is not absorbed it can bounce back and fourth between the surfaces thereby changing the exact values of the absorption. σ is the Stefan Boltzmann constant in $\frac{W}{m^2 \cdot K^4}$ and T is the temperature of surface 1 and 2 in K.

5.1.4. Convective Heat Transfer

Convective heat transfer occurs when heat is transferred by moving a fluid. When the fluid travels the heat that is absorbed within it travels along with it. As there is a negligible amount of fluid in low earth orbit, there is no significant amount of convective heat transfer in space. Only if fluid is dumped overboard will there be any heat transfer, as is the case with thrusters. Within a satellite there can be convective heat transfer in for instance pumped fluid loops or in heat-pipes. The amount of heat transferred through convection can be calculated using equation 5.7.

$$q_s = h_c \cdot \Delta T \tag{5.7}$$

In this equation q_s is the heat flux due to convection in $\frac{W}{m^2}$, h_c is the convective heat transfer coefficient in $\frac{W}{m^2 \cdot K}$ and ΔT is the change in temperature in K.

In an actual vacuum environment the convective heat transfer to the ambient atmosphere is not relevant as there is hardly any atmosphere present. But for the test on the ground this can become an issue. If thermal tests are performed outside of a vacuum chamber there will be convective heat transfer. Just by letting the TSD sit in the ambient air while heating up there will be natural convection, due to the warm air surrounding the casing rising, causing circulation. This type of heat transfer is hard to calculate as it is highly sensitive to the slightest perturbations in the surrounding environment.

Another possibility is forced convection. Here a stream of air is forced to flow over the casing. This type of heat transfer is more predictable assuming the fluid flow has a known temperature, although this will increase the heat transfer to the fluid.

5.2. Numerical Models

Calculating the thermal responses of objects is very useful for engineering prototypes, as it allows for quick comparisons between designs. These calculations are governed by differential equations. For conductive heat transfer this is determined by the shape and the thermal conductivity of the material used. All these together determine the differential equation that determines the behaviour of the system. The differential equation is based on conservation of energy shown in equation 5.3.

These equations do not always have analytical solutions or can become extremely complicated very quickly. To solve them engineers often have to make a number of simplifications that lower the accuracy of the calculation. Another possibility is to divide the calculation up into small pieces and solve linearized versions of the differential equations in small steps. This way whole differential equations need not be solved over a long period of time but a simple calculation can be used and with a local derivative to calculate the solution with short steps in time. This linearization over small timescales leads to errors, but if the time-step is kept small these errors remain small as well. Sometimes the simplifications required for analytical equations create greater errors in the results than the numerical time-step errors. For instance the changing amount of energy in a system over a small time-step can be approximated by combining equations 5.1 and 5.2 as shown in equation 5.8:

$$Q_{p+1} = Q_p + \dot{Q}_p \cdot \Delta t \tag{5.8}$$

In this equation Q_p is the amount of energy in a numerical node at time-step p in J, $\dot{Q}_p$ is the change in energy in a numerical node at time-step p in W. Δt is the time step of the numerical model in s.

5.2.1. Finite Element Model

The program used for a Finite Element Method (FEM) model in this thesis was Comsol Multiphysics. A FEM is a computer model that discretizes a geometry into non-overlapping areas. An energy function and degrees of freedom then describe how this area should behave. Comsol then minimizes the energy function of each of these elements. This is because Comsol can easily be used for multiple physics calculations. For instance heat and pressure changes to properly model the effect of the PCM on the casing. A 3D model of the prototype can easily be modelled in a Computer Aided Design (CAD) program and imported onto Comsol; in this case Solidworks was used. This allows for making more complex designs and leaving Comsol to cut the design into nodes using a meshing function. This allows for rapid design updates and optimizations of the model. If the model can be validated so that it accurately enough predicts the real world, it can be used to rapidly design a TSD prototype.

5.2.2. Finite Difference Model

The Finite Difference Method (FDM) model is a fairly simple numerical modelling scheme. It works by modelling nodes in specific places. A differential equation and boundary conditions need to be defined and then a steady state or a changing state through time can be calculated. This numerical modelling scheme can be used for thermal conduction modelling of heat between nodes. The important boundary conditions are determined by the temperature and fixed heat flows. The node properties are determined by their thermal capacity. The flow of heat between nodes is dependent on the thermal resistance of the node.

The basic setup of the model is the thermal capacitance of a node. The capacitance of a node can be calculated with equation 5.9

$$C = m \cdot c_p \tag{5.9}$$

In this equation C is the thermal capacity in $\frac{J}{K}$, m is the mass of the node in kg and c_p is the specific heat in $\frac{J}{K \cdot kg}$.

The state of these nodes is defined by its temperature. The energy flow between nodes is dependent on the temperature and the thermal resistance between the nodes as seen in equation 5.10. An analogy can be drawn between thermal problems and electrical circuits, where the temperature is equal to the voltage and thermal resistance is electrical resistance. The thermal resistance that can be calculated with equation 5.12 is a combination of the equations in section 5.1.2. If the material between nodes is made of two different materials or has different cross sectional areas then the thermal resistance of the individual materials can be added together by equation 5.11.

$$R = \frac{L}{A \cdot k} \tag{5.10}$$

$$R_{tot} = \frac{1}{\frac{1}{R_1} + \frac{1}{R_2}} = \frac{1}{\frac{A_1 \cdot k_1}{L_1} + \frac{A_2 \cdot k_2}{L_2}} \tag{5.11}$$

In this equation R is the thermal resistance in $\frac{K}{W}$, L is the length between the nodes in m, A is the cross sectional area of the node in the direction of the heat transfer in m^2 and finally k is the thermal conductivity of the material in $\frac{W}{m \cdot K}$.

To calculate the heat flow between nodes in a one dimensional model equation 5.12 can be used.

$$\Delta T_n = \frac{(T_{n-1} + T_{n+1} - 2 \cdot T_n) \cdot \Delta t}{R \cdot C} \tag{5.12}$$

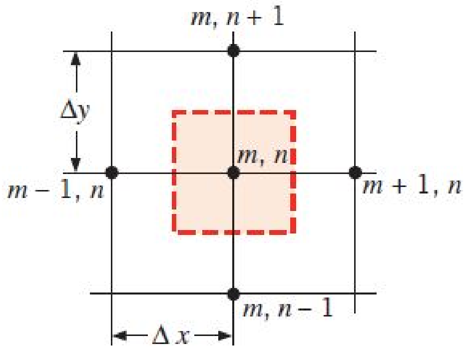

Figure 5.2: Node locations in numerical model [56]

$$\frac{(T_{m,n}^{p+1} - T_{m,n}^{p})}{\Delta t} = \frac{(T_{m+1,n}^{p} + T_{m-1,n}^{p} - 2 \cdot T_{m.n}^{p})}{R_m \cdot C_{m,n}} + \frac{(T_{m,n+1}^{p} + T_{m,n-1}^{p} - 2 \cdot T_{m.n}^{p})}{R_n \cdot C_{m,n}} \tag{5.13}$$

T is the temperature in K, t is the time step in seconds, R is the thermal resistance in $\frac{K}{W}$ and C is heat capacity in $\frac{J}{K}$.

For a two dimensional model the equations need to be expanded in the extra dimension as seen in equation 5.13. This can also be expanded to three dimensions using the same method. A schematic representation of how the nodes are set up is shown in figure 5.2.

5.2.3. Model Setup

An FDM model was made in Matlab using the equations in section 5.2.2, the code of which can be found in appendix C. This section describes the setup of that model. The model is meant to get a quick representation of the thermal response of the TSD in different configurations. Due to the high thermal resistance and complex melting behaviour of the paraffin, many nodes are needed to capture its behaviour. To make the model as simple as possible two different types of nodes are used. A schematic cross sectional representation of the FDM model node layout can be seen in figure 5.3. The outer casing of the TSD is represented a single layer of nodes around the PCM and has different sizes depending on what piece of the casing it is modelling. The inside of the casing all have the same sized nodes. To capture the effect of pockets of un-melted PCM inside the casing between every fin node three PCM nodes need to be placed. This allows for a pocket of PCM to remain un-melted in between the casing and shows the insulating effect of the PCM.

The heat source is attached to the base plate near the top of the casing as this is where the heat will enter the prototype as is shown in section 6.18. The nodes are defined to be in the centre of equally sized cuboids. To calculate the thermal resistance between nodes the resistance from one centre to the edge of each node needs to be calculated and combined using equation 5.10 and 5.11. Once the PCM nodes reach their melting temperature the energy entering the system starts to go into the latent heat storage of the node. This is done over a melting range to try to get a more realistic melting behaviour. This melting range is taken to be $6°K$. The amount of energy in the stored in the latent heat of a node also controls the temperature and thermal conductivity of the node which gradually switches from the solid to the liquid state. Radiation and convection are ignored in this model as it is unclear how they will behave and ignoring them gives more conservative results. The property values of the aluminium are from the 6082 T6 aluminium as defined in section 4.2.2. The eicosane properties are taken from table 3.5.

To determine how easily heat transfers through a system the thermal diffusivity number is used. The thermal diffusivity shows how at constant pressure heat travels through a system

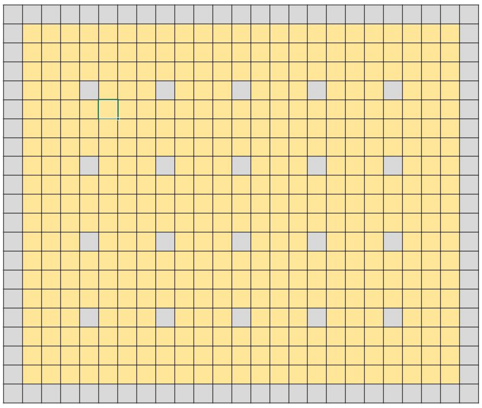

Figure 5.3: cross-sectional view of FDM with casing walls fins and PCM, yellow = eicosane, grey = aluminium

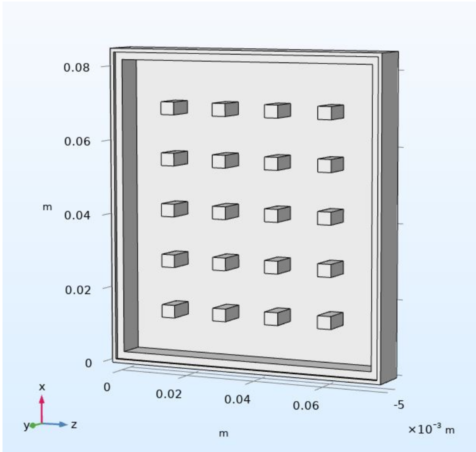

Figure 5.4: 3D representation of FDM model shown in Comsol

through conduction. It is defined in equation 5.14.

$$\alpha = \frac{k}{\rho \cdot c_p} \tag{5.14}$$

In this equation α is the thermal diffusivity in $\frac{m^2}{s}$, k is the thermal conductivity in $\frac{W}{m \cdot K}$, rho is the density in $\frac{kg}{m^3}$, c_p is the specific heat coefficient of the material in $\frac{J}{kg \cdot K}$

Numerical stability within the model determines the maximum step size that can be used. A simulation can become unstable if small perturbations grow exponentially and to unbounded heights. This happens when a small numerical error becomes larger in a feedback group. If a small perturbation is produced it has to have a larger effect on the system than the original perturbation. A tool for calculating these growth-rates in conductive systems is the Fourier number. The Fourier number is shown in equation 5.15.

$$F_o = \frac{\text{diffusive transport rate}}{\text{storage rate}} = \frac{\alpha \cdot \Delta t \cdot A}{L \cdot V} = \frac{\alpha \cdot \Delta t}{L^2} \tag{5.15}$$

In this equation F_o is the Fourier number, α is the thermal diffusivity in $\frac{m^2}{s}$, Δt is the timestep in seconds, A is the surface area in m^2, L is the length in m, V is the volume in m^3 and L_c is the characteristic length in m.

This equation can be used to define the stability of a system. The system in three dimensions is considered stable if the Fourier number is $\leq \frac{1}{6}$ [56]. The problem with using the equations above is that they assume all the cells are the same size. For the FDM model there are multiple types of nodes having different materials and lengths and in different directions. Therefore for calculating the maximum step-size for each of these models, the heat capacity of and thermal conductivity between each node needs to be determined. Also this is the step-size where the model starts to become unstable therefore a small safety factor should be used to keep it within a stable region. The step-size is therefore multiplied by 0.75. The eventual model uses different node sizes depending on the inputs and discretization of the model. The order of magnitude of the step-sizes is 10^{-3} seconds. This is an extremely small step-size and causes the model calculation time to be very large. This could be addressed by increase the size of the nodes. For instance the fins and walls of the highly conductive aluminium could be modelled as a single node. Although this would increase their effectiveness and would therefore overestimate the effectiveness of the system. Therefore it was chosen to keep the node size and the time-step small for this model.

5.2.4. Thermal response

The thermal response of the casing can be seen in figure 5.5. These models calculate the thermal response of 8 W of input power for 30 minutes. A slight difference can be seen in these models. This is assumed to be because of slight differences in element shapes and sizes and different methods of calculating the melting behaviour between the two models. These slight differences in turn cause slight differences in melting behaviours, although they show similar results and are within the tolerance range of 5 K taken for this thesis.

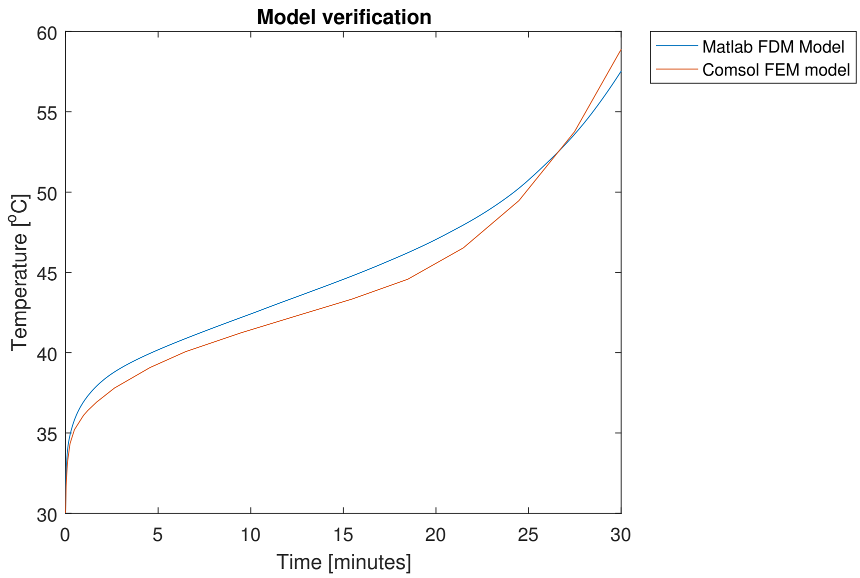

Figure 5.5: Model comparison of Matlab and Comsol models,
the model geometry is shown in figure 5.4 and has 8 W of input power and 1.778 W of ambient heat loss

The Comsol FEM model was used to calculate the thermal response of the prototypes in the section 4. The Matlab FDM model was used to determine design sensitivities in the casing. Appendix C shows the results of the sensitivity of the thermal response to different design changes. The results of these graphs are summarized in table 5.2

Logically the more mass is introduced the more the temperature will drop in the casing. Also, adding more mass to the system will increase the volume of the system. Therefore two different types of optimizations can be considered, the first being mass optimization and

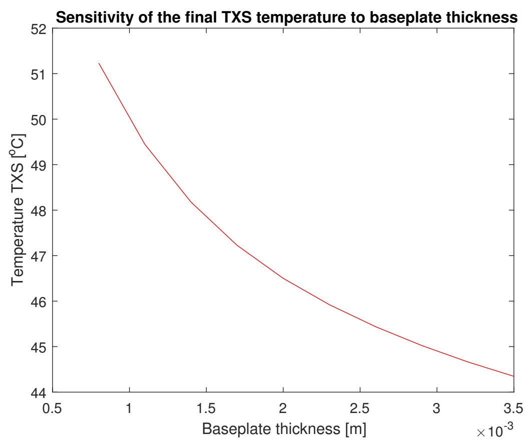

Figure 5.6: Sensitivity of the maximum temperature of the thermal response to base plate thickness

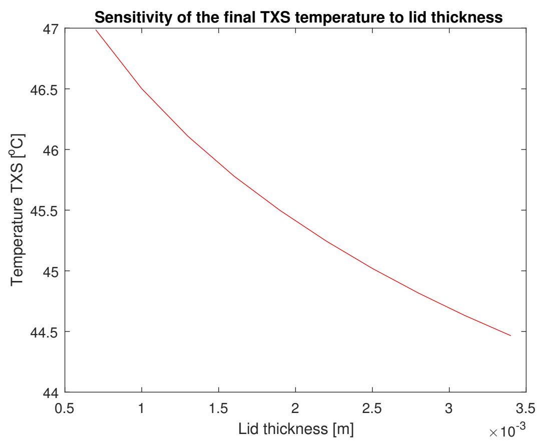

Figure 5.7: Sensitivity of the maximum temperature of the thermal response to casing lid thickness

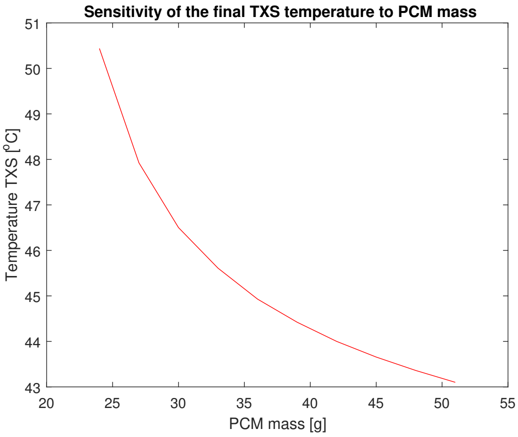

Figure 5.8: Sensitivity of the maximum temperature of the thermal response to PCM mass

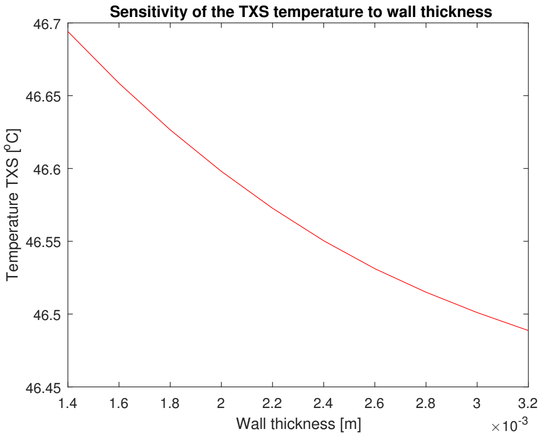

Figure 5.9: Sensitivity of the maximum temperature of the thermal response to casing wall thickness

Table 5.2: Local temperature sensitivity to model parameters with setup shown in figure 5.4 all sensitivity results are shown in Appendix C

Parameter	Size	Step size	Mass sensitivity in $\frac{K}{g}$	thickness sensitivity in $\frac{K}{mm}$
PCM mass	30 g	3 g	-0.18	-1.48
Casing base plate	2 mm	0.3 mm	-1.9	-0.109
Casing lid	1 mm	0.3 mm	-0.07	-1.3
Casing wall thickness	3 mm	0.2 mm	-0.01	-0.19

the second being volume optimization. Therefore the sensitivity plots show the sensitivity of the temperature as function of the added mass or added thickness of the casing. This is calculated by varying certain model parameters with certain step sizes and calculating the gradient in the result as shown in equation 5.16. The local starting point for these models is the configuration shown in figure 5.4. And the sensitivity of the final temperature, final temperature to casing thickness ratio and final temperature to casing mass ratio are shown in table 5.2.

$$\frac{\Delta T}{\Delta x} = \frac{T_{n+1} - T_n}{x_{n+1} - x_n} \tag{5.16}$$

In this equation T is the temperature in K, x is a variable to which the gradient is calculated, n is the step number at which the sensitivity is being calculated.
To determine which model is better for calculating the thermal response, they would have to be compared to the measured results.

The main issue with the FDM model setup this is that the casing geometry can not easily be imported into the software as with Comsol, therefore it can easily be used. This is the main reason this model was chosen to calculate the response of the casing.

To use the FDM model, more thought must be given to how the nodes are structured in order to accurately model the prototype. The main advantage of the FDM model is that it was designed specifically for this problem and the governing equations of the phase change reaction can easily be tweaked. For the FEM model there is a built-in Phase Change Material module, and while the governing equations are explained in the module they are not as easy to tweak.

The determining factor for using one model over the other is the time invested in creating the model and how much detail must be added.

6

TSD prototype

A general design for a CubeSat TSD was discussed in section 4. This section will size the TSD for a specific heat load and use case. Although this will be a specific use case, it is designed for use by any use case with a similar heat load. A set of standard sized PCM TSDs can be designed for a range of different heat loads and use cases. If two use cases are similar then a standard size developed for one can be used in both. It was chosen to make a specific design use case for the PCM TSD. This way the design can be tested to see if it works in practice and if it is possible to answer the research questions using this design. As mentioned in section 2.2.3, a radio transmitter is an ideal case where a lot of power is used intermittently on a CubeSat. An example of the temperature profile this creates can be seen in figure 6.1. There is always a need to transmit data from a satellite to ground, therefore this is an optimal general use case.

This section will explore the specific use case of the TXS S-band radio transmitter made by ISIS. This use case will define the size and dimensions for the TSD. This prototype TSD can in turn be built and tested to determine the feasibility of the design. Once the performance of the PCM TSD is determined and predictable, designs can be optimized and be made for very specific use cases. The best sizes for general use cases can be categorized and designed into PCM TSDs. This will be left for future work as it depends on the needs of future satellite missions.

6.1. Heat Source

The heat load of the TXS can be simulated using a heater, allowing the characteristics and thermal response of the TSD to be mapped out. To benchmark how effective the TSD is at cooling the TXS, the components should be tested together to see if the heat properly transfers into the TSD. As an actual TXS is an expensive complex piece of flight hardware that would require additional software to run, a different PCB was used as heat source. This is a PCB used at ISIS that can produce heat loads in the centre of the board using resistors. The layout of this PCB can be seen in figure 6.2. This custom PCB has been used in previous thermal tests at ISIS. The PCB's thermal characteristics will be slightly different but the characteristic of the copper heat sink should be similar. The TXS has a heat sink attached that weighs about 80 grams. The TSD was machined to be able to be attached to the TXS attachment points on the heat sink. For the custom PCB a piece of copper had to be machined with the same connection points on the copper heat sink as the TXS would have had, while of course being attached to the heat source on the PCB. The heat sink was clamped onto the board with a conductive gasket between the resistors and the heat sink. The heat sink was also sized to be around 80 grams so as to have the same thermal mass as the actual TXS. The design of this heatsink can be seen in figure 6.3. Next this heat source and heat sink where integrated into a 2U CubeSat frame as can be seen in figure 6.4.

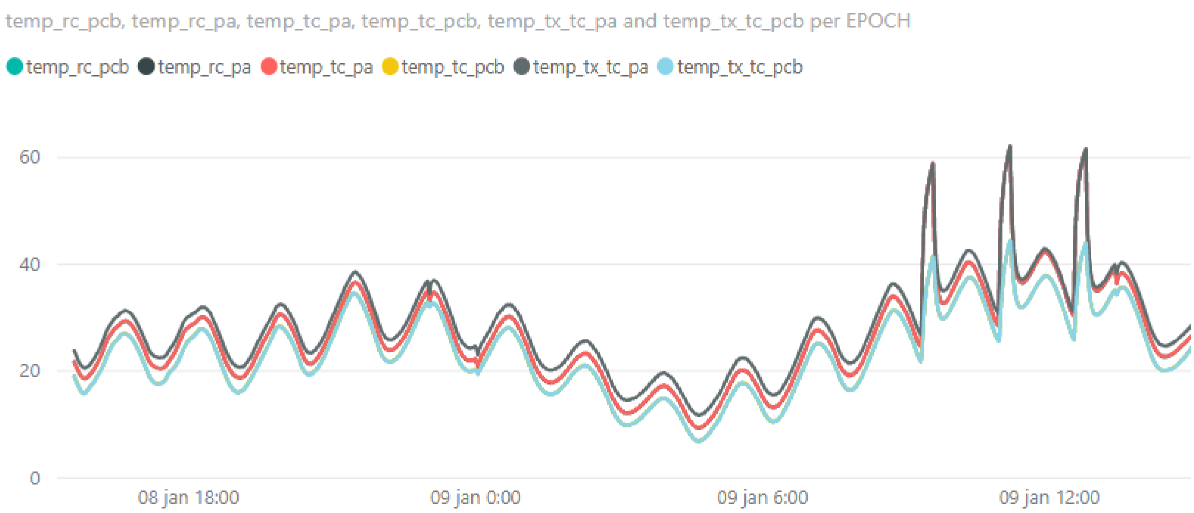

Figure 6.1: On orbit temperature measurements of a TRXVU on a Hiber satellite by ISIS, x-axis shows the local date and time the measurement was done, the y-axis shows the measured temperature in $^{\circ}C$, temperature swings can be seen throughout the measurement due to the satellite passing in and out of eclipse, the last three orbits show larger temperature spikes due to the use of the radio

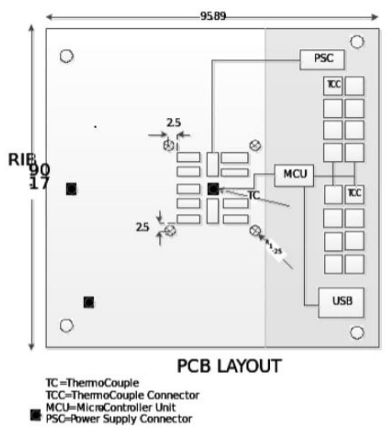

Figure 6.2: Custom thermal test bed PCB layout [8]

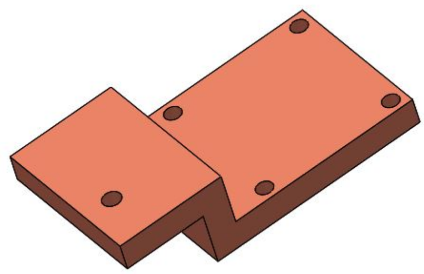

Figure 6.3: Custom test setup heat sink

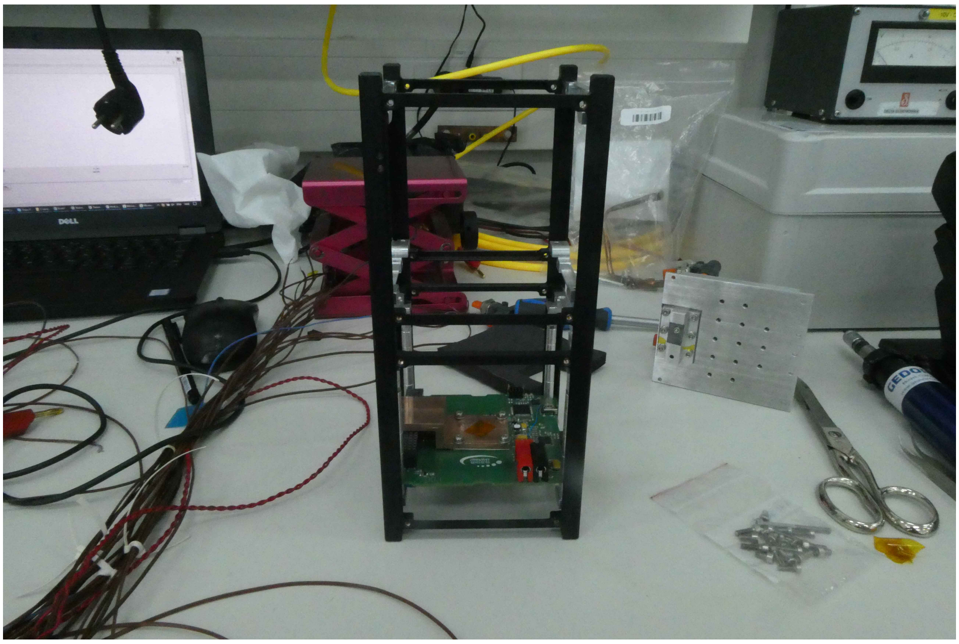

Figure 6.4: Integrated custom PCB (A Thermal testbed PCB) with heaters and heat sink with similar characteristics to the TXS

6.2. Sizing the TSD

In this section the basic design choices are described. They where based on the CubeSat and the specific use case for this project. In section 4.1 multiple possible casing designs where shown. In this section these designs will be fully developed for the heat load from the TXS. These designs include three different filler materials: fins, honeycomb and metallic foam. Also, two different sealing methods were made: the first was a welded lid with fill ports glued on, the second was a lid glued on with clamped-on fill ports with O-rings to seal it off.

6.2.1. Sizing the PCM

As described in section 2.4, the PCM enables the CubeSat to be designed for the average thermal load instead of the maximum and minimum loads. This means that the thermal load selected will have to be dissipated within one thermal cycle for the PCM device to work. If all the heat is not removed before the next cycle then the PCM device will become more saturated during every heat cycle and eventually won't be able to store any more energy in the form of latent heat.

Assuming the orbit duration is 90 minutes and the TXS S-band transceiver is used for 20 minutes, a total energy of 9600 J is generated. If the net energy in the 90 minute cycle is 0 there needs to be an average heat loss of 1.778W. If the average heat loss is assumed to be the actual heat loss during the 20 minute transmitting time, then 7466.4J of energy needs to be stored by the TES device. Paraffin has a latent heat of fusion of $246\frac{kJ}{kg}$. So if all the heat that needs to be stored as latent heat then using equation 3.1, and assuming ΔT over an orbit to be 0, then 30.35 grams of eicosane wax is needed.

This calculation is conservative because there will also be heat stored as sensible heat in the paraffin and the casing. The specific heat of eicosane is two orders of magnitude less than the latent heat storage, so unless the ΔT is around 100 $°C$ or more the latent heat storage will be dominant. Also heat could be lost to the satellite frame and through radiation to space. Although, these losses are represented in the 1.778 W of heat-loss assumed in the heat cycle calculation. Figure 6.5 shows the results of an FDM model which simulates the temperature of a TSD after 20 minutes of producing 8 W. The effectiveness of increasing the PCM mass diminishes greatly after more than 30 grams of eicosane is used. This shows that

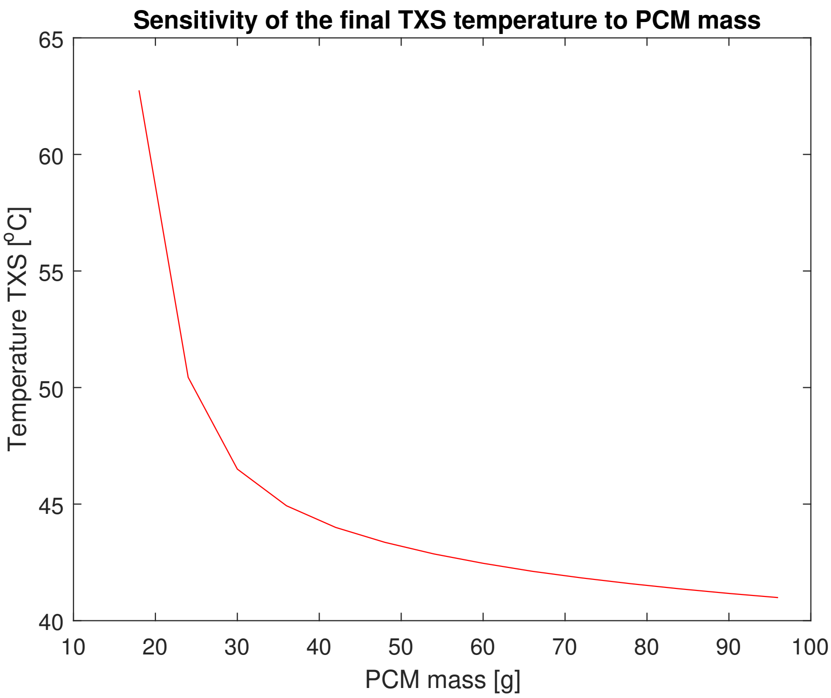

Figure 6.5: Sensitivity of the casing to mass of the PCM for this specific use case (8 W of input power for 20 minutes with 1.778 W of ambient heat-loss)

the assumptions that the latent heat storage of the PCM is a dominant factor in this model.

Using the mass of eicosane the total volume and therefore height of the casing can be calculated. The total volume of the casing can be calculated using the density at the highest expected temperature. If it is assumed that this is $50°C$ then the total volume is $3.95 \cdot 10^{-5} m^3$. The height can be calculated if we know the surface area over which it is spread out. If the same assumptions are used as in section 4.5 then the height of the paraffin is around $5.88mm$. This does not include the thickness added by the base plate or cover thickness. Also the area used to calculate the thickness also needs to include the area of the wall of the casing and all the filler material, including the fins that have the threaded holes with other filler material. These will all increase the thickness of the casing. The best design would be to have a casing that is as flat and with the largest heat storage rate as possible.

An important note is that an area around the fill ports needs to be clear of filler material to allow for the fill-ports to protrude through the casing. This allows for any attachment method and allows for a stream of liquid eicosane to enter casing. As can be seen in figure 6.8 the fins of the first casing near the fill-ports were removed, this was also done at the bottom, this is to add symmetry to the design and allow for more paraffin to be added to the system.

6.2.2. Paraffin Casing

The paraffin casing needs to be able to withstand the internal pressure changes over the lifetime of the satellite. If the casing is filled at the highest expected temperature then in principle it will only experience a pressure difference with the ambient when on the ground at about one Bar of air pressure. Once the casing is placed in a vacuum then the only pressure difference will be the vapor pressure of the paraffin coming from the inside. As this is extremely low for Eicosane as shown in table 3.5, this is not a structural concern for this design. The casing needs to be designed to withstand the pressure difference at one Bar.

Also the deflection should not be too large on ground as this is the level the satellite will be assembled. If the deformations are too large at sea level then when the casing is placed in a vacuum it will further deform and systems can either misalign or thermal interfaces can start acting in unexpected ways. The main structural concern would be if the casing is not completely airtight when at sea level and the casing fills with ambient air while on the ground. If air is trapped while the paraffin is solid, and then the casing is put into a vacuum and the PCM melts, it can cause a pressure spike. This can be mitigated by leaving extra room in the casing, although logically one would assume if ambient air can leak into the casing at air pressure it would escape again when placed in a vacuum. This would mean that the casing is leaking and will have all the negative side-effects associated with that.

An added advantage of filler materials is that they can be extended to the lid of the casing where they can be connected with either a weld or glue. This increases the structural integrity of the casing and allows for a thinner casing with less deformations. A figure showing a schematic representation of this can be seen in figure 6.6.

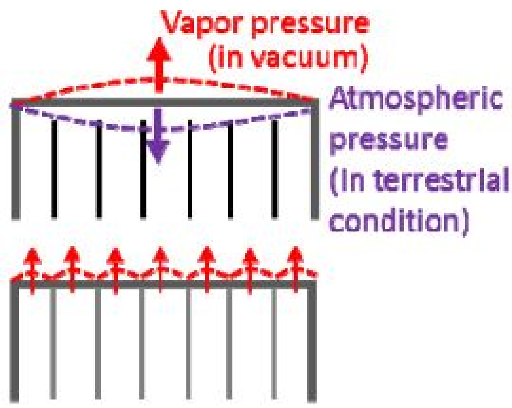

Figure 6.6: Conceptual design behind attaching fins to casing to increase structural integrity [50]

For this analysis it is assumed that the only pressure difference the casing has to be able to withstand is a pressure difference of 1 Bar. By gluing the tips of the fins to the casing, the deformations can be reduced by two orders of magnitude. This can be determined using Comsol to measure the strain of the casing when a pressure of one Bar is applied from the outside of the casing. The results of this can be seen in figure 6.7. These simulations show that at most the casing never bulges more than $10\mu m$. High strength aluminium can easily withstand these pressures, the main difficulty will come if these pressures become cyclical, this could cause high cycle fatigue. It also shows that the stress of the casing at one Bar is about $1.5MPa$ and would allow for the casing to survive the heat-cycles of a mission longer than 3 years, assuming the material properties shown in section 4.2.2.

To make sure the casing is airtight it has to be machined to a certain tolerance. The tolerances of the casing and lid were machined down to a H7 g6 tolerance. This is a tight fit tolerance. They should be milled down to be as small as possible as this will create the most lightweight structure. However there is a limit to this due to the vibrations caused by the milling machine in open end thin walls which can cause inconsistencies on its surface. On the first casing the walls were milled down to 3 mm and on the second to 2mm. The base plate and lid thickness were kept as thin as possible, but this became difficult to do as the casing had to be clamped into the milling machine. This can cause the casing to bend once the material has been machined out and therefore the casing bottom was left to 2mm in the first casing and to 1 mm in the second. The exact dimensions of each part of the casing can be seen in appendix B. The flanges connecting the casing to the CubeSat stack were

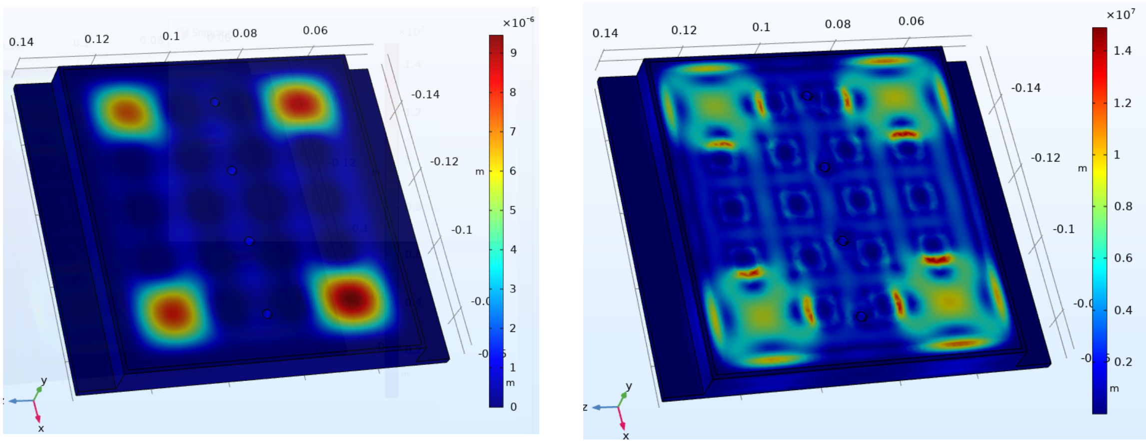

Figure 6.7: Strain [m] (left) and stress [Pa] (right) FEM simulations of the fin casing using Comsol

also milled to be 3mm as these are also open ended flanges. These could be machined down further as well to minimize mass in future iterations.

6.2.3. Filler Material in the Casing

Filler materials were already discussed in section 4.5. Filler materials in the TSD have the following functions:

- Increase the speed at which the PCM absorbs and releases heat. The effectiveness of the filler determines the slope of the temperature gradient throughout the TSD at a certain power input.
- Increase the stiffness of the casing to that it can keep its structural integrity while reducing the mass.
- To create a capillary effect so that the PCM is collected close to the heat source and the filler material. This can become a issue when cavities form in the PCM due to the volume change during the phase change reaction. Although this requires filler material with thin gaps to create a capillary effect.
- To allow for threaded holes in the casing so the heat source can be clamped onto the TSD minimizing the contact resistance.

During the expansion and contraction cycle of the PCMs the filler material will experience stresses, therefore it is important to have the filler material itself be structurally sound or they could be damaged during their operation reducing the effects listed above.

Three different types of casings were made with three different filler materials. Each of which filled the casing a certain amount:

- Fin filler = 11.4%
- honeycomb ≈ 20%
- foam ≈ 20%

Due to the different construction methods between the first and the second series of casings, it was chosen to only create the honeycomb and the foam to have the same volume fraction. This was done because these filler materials generally took up more volume, and therefore to be able to compare the differences between filler materials a sufficiently large volume fraction of the casing needed to be occupied by the filler to show a meaningful difference (especially the foam, as the specific gravity of the foam is already about 25%). There is a slight uncertainty in the filler fraction of the honeycomb and the foam casings due to the shape and effect of the fill ports in these casings.

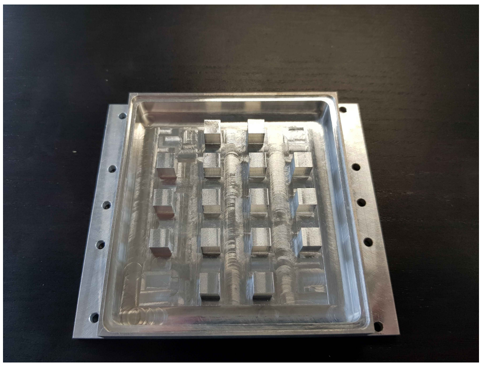

Figure 6.8: Fins TSD casing

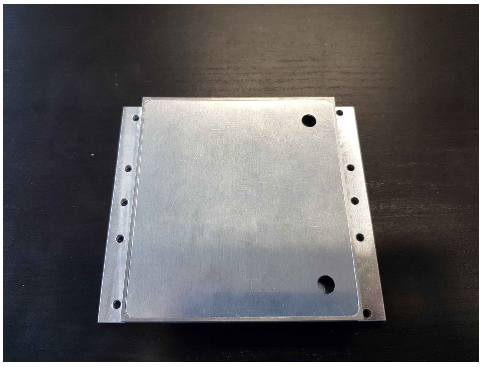

Figure 6.9: Fins TSD prototype

Most of the casing components were milled out, exception include the fin casing lid and the foam filler material. The fin and honeycomb filler materials were milled out. This was done to minimize the contact resistance from the base plate into the filler material. In practice a milling tool has to be able to actually fit where it needs to remove material. Because the fins and honeycombs were chosen to be milled out and standard milling machines have milling tools that go down to a $6mm$ diameter, the minimum gaps that could be formed between the filler materials was designed to be $6mm$. These gaps are too large to create a meaningful capillary effect on the paraffin, but it still does increase the surface heat-transfer area to the PCM. More specialised tool-kits would be able to create smaller gaps.

All the casings have fins in them to allow for the threaded connections and to increase the strength of the casing. The ones in the fin filler casing are square due to the fact that it was milled by hand, the other casings were CNC milled and therefore were able to have round fins, which requires less material. The minimum thickness of the fins is determined by the fact that they where designed to have threaded holes in them. This meant that there needed to be enough material for the hole and the threads to be cut out of the fins, and enough material to distribute the clamping force over the threads. Therefore the fins required a minimum thickness of 5mm; for safety a thickness of 6mm was chosen on the first design. The results of the first casing manufacturing can be seen in figures 6.8 and 6.9. Its exact dimensions can be found in Appendix B.

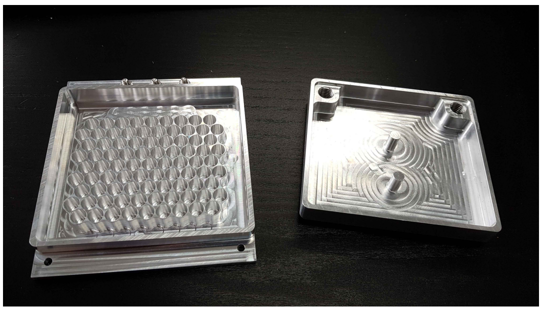

Figure 6.10: Honeycomb TSD prototype

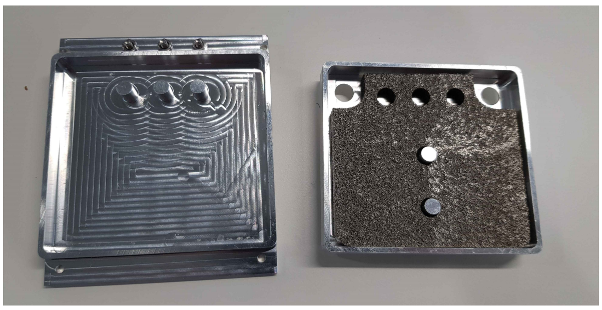

Figure 6.11: Foam TSD prototype

The honeycomb filler material size was partially determined by the machining tools as with the fins; the cells of the honeycomb have a diameter of $6mm$. The honeycomb wall can not be made too thin as this would create difficulties in machining. The thickness of the honeycomb structure was machined down to 0.5mm at its thinnest part. The thickness of the honeycomb, and how far it protrudes from the base plate, determine how much volume it will occupy. These were designed to match the foam filler in the its casing. The honeycomb filler can not protrude all the way out as it would prevent the PCM to flow into the cells once the casing is assembled. The honeycomb filler only protrudes 7mm out from the base plate, this leaves 1mm of space between the honeycomb and the lid. To allow for the threaded bolt holes to be made in the base plate some of the honeycomb cells were not cut out but left as solid aluminium cells. This allowed for a bolt to clamp onto the base plate at the exact location of the honeycomb cell. To allow for bolts to be clamped onto the casing fins and threaded holes were machined out of the casing lid as can be seen in figure 6.10. These fins were designed to fit into the honeycomb cells with a clearing. Its exact dimensions can be found in Appendix B.

The aluminium foam filler material (Racemat [57]) was used for the third casing. The foam filler was not machined out of the casing but glued on. Figure 6.11 shows the foam filler casing, its exact dimensions can be found in Appendix B. The foam will cause a capillary effect in the paraffin. To make sure it collects the PCM near the base plate, the foam should not protrude all the way through the casing. This way it will keep the eicosane close to the base plate. For this reason the foam was machined down to a thickness of 7mm. Fins where machined out of the base plate and the lid of the casing to allow for bolted connections with connector pieces. The holes for the fins and foam outline was laser cut from an aluminium foam plate. The final assembled TSDs (with fin and honeycomb filler materials) can be seen in figures and 6.14 and 6.15.

Stress and strain simulations were also done on the honeycomb and foam casings. The results of these simulations can be seen in figures 6.12 and 6.13. Due to the smaller fins and the fact that only two of them were used, the stresses in these casing were more than 5 times higher than in the fin casing at the same pressure. More of them were not used in these designs as this would have taken up too much of the filler space reducing the effect of the TSD. It was chosen not to do this in order to better measure the differences in filler materials. An easy solution would be to fill the casing less so that the stress on the casing never exceeds one Bar. Redesign through extra fins or small increases in thickness on the lid around the fins could also reduce peak stress concentrations, but it is not obvious that this is required for these casings. For the test prototypes these designs were definitely strong enough, but if a CubeSat prototype is made these peak stresses might have to be reduced to avoid fatigue in the aluminium.

The foam filler material has similar strain and stress peaks as the honeycomb model. It is not obvious how to model how much stiffness of the glued on metal foam would introduce to the casing. Therefore the stiffness of the casing without the metal foam was modelled. But logically they would only increase the stiffness and therefore this is a conservative calculation. But if reductions in stress are required similar redesigns can be applied to the foam filler casing as was described for the honeycomb filler casing.

6.2.4. Predictions

Once the designs were made some comparative predictions could be made on how well the casings would perform. As a lot of the information needed to make a model, like contact resistance and ambient heat loss were not available until the casing is tested, similar inputs to those used in the FEM model in section 5.2.3 was used. Here an input power of 8 W for 30 minutes and a heat-loss of 1.778 W from the casing lid were assumed (these values are based on the calculations done in section 6.2.1). The honeycomb and foam casings are of similar size; the fin casing has slightly less volume for the PCM. To make a proper comparison, the eicosane density in liquid form was increased in the fin casing so that the mass of the PCM matched the other two casings. Also the honeycomb and foam casings weighed slightly more,

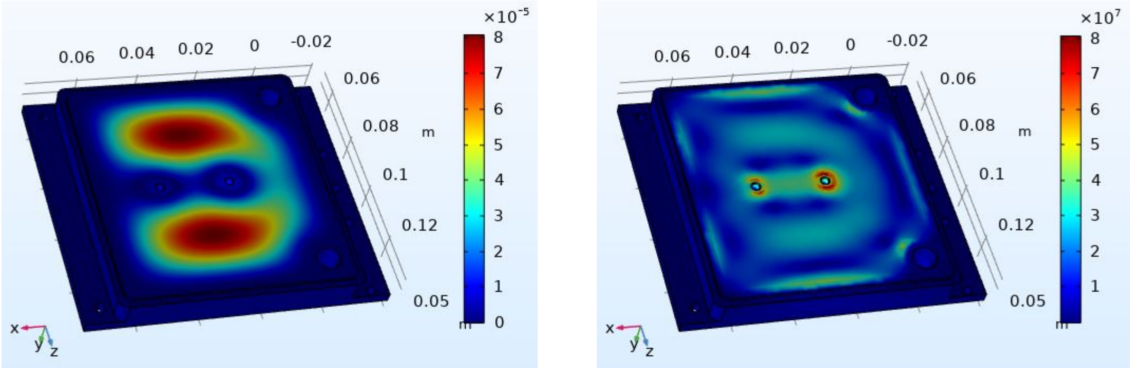

Figure 6.12: Strain [m] and stress [Pa] simulations of the honeycomb casing using Comsol

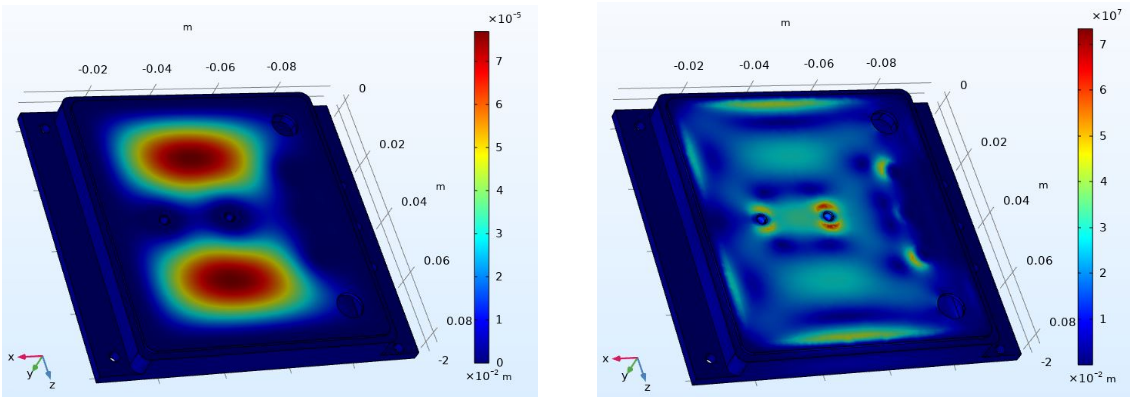

Figure 6.13: Strain [m] and stress [Pa] simulations of the foam casing using Comsol

therefore the density of the aluminium was also increased in order to do a proper comparison of the filler types. The results of the simulations can be seen in figure 6.16.

The calculated performance results of these casings are similar although some clear differences can be seen. The best performing filler material seems to be from best to worst performing:

- The foam filler
- The honeycomb Filler
- The fin filler

This judged on how low the casing is able to keep the heat source temperature throughout the heat up phase. Although the differences are not extremely significant. Increasing the input power or the by using a finer filler material (thinner with smaller gaps between them) these differences would likely become larger. The filler materials for these prototypes also decrease in complexity and price in that order.

6.3. Integrated setup

To test if the prototype could be integrated into a CubeSat and to measure the effects the TSD had on a CubeSat, an integrated test-setup was made. The thermal storage device has to not only be able to work properly on its own but also in combination with all the other components and the CubeSat itself. This section will describe the test setup and the connections with these other components.

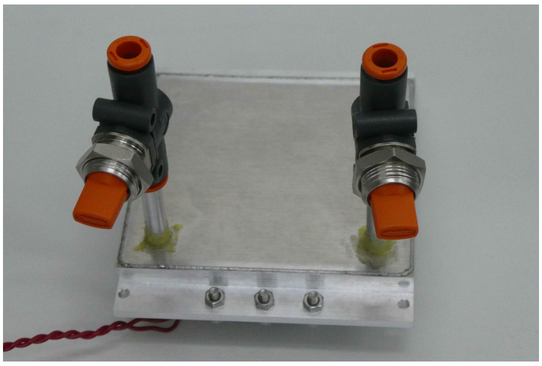

Figure 6.14: Finished TSD with a fin filler and welded on lid

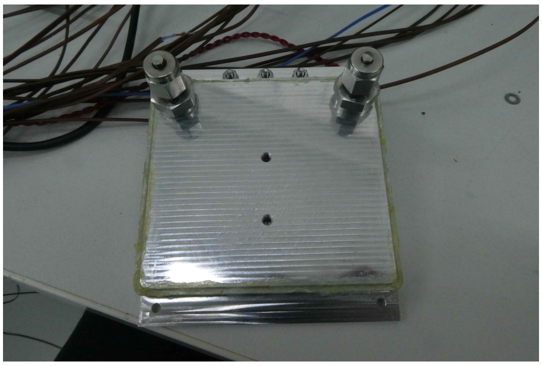

Figure 6.15: finished TSD with a foam filler and glued on lid

6.3.1. Heat Transportation Connector

To make a proper connection with the TSD, multiple small bolts were used to clamp the surfaces together. The reasons for this are explained in 4.4.1. M3 stainless steel bolts are used in this design. Smaller bolts could be used if this would allow for more of them to be attached to a connector piece, or for a smaller fin size in the first TSD design. For smaller bolt sizes in an aluminium tapped hole it is common practice to insert a helicoil. This allows for the stresses caused by a bolt to be spread out over more material. This has as a goal to try and make the first failure point of a bolted connection the bolt and not the threaded hole. If the tapped hole thread fails then a new casing would need to be built. If the bolt fails then only the bolt would need to be replaced. Also, larger clamping forces can be applied to these bolts and therefore create a better thermal interface between the casing and a connector piece. To further increase the effectiveness of these clamped interfaces Sigraflex was added between the non copper-copper interfaces, decreasing the interface resistance between the components. Copper-copper connections transfer heat well enough without the Sigraflex in between them.

For this thesis experiment the PCM device was mounted close to the TXS. The TXS has a shape that does not allow it to be directly clamped on to the PCM casing. A connecting rod between the heat sink and the PCM casing was milled out to have the right shape which can be seen in figures 6.17 and 6.18. An extra use for the connector rod can be to spread the heat over the surface of the casing. A thin rod can be milled out to minimize weight, and create accessibility to the heat sink while allowing for bolt heads to clamp the rod to the PCM device. Another view of this piece can be seen in figure 4.18. Figure 6.19 shows the connector piece integrated into the CubeSat frame.

The other transportation method discussed in section 4.4.1 are the flexible heat straps. Improvised flex straps were used in these tests. Copper pipe fittings were used to easily connect different components together. This can clearly be seen in figure 6.19.

It is also possible that a component on a CubeSat would benefit from being thermally isolated, for instance if the TSD is designed to store heat for the batteries at a later time. If the casing is attached to the frame then all the heat could be transported through the frame and be radiated away before it can be used to keep the batteries warm. Therefore the option of adding peak nuts to the steel rods in the CubeSat stack was explored in these tests. This was instead of the aluminium spacers that are usually used to keep components in their stack locations. These nuts can also be seen around the TSD in figure 6.19. Although the test setups did not show any significant differences when using the PEEK nuts, therefore heat was leaking from the TSD to the frame through some other way. If more thermal insulation is required, then the casing could also be attached to the frame with peek brackets. This

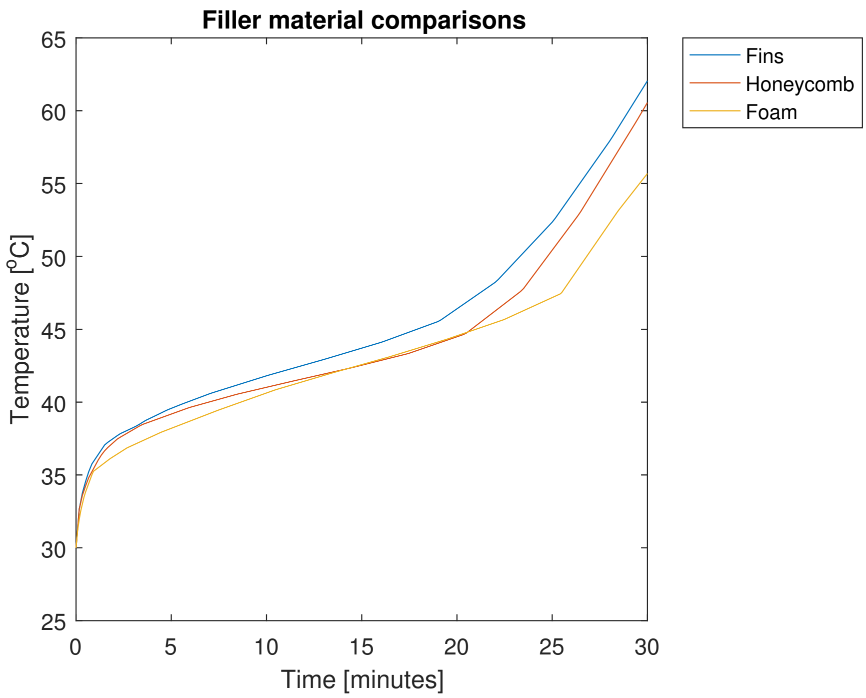

Figure 6.16: FEM model thermal responses of different filler materials
The geometries are the same as the actual casing prototypes, these predictions are calculated using 8 W of input power and 1.778 W of ambient heat-loss

would decrease the conductive thermal coupling between the TSD and the CubeSat frame even further. If this is done then further steps would have to be taken to insulate the TSD from radiative heat transfer. Methods for doing this were shown in section 4.4.1, but are not further explored in this project.

6.3.2. Battery Pack Mass

The effect of the TSD is that it will store heat that is released for a later moment. This can be to keep the system it is attached to warm or to heat another system. The integrated setup was built to test how the TSD works together with other systems. This setup tested how the TSD stored heat from a TXS and release it slowly to a battery pack. For safety reasons a block of aluminium with similar mass/heat capacity as the battery pack was used instead. The heat capacity of the batteries used in a CubeSat are $0.75\frac{J}{g \cdot K}$. Using equation 2.2 and a specific heat of aluminium of $0.91\frac{J}{g \cdot K}$. $190g$ of aluminium is required to simulate the heat storage capacity of a four cell battery pack.

6.3.3. Assembly

The TSD prototypes and the custom PCB were integrated into a 2U CubeSat frame and thermally connected using the connector piece shown in figure 6.18. This was done to measure how the use of the TSD and the rest CubeSat system behave together. The aluminium block was connected to the TSD by clamping it to a copper strap using M3 bolts. To do this an M3 hole needed to be tapped into the block. This setup can be seen in figure 6.19. This frame is missing the side panels and therefore the frame has less mass then it otherwise would, this will cause it behave differently than when used in practice, but it should at least resemble the behaviour that can be expected from the CubeSat frame.

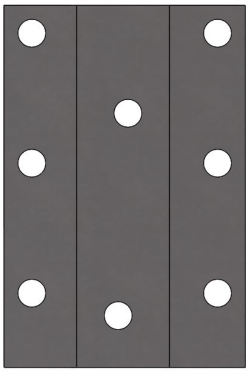

Figure 6.17: Connector piece top view

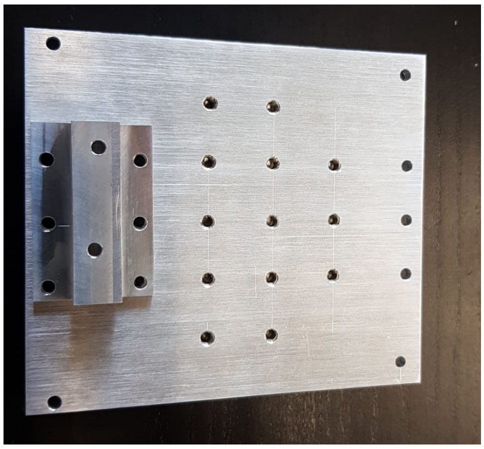

Figure 6.18: Photo of the Connector

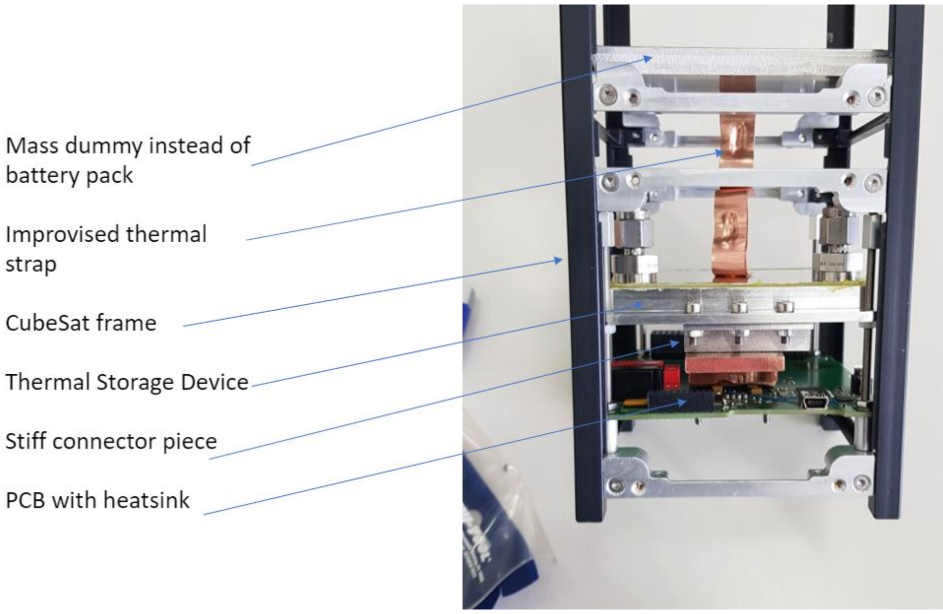

Figure 6.19: Integrated satellite test setup

All the prototypes were integrated into the CubeSat frame made available by ISIS. A design flaw was discovered as the clearing between the corners of the casing and the frame was not large enough, and therefore slight misalignments in the assembly would cause the frame to touch the TSD. This would create an extra thermal connection with the aluminium CubeSat frame. To avoid this, on a second assembly attempt the TSD corners were filed down leaving a larger clearance between the casing and the frame. In the next design iteration, the casing should have rounded corners or shorter flanges to avoid this issue.

7

TSD experimental setups

This section describes the tests that were done for this experiment. The main goal of these tests was to validate the models that was described in the previous chapters. These tests were meant to map the characteristics of the TSD, and how it interacts with its environment, such as gravity or the CubeSat structure. These tests where performed at the thermo-vacuum lab at the NLR.

7.1. Test Plan

The test plan has multiple objectives. The list below describes the research questions that were posed in section 1.2 and the tests that were designed to answer them.

- **What is the thermal response of the TSD?**
  - By measuring the thermal response with and without PCM.
  - By measuring the effect of gravity on the casing.
  - By measuring the effect the different filler materials.
  - By measuring the effect a TSD has on a CubeSat frame in a similar thermal environment as would be expected in LEO.
- **Can the TSD be designed to perform reliably?**
  - By measuring the effect of multiple thermal cycles on the endurance of the casing
  - By measuring if the multiple cycles cause a change in performance
  - By measuring how casings with various filler materials compare with respect to their durability of multiple thermal cycles.
- **Is the TSD useful and does it perform better than traditional thermal control systems for the given use case?**
  - By measuring the thermal response of the TXS with and without a TCS.
  - By measuring the difference between a heat sink and a PCM TSD of the same mass.
- **Can the model predictions be verified with the experimental tests?**
  - By measuring the thermal responses of the same systems that were modelled in the previous chapters and comparing the results.
  - By measuring the thermal response of the TSD's with different filler materials.
  - By measuring the thermal response of the filler materials at different power inputs.

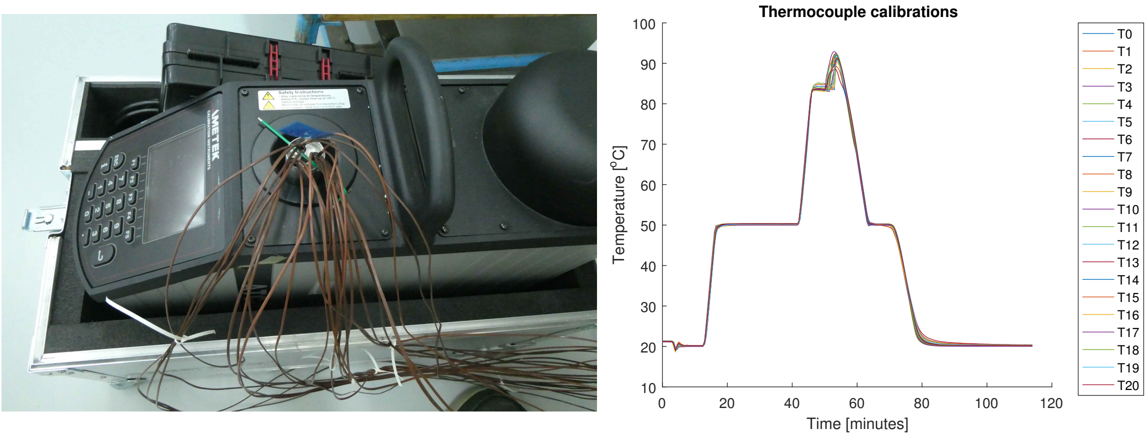

Figure 7.1: Calibration of the thermocouples using IPA at 20, 50 and 100 $°C$ with limitations of the boiling point of IPA

A complete overview of the tests and the test requirements can be found in the test plan in Appendix D.

It is important to note that at the setup for each experiment steady state heat losses are attempted to be measured. If the input power required to keep the setup at specific temperatures is measured then estimations of the heat losses at certain temperatures during the experiments can be made. Also at steady state temperatures the temperature drops over contact interfaces can be measured. These values are important for modelling the behaviour of the casings in the numerical models. These measurements and the resulting model inputs can be found in Appendix E.

7.2. Test hardware used

This section will describe the thermal hardware used in the test setups; which hardware was used, why they where needed and how they were implemented.

The thermocouples (TCs) used in this experiment were type-T TCs, made out of a junction of copper and constantan. These are standard TCs used to measure low to modest temperatures ($-200°C$ to $200°C$). To measure the temperature on the device the voltage difference of the TC junction needs to be measured. If the junction is in contact with other metals this will also generate a voltage difference and the wrong temperature will be recorded. Therefore the TC cannot be in contact with the casing and has to be electrically isolated. In figures 7.7 and 7.9 it can be seen that Kapton tape is used to electrically isolate the TCs from the casing as well as to attach the TC to the casing. To make sure all of the TCs worked properly and to map the exact voltages certain temperatures generated, the they were calibrated. Figure **??** shows the TCs being calibrated. They were calibrated at $20°C$ and $50°C$. Most TCs measured the temperature within 0.1 degrees, the largest deviations where around 0.4 degrees. These deviations are an order of magnitude smaller than the 5 degree accuracy requirement set at the start of the project.

A thermal chamber was used to melt the PCM during the filling stage. This thermal chamber was also used to produce the large temperature swings of the CubeSat frame during the integrated tests. A thermal chamber can also be used to accurately control the amount of convective heating or cooling experienced with the casing. The chamber was not required for the tests with a constant ambient temperature. For these tests the insulating foam was used to control the convective cooling.

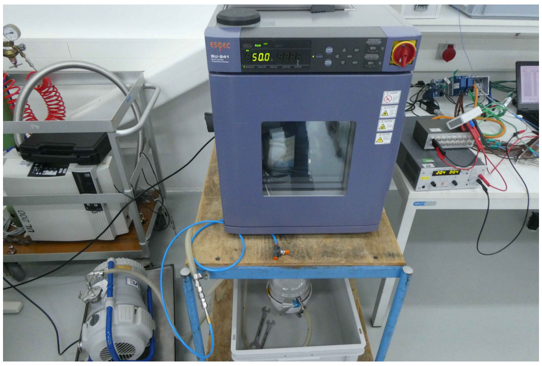

Figure 7.2: Thermal chamber at the NLR

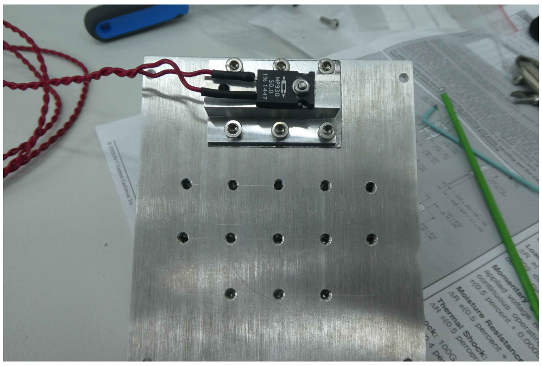

Figure 7.3: MP930 Kool-Pak Heater attached to casing

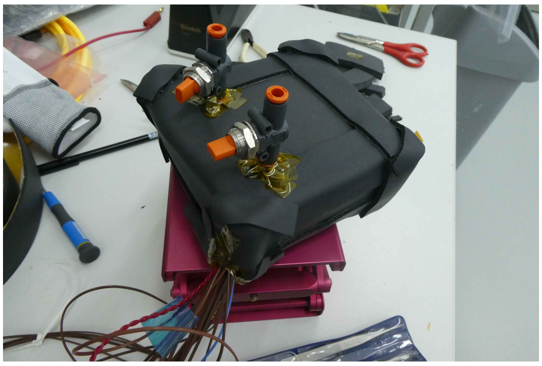

Figure 7.4: Insulated casing setup

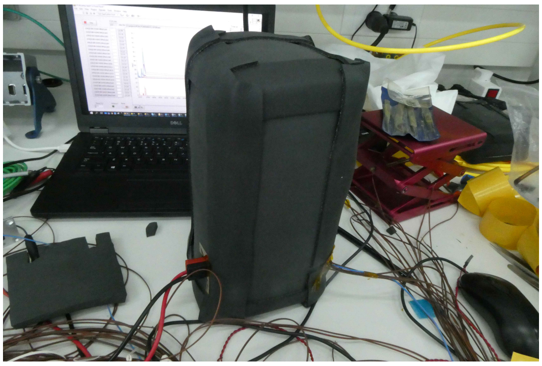

Figure 7.5: Insulated integrated CubeSat setup

To measure the thermal response of the non-integrated casing a heater was used to model the input power of the TXS. This heater could supply up to 30W of power depending on the temperature, which was sufficient for the test-case of this heater. The heater was attached to the connector piece on the casing. This is because the M3 bolts needed for the casing are too large for the heater. This also allows the proper measurement of the contact resistance between the connector piece and the casing. To get a good thermal contact resistance the heater was clamped onto the connector piece with Sigraflex between them. To reduce the risk of accidental overheating and damage to the setup, an extra TC was placed on the heater with a switch connected to the power-source. If the heater exceeded $80°C$ then the power to the heater would be cut. This temperature is higher than would be expected for the experiment under normal circumstances. This is also the temperature limit after which the power amplifier on the TXS would stop working. Therefore if this temperature was reached then the TSD would not be able to cool the TXS properly.

To remove the large effect natural convection has on cooling the casing, it was wrapped in thermally isolating foam which traps air and uses it as an insulator to protect the casing from rapid convective cooling. The foam used was Fleximat which has wide range of usable temperature ranges thereby minimizing the risks of a fire. All the junctions in the foam were taped so as to not leave any cracks where air can flow by the system. If a crack were to remain then the casing could have a chimney effect which would drastically change the insulating characteristic of the foam. Figures 7.4 and 7.5 show the test-setups of the casing and the integrated setup. For the integrated setup foam was also cut into pieces and placed between the subsystems to prevent convective heat transfer between them.

The software program used to measure and control the thermal tests is Labview. The software records the TC temperatures, the input power and the time of the tests. Other control mechanisms like safety relays and other control relays could also be triggered by events in the software. This was especially useful for the thermal cycled tests as these would take

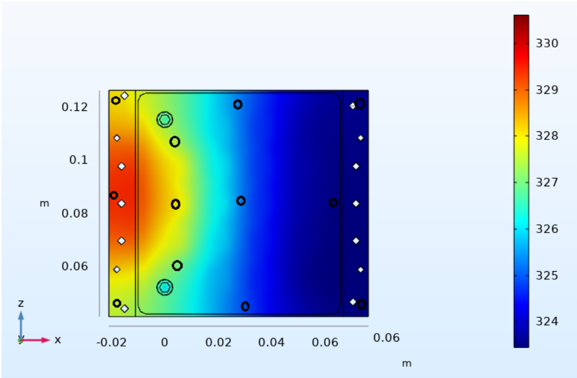

Figure 7.6: Placement of top thermocouples based on simulation

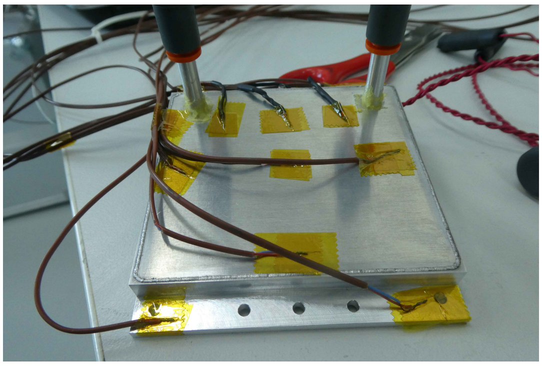

Figure 7.7: Top view of thermocouple locations

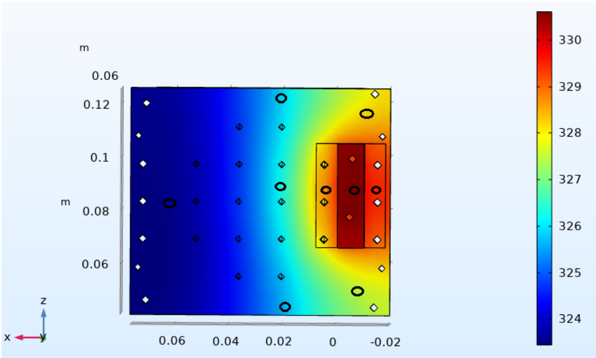

Figure 7.8: Bottom view of thermocouple locations

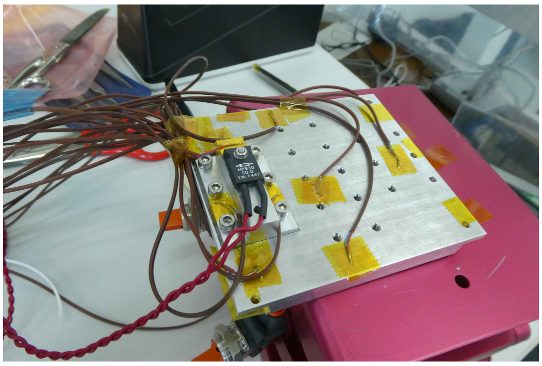

Figure 7.9: Bottom view of thermocouple locations

many hours a day to perform. By using the software the input power can be automated. To speed up the heat cycle a fan was used for forced convection to decrease the cool down time. The fan and input power were controlled by relays and by the software; the whole process could then be automated.

For one of the tests, instead of using the PCM TSD a heat sink was attached to the PCB. This can be seen in figure 7.25. This heat sink was a copper mass of about 150g while the TSD was only about 130g. This setup was made to see if the PCM would outperform a traditional heat sink. If not then the system would be a very complicated, expensive and less effective TSD suggesting the project should be abandoned. Luckily this was not the case as shown by the test results.

7.3. Test Setups and Results

This section will explain how each experiment was set up and why it was done that way.

7.3.1. Prototype Setups

The first setups that will be discussed are those of the individual prototypes. These were measured individually before being integrated into a CubeSat frame.

Placement of the TCs was determined by looking at simulations of how the temperature is likely to spread through the casing as shown in figures 7.8 and 7.9. The TCs where placed on both sides of the casing, at multiple distances from the heat source, this was to check if the casing performs as expected in these locations. TCs where also placed near locations of interest like the connector holes to the CubeSat, also on and around the connector piece. The TCs where also placed in pairs or groups of three at certain distances, this is for redundancy in case a TC fails and to check for symmetrical heat distribution through the TSD.

In total, 21 TCs were placed on the casing. Some TCs did fail as electrical contact with the wire was lost or because the tape separated from the casing causing the TC to measure the ambient air temperature. These cases were fairly obvious to spot during or after the tests as the TC temperature would change rapidly or have clearly incorrect values. The results of the malfunctioning TCs were removed from the results. Another reason for the large number of TCs is the fact that a model can be checked in multiple locations for its accuracy. Therefore, if correct the model is more likely to be able to predict future temperatures then if it only correlates at one point. These TCs are meant to capture the heating behaviour, the thermal gradient through the casing and the contact resistance of the interfaces between objects. No TCs could easily be placed inside the casing, therefore the behaviour inside the casing was inferred from the data obtained on the outside to the extent that was possible. This setup was repeated for the other casing as well. The TC locations were placed in similar locations, though no precise measurements were made to determine that they were exactly the same.

7.3.2. Prototype measurements

After attaching the TCs a number of baseline measurements were made. The thermal response of the casing before being filled was measured first. This gives a good baseline for the measurements so the effects of the PCM can be seen and the model can be built accurately. The casing was then filled with eicosane paraffin and the test was immediately repeated. The results of the thermal responses of the empty and filled casings are shown in figure 7.10. Here the effect of the PCM can clearly be seen with the large increase in heat capacity of the casing from about minute 8 until about minute 28. This is the PCM melting. The melting profile isn't as flat as one would expect. This is due to the melting interface of the PCM moving farther from the heat source, thereby creating a larger thermal gradient through the melted eicosane, thereby increasing the casing temperature. The same was done with the casing while letting it cool down; the results of these measurements can be seen in figure 7.11. The same results as before can be seen as the outside of the casing drops below the melting temperature as the heat is flowing the other direction. The heat flux is much lower than the heating up and therefore takes much longer. The paraffin can clearly be seen solidifying starting at minute 40 and finishing at around minute 150.

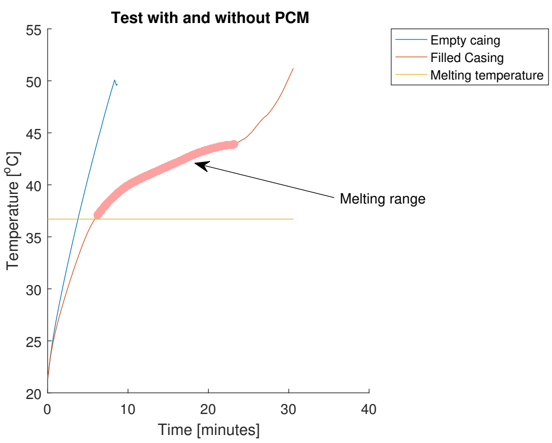

Figure 7.10: Thermal response of casing with and without PCM at 8W of power input

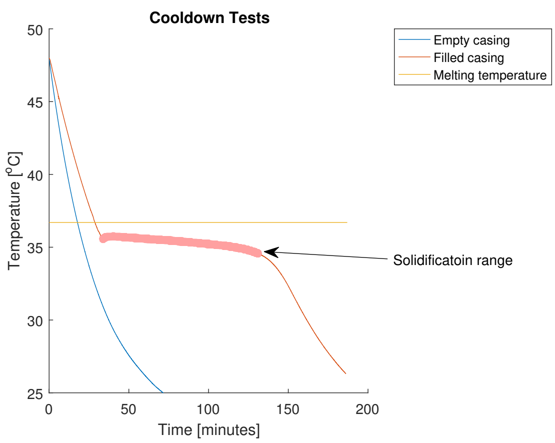

Figure 7.11: Cooling down of insulated casing in ambient environment with natural convection, conduction and radiation

After these measurements were complete the effect of gravity on the TSD was measured. The first prototype was measured in multiple orientations, the setups for which can be seen in figure 7.12. The results of these different orientations can be seen in figure 7.13. Here it can be seen that there is a slight variation in the final temperature but that is due to different starting temperatures of different setups. Some were started at 21 $^{\circ}C$ and others at 30 $^{\circ}C$ therefore the casings that started at 21$^{\circ}C$ have more of a thermal gradient when they reach

$30°C$ than those that started at that temperature.

Besides these complications the results clearly show a trend that gravity has an effect on the melting behaviour of the PCM. These measurements were done on the casing with the fins that run all the way to the lid of the casing. If the heater is placed near the bottom of the casing then it starts to melt from the bottom, causing the filler material to be suspended from the fins near the lid of the casing. Once enough of the PCM has melted a solid piece of PCM sinks towards the heater and causes a dip in temperature. This effect disappears when the heater is located above the PCM. In space, gravity will have much less of an effect and therefore it is unlikely for this large dip to occur in space. Small forces like inertial forces due to rotation of the satellite will have a much larger effect on this temperature drop. These are more difficult to predict however so the orientations where the heater is placed near the top of the casing are more conservative estimations on how the PCM device will respond in a micro-gravity environment. This effect is absent with the honeycomb casing as the honeycomb filler is only attached to the base plate where the heater is mounted, Because the honeycomb filler does not extend to the lid of the casing the PCM is supported by the honeycomb filler and does not sink to the bottom until it has shrunken significantly more than in the case of the fin filler casing.

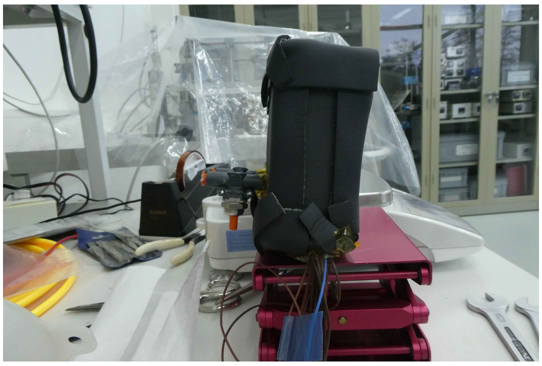

Figure 7.12: TSD oriented on its side with the heater near the bottom of the casing

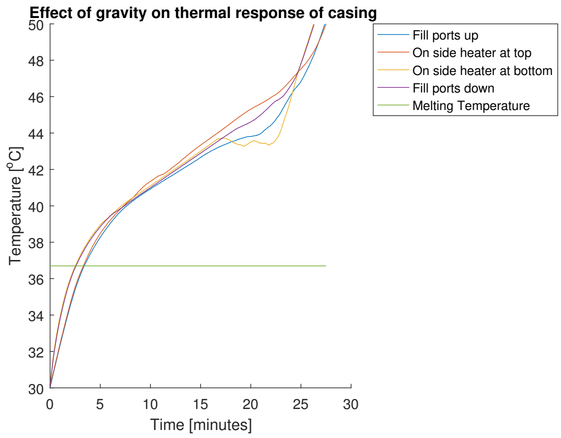

Figure 7.13: Results of casing thermal response at 8 W of power input in different orientations

The thermal response to multiple different input powers were tested for both of these casings. The thermal responses with 6, 8, 10 and 12 W of input power were measured. The results of the fin filler casing can be seen in figure 7.14 and the honeycomb filler casing in figure 7.15. A clear trend can be seen where the temperature of the casings increases as the input power increases. Also, a shorter melting period and an increase in the thermal gradient through the PCM is demonstrated by the steeper slope of the temperature increase.

To properly compare the different filler materials the 6 W thermal response of each casing is compared in figure 7.16 and the 12 W thermal response in figure 7.17. Here it can be seen in both graphs that the fin filler material casing is able to keep a slightly lower temperature than the honeycomb casing during the heat up phase, although not by any significant margin. The fin filler has the advantage of the sinking PCM in both cases although the final results are similar for both casings. These filler materials would probably be more significant if higher input powers were used and a finer filler material structure was used. Therefore it is expected that the foam filler material casing would have outperformed the other casings. Also as the fin filler casing uses less filler material and has a stiffer casing design, these results favour the fin filler casing for this design and use case.

To check if there are any issues in low cycle durability of the TSD a thermal cycle at least

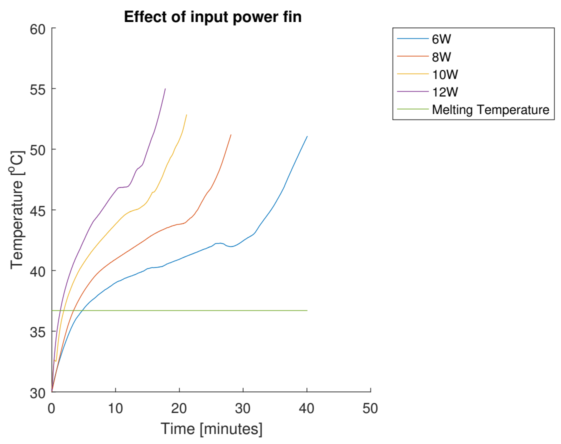

Figure 7.14: Effect of different power inputs to thermal response of the fin casing

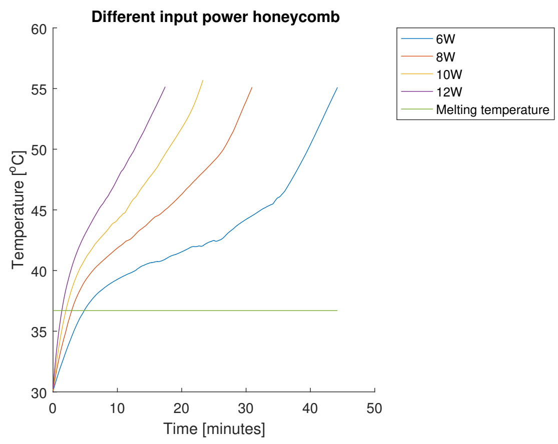

Figure 7.15: Effect of different power inputs to thermal response of the honeycomb casing

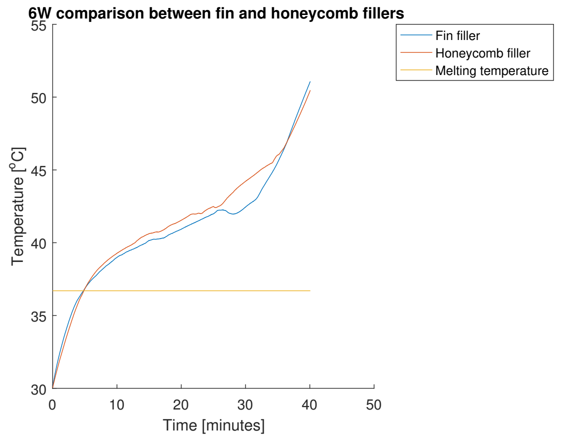

Figure 7.16: Comparison of the fin and honeycomb filer material at 6W of input power

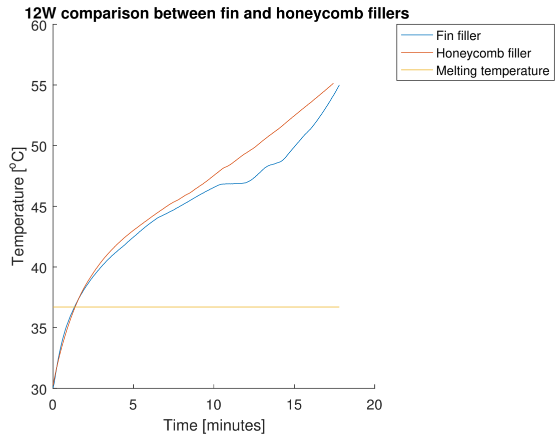

Figure 7.17: Comparison of the fin and honeycomb filer material at 12W of input power

12 times. 12 cycles where chosen as this is about the amount that could be fit into one day without stopping. It was chosen not to let the automated test continue at night for safety reasons. The results were then compared to check for any differences. The theory behind this reasoning is that changes in the amount of PCM or shape of the filler material in the casing would lead to a change in its thermal response, where this to happen it could be seen on a test.

- If a significant amount of PCM leaks from the casing:
  - The melting and solidification period will be shorter
  - The final temperature will be higher
- If the filler material were damaged:
  - the thermal transportation into the casing would be less effective thereby increasing the thermal gradient through the casing thereby increasing the final temperature of the heat source

As can be seen in the previous tests, there is little difference between the fin and the honeycomb filler materials, therefore even if the filler material were to be damaged somehow this would have little effect on the thermal response. These filler materials are robust and are not expected to break or deform in any meaningful way. The main experiments where the effect

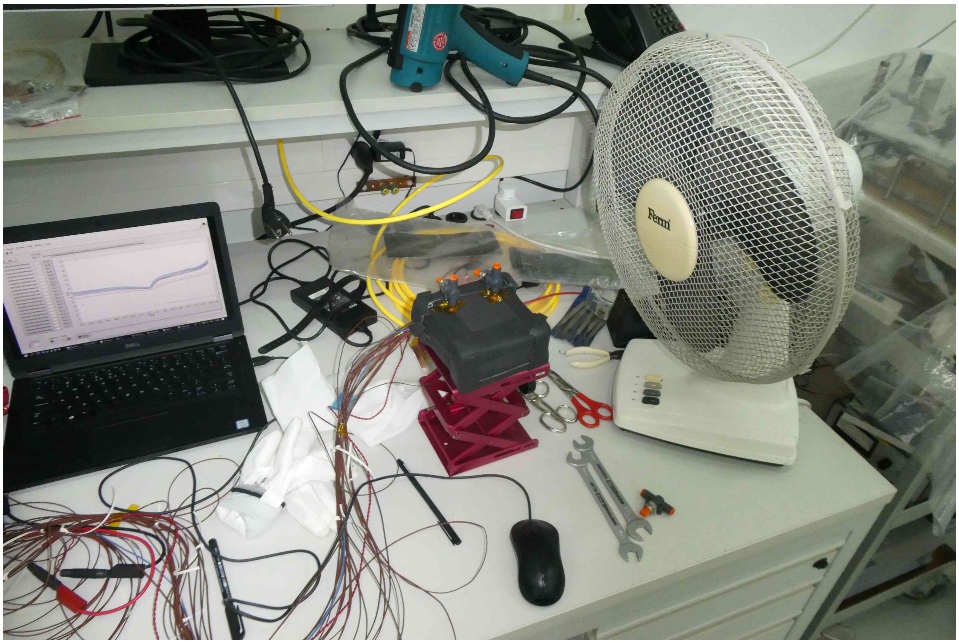

Figure 7.18: TSD setup with a fan for the thermal cycle tests

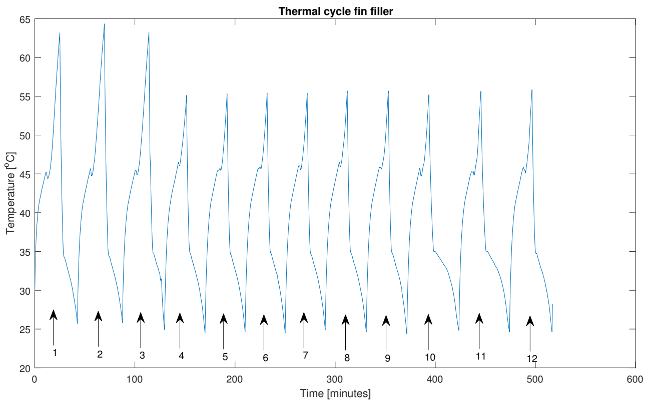

Figure 7.19: 12 thermal cycles of the fin casing

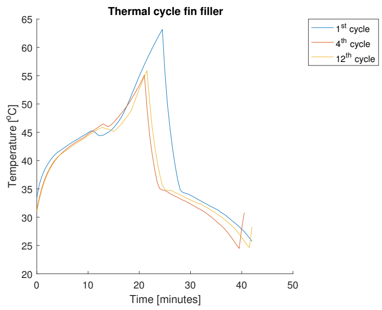

Figure 7.20: Endurance of the fin filler casing over 12 thermal cycles

of the thermal response should have been seen is the foam filler casing, as the cells in the foam are more fragile therefore more prone to breaking. The foam is also glued on, and since this glue could break after repeated thermal cycles and therefore a large change in thermal response should be measurable if this happens.

Multiple thermal cycles are difficult to measure because of changing thermal factors from day to day. The thermal cycles were not permitted to run overnight as it was still considered to be a fire hazard. To speed this process the input power for the thermal cycles was set to 12 W. To speed up the cooling section of a cycle the power was turned off and a fan was turned on. The fan caused forced convection over the casing and therefore had a more uniform heat transfer coefficient than natural convection would. This is because natural convection would be highly dependent on the buoyancy of the air and minor air currents in the laboratory.

The honeycomb casing-cycled experiments had the same setup as for the fin filler casing. The results of this test can be seen in figure 7.21. This setup did not have the difficulties experienced with the fin filler casing. The cycles were performed all on the same day and

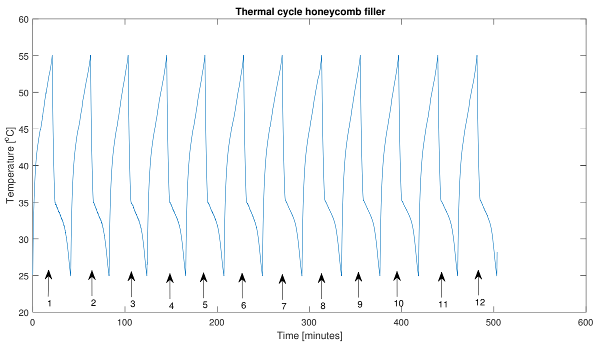

Figure 7.21: 12 thermal cycles of the honeycomb casing

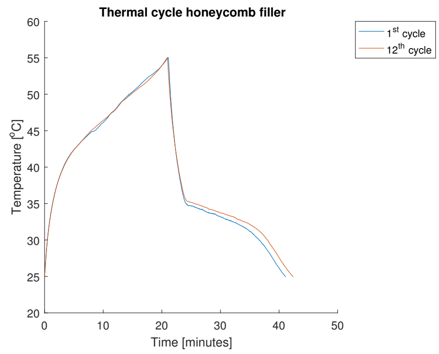

Figure 7.22: Endurance of the honeycomb filler casing over 12 thermal cycles

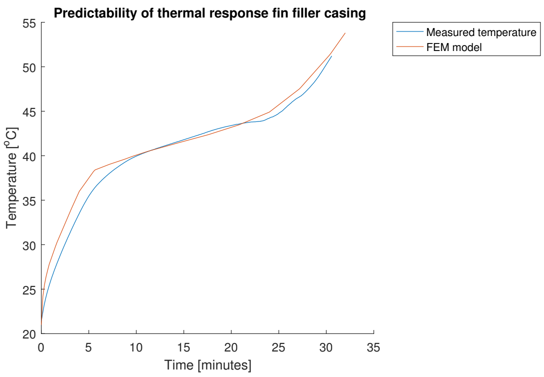

Figure 7.23: Fin filler prediction

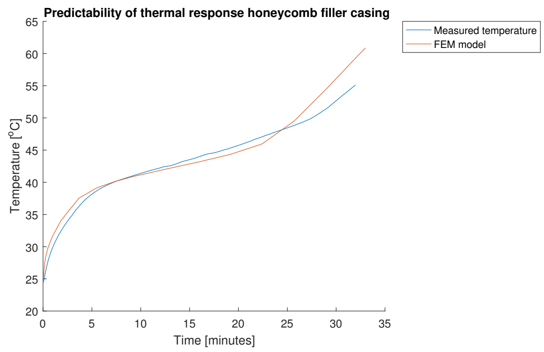

Figure 7.24: Honeycomb filler prediction

have almost identical thermal profiles as can be seen in figure 7.22.

The results of the thermal cycle tests conclude that this small number of cycles does not affect the filler material or the amount of PCM in the casing in any significant way. Although the first casing showed evidence of leaking PCM, the second casing was much better sealed. These small number of cycles did not seem to have an effect; a next step would be to increase the number of cycles to the expected life cycle of the satellite and see if it can endure these cycles. The measurement of the casing endurance should also be changed to allow for measuring small amounts of PCM leaking from the casing somehow. Also the experiment should be repeated in vacuum as this would increase the peak pressure differences in the casing, therefore increasing the risks of a leak forming in the casing.

The FEM models described in section 5 predict the performance of the TSD within the specified tolerances of 5 K. The comparison between these predictions and the measured results can be seen in figure 7.23 and figure 7.24. These models focus on conservation of energy, mass and heat transfer through conduction. The main things that needed to be measured were the heat loss to the environment and the contact resistance of the connector piece. The exact input parameters of the models are determined and displayed in Appendix E. The models are very accurate until and during the melting period of the phase change of the eicosane. After the melting period small differences in melting behaviour create large differences in the final temperature. Therefore if more accuracy is desired the models should be expanded to include in more details and the experiments should be performed in a better controlled environment. Ideally this environment would be a vacuum as this would remove the convective heat transfer and therefore much of the complexity in the model. This is of course also the environment in which the TSD will ultimately be used.

7.3.3. Integrated Setups

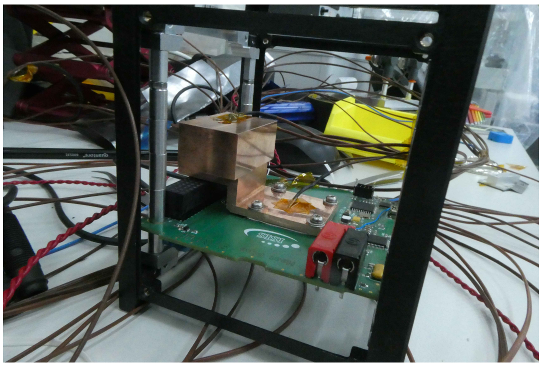

Figure 7.25: Integrated custom PCB with extra heat sink setup

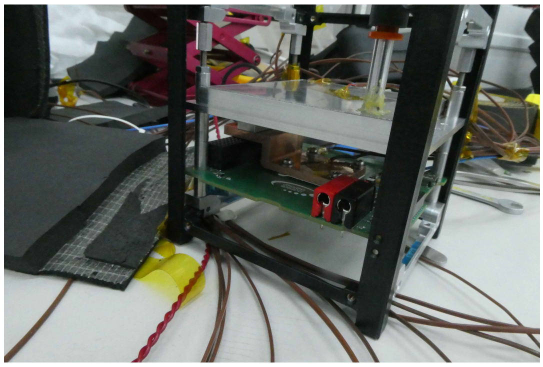

Figure 7.26: Integrated custom PCB with PCM TSD setup

The following setups are the subsystems that were integrated into the CubeSat frame. For these setups the custom thermal testbed PCB was used as heat source instead of the heater, this was meant to simulate the TXS. To show the effect of the TSD compared to a traditional copper heat sink the tests were performed with 8 W of input power until the casing reached about 50 $^{\circ}C$. First the PCB with the regular heat sink was tested; the setup can be seen in figure 6.4. Next the large copper heat sink was clamped onto the heat sink and the measurement was repeated. The setup of this experiment can be seen in figure 7.25. Finally the PCM TSD was attached and the test was again repeated. This setup is shown in figure 7.26 and the results can be seen in figure 7.27. The superiority of the TSD can clearly be seen over the regular heat sink setups.

In the next step, an aluminium block was attached to the TSD and the assembly was set in the thermal chamber. This was meant to replicate the temperatures the satellite is expected to experience in LEO. This was done to determine if the PCM still behaves as is expected in these environments. Also the mass dummy was meant to simulate the CubeSat battery pack. This test measured when and where the heat produced by the TXS flows. As can be seen in figure 2.2 the CubeSat frame temperatures rose from +40$^{\circ}C$ to -20$^{\circ}C$. These are of course the extreme temperatures of the casing and not all of the panels reach these extreme temperatures. Nevertheless the thermal profile set into the thermal chamber was meant to replicate these temperature swings in roughly the same time periods. As can be seen in figure 7.28 this was achieved. By raising the chamber temperature to 50$^{\circ}C$ degrees and lowering it to -30$^{\circ}C$ the frame followed the correct temperature profile. The main issue is that the heat conducts through the insulation and into the frame causing it to cool. It also conducts through the air in the frame, causing the subsystem temperatures inside the assembly to have much larger temperature swings then is usually the case in orbit. Usually these temperature swings are on the order of 15 K and not 30K as seen in figure 7.28. Although these temperature swings can still be seen in CubeSats with different configurations, orbits and orientations.

The following figures show how the heat was absorbed into the casing, although the full use of the casing was never reached. In fact only at the end of the power transmission did the heat from the TXS start to melt the eicosane. Nonetheless some effect of the melting can clearly be seen. The temperature slopes of the subsystems clearly decrease after the temperatures rise above the eicosane melting temperature. Also a slight extension in the elevated temperature can be seen after the temperatures drop below the solidification of the eicosane. The duration and start period of the input power can be varied to measure different results. The variations of these can be seen in figures 7.29, 7.30 and 7.31.

Figure 7.32 compares the battery temperatures of the integrated thermal chamber tests. This was done to see how much of the TXS power entered the battery mass dummy. An important thing to note is that all these comparisons had different starting temperatures. This is due to the dynamic behaviour of these tests. None of the tests were done from a steady

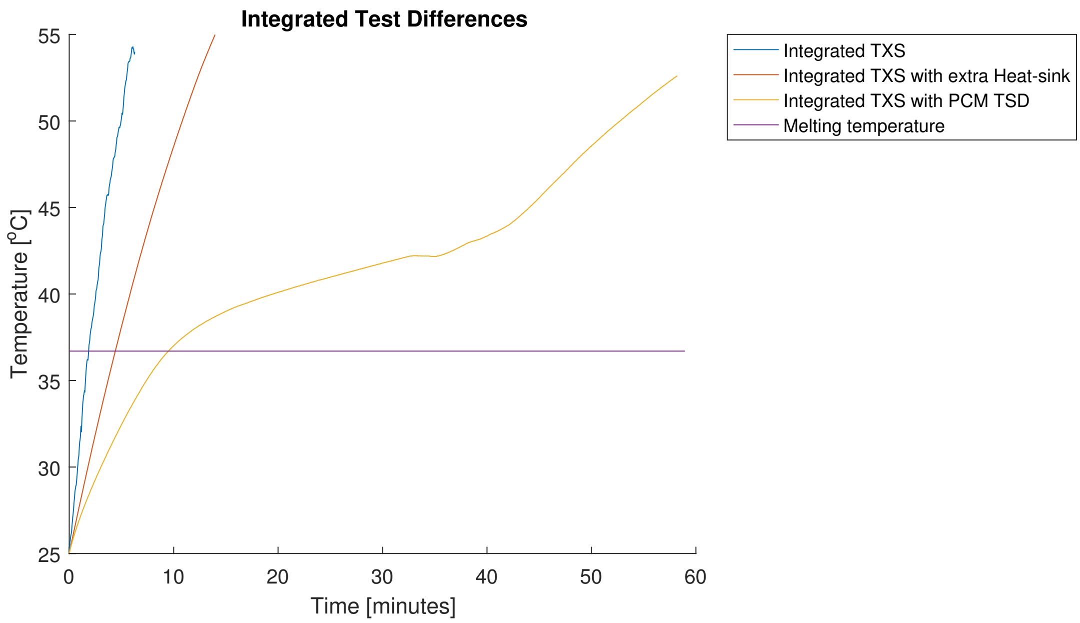

Figure 7.27: Different setups comparison

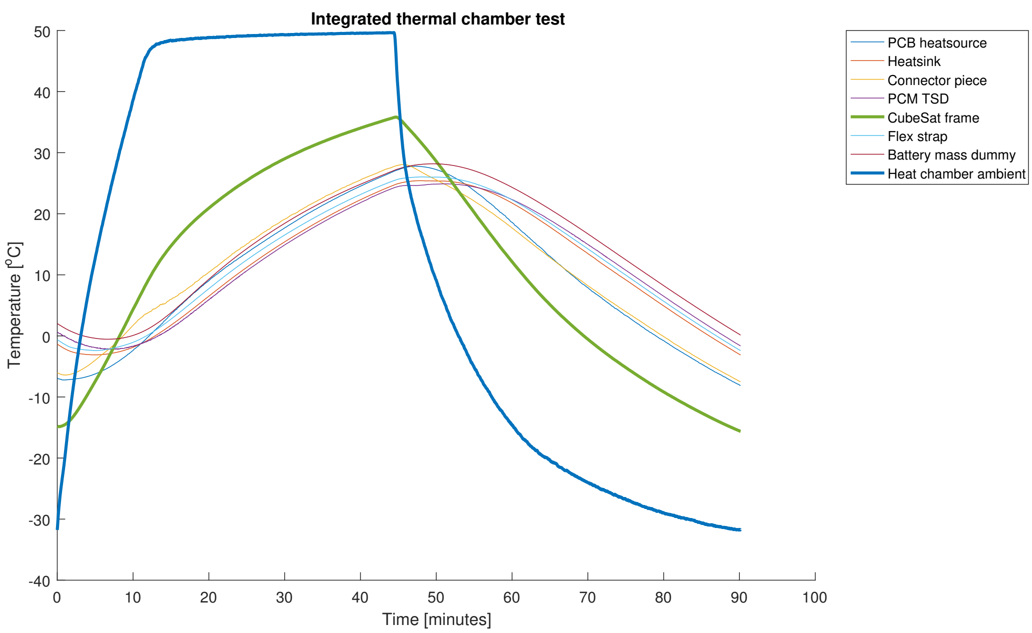

Figure 7.28: Integrated thermal chamber setup with no power input

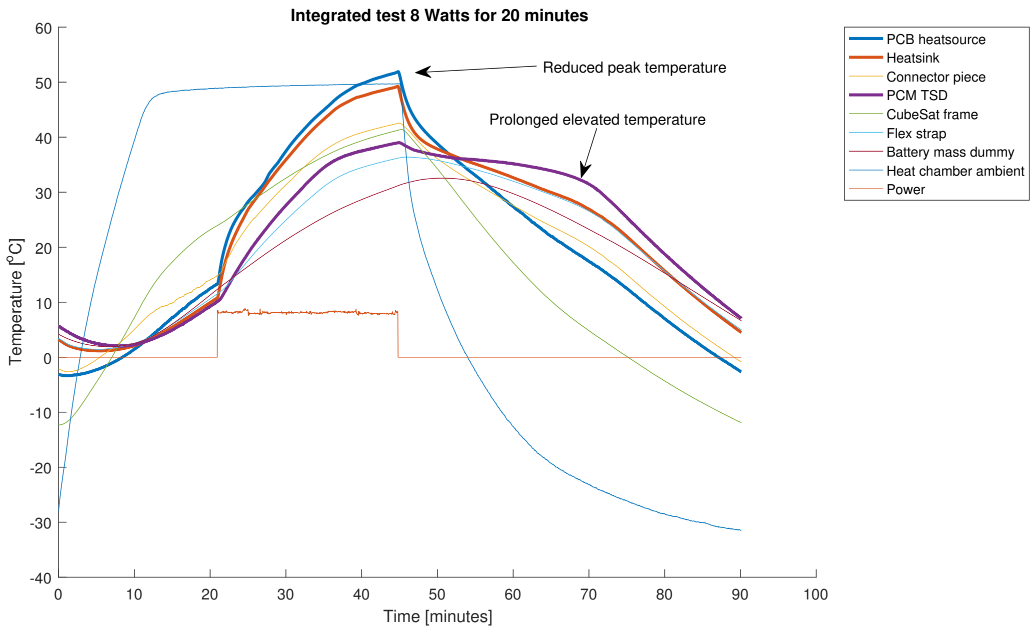

Figure 7.29: Integrated thermal chamber setup with 8 W of power for 20 minutes

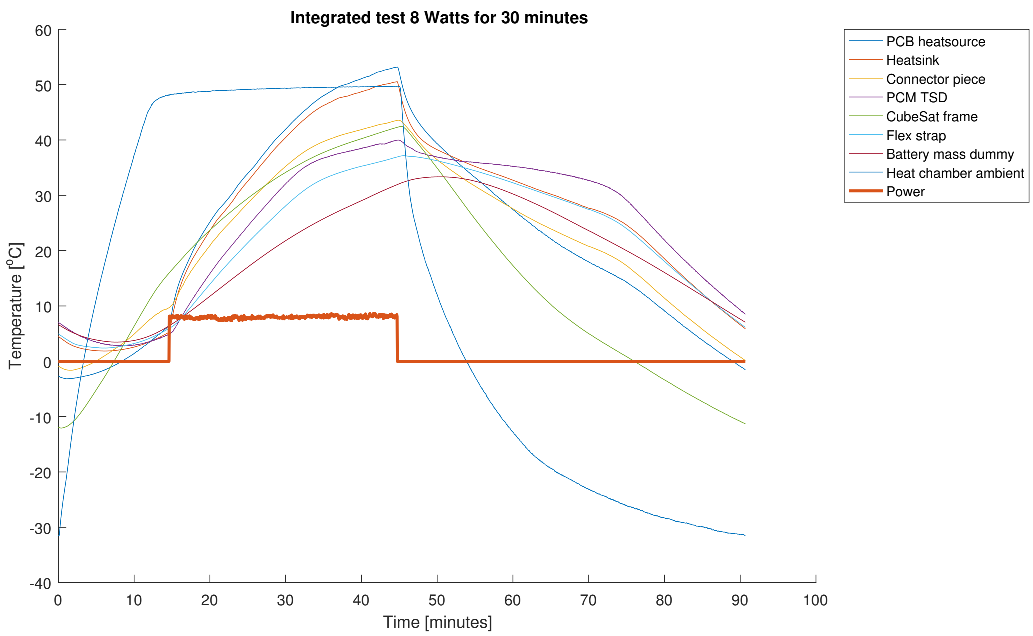

Figure 7.30: Integrated thermal chamber setup with 8 W of power for 30 minutes

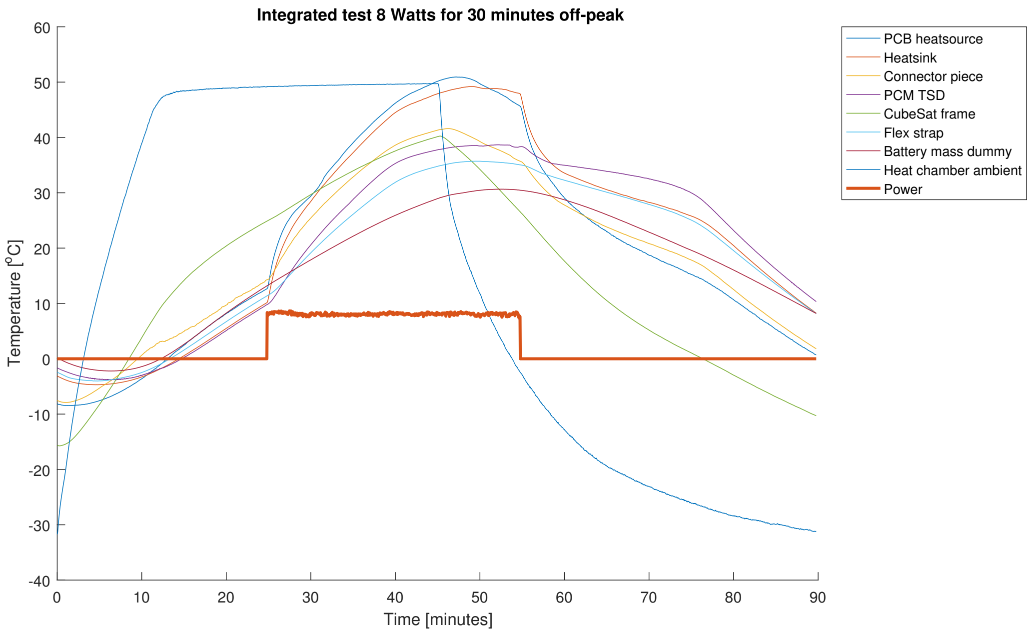

Figure 7.31: Integrated thermal chamber setup with 8 W of power for 30 minutes slightly delayed

state temperature, therefore it is very difficult to control the starting temperature of all the sub-components. This is done because in an actual LEO environment the satellite will also not be in a steady state but continually in a transient state. Even though the battery had different starting temperatures, the battery tests that had the power input and therefore a phase change reaction ended up at similar temperatures whereas the one that did not end up at a much lower temperature. This setup is meant to elevate the minimum temperature of the battery pack mass dummy. Therefore the peak temperature of the battery pack mass is also much higher. If this peak also needs to be reduced then either the thermal resistance to the TSD needs to be increased or a PCM with a lower melting temperature is needed. This is a trade-off that needs to be made as this would reduce the effectiveness of the TSD for the TXS.

Another option to decrease the thermal peak of the casing would be to have a hot and a cold side of the TSD. The problem with this is that the aluminium casing conducts very well and therefore evens out the temperature. To reduce this effect the wall thickness of the casing would have to be decreased and the fins would not be allowed to run all the way through the casing. This would have structural consequences for the casing but could be a possible solution. One final option would be to somehow add a separate poorly conducting material between the two casing halves. These designs would have beneficial properties, but they would increase complexity in the design.

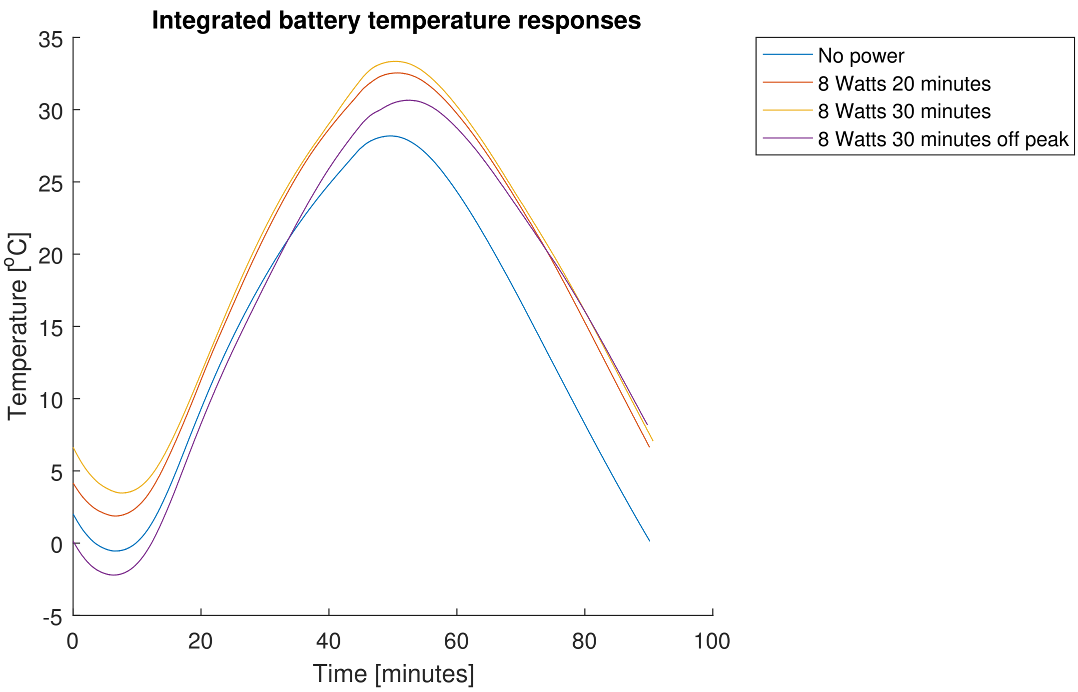

Figure 7.32: Comparison of battery temperature tests with the different integrated setups

7.3.4. Conclusion of Results

This section is a brief summary of the results and the conclusions that can be drawn from them. The following is a summary of the tests done to determine the characteristics of the casings:

- The PCM TSD is able to greatly increase the heat up and cool down time for the heat source when the PCM goes through a phase change (figures 7.10 and 7.11).
- Depending on the orientation of the casing in relation to its heat source and gravity the solid PCM tends to have a negative buoyancy and therefore will start to sink in the direction of the gravity. This positively effects the thermal response of the TSD. Although, in orbit this effect would be dominated by inertial forces on the satellite or currents within the liquid PCM (figure 7.13).
- Increasing the power of the heat source decreases the melting period and increases the final heat source temperature when all the PCM has melted (figure 7.14 and 7.15).
- The fin filler casing was able to keep the temperature of the heat source lower than the honeycomb filler casing could during its melting period. This is the opposite of what it was modelled to be in the previous chapter. Although these differences are small and don't show a large advantage either way. This can be explained through possible differences in ambient temperature, clamping pressure or possibly the different manufacturing methods between the casings (figures 7.16 and 7.17).
- The PCM TSD seems to have a stable heat up and cool down cycle throughout the 12 thermal cycles done during the thermal cycle tests. The honeycomb casing was especially consistent. Although during later inspection it turned out that the fin filler casing did end up leaking paraffin after the thermal cycles and was therefore not properly sealed. The fact that this could not be seen on the thermal cycle tests indicates that this test is not enough to show that the casing properly seals the PCM (figures 7.19, 7.21, 7.20 and 7.22).

- The casings followed the predicted temperatures well once all the heat fluxes and contact resistances where measured and properly modelled. Although some deviations still exist these could be prevented by repeating the tests in a more controlled thermal environment where the heat fluxes can be calculated more precisely (fures 7.23 and 7.21).

Next is a summary of the results of the integrated test setups:

- The integrated tests show how the TSD performed compared to a traditional heat sink of the same mass. When the TXS was attached to the TSD its heat up period and therefore possible transmission time was increased to more than an hour (figure 7.27).
- The final tests created a temperature profile that can be expected of a satellite in LEO. The TXS was testes in this environment and was able to transmit without overheating for extended periods of time during different phases of an orbit. in all cases the heat source peaked at around 50 $^{\circ}C$ and the TSD maintained an elevated temperature during its solidification period when the heat source was used. This heat was slowly transferred to the battery pack mass thereby increasing its peak and minimum temperatures by about 10 $^{\circ}C$ (figures 7.28, 7.29, 7.30, 7.31 and 7.32).

8

Discussion

This chapter discusses the findings of the thesis. Most of the results of this thesis show that the TSD design is a feasible TCS for a CubeSat. Designs where made that passed the test criteria and after some optimization have high potential to be a feasible prototype for on a CubeSat. The TSD was able to keep the TXS subsystem within its operating temperature for extended periods of time, more effectively than classical methods.

The casing was also able to store the heat produce by the subsystem and use that heat later to keep the battery warmer. Although the casing design could be changed by making a casing with hot and a cold attachment points. The thermal response of the casing was also predictable within the five degree tolerance set at the start of the thesis. This validates the modelling method and allows for rapid redesign thereby optimizing the casing.

These results are promising and show a successful test campaign. The rest of this chapter will focus on issues that could possibly lead to problems with these results.

8.1. Models

The model predictions seemed to predict the test results fairly well. This was confirmed by measuring the casing at multiple points with several different input variables. For a higher degree of accuracy a more controlled thermal environment is needed to keep track of the heat entering and leaving the system. The tests will also have to be repeated in a vacuum to be able to see if temperature predictions are still valid when its orbit.

The models were inaccurate in predicting the buoyancy effect due to gravity. This is mostly because no attempted was made to model it has little effect on the final casing temperature. This effect could become dominant in different temperature ranges and environments. This is another reason that the tests need to be repeated in the expected use case environment.

8.2. Experiments

Early on in the testing a mistake was made in using the wrong type of TC. A type-t TC was attached to a type-K TC. In principle this only resulted in a small error as these TCs have very similar voltage readings in the temperature range in which the tests where conducted. This is also borne out by the lack of error in the TC calibration.

Having said that the fact that two different types of TCs were attached to a junction causes another error: at this extra junction a second thermoelectric effect takes place because different metals used in the TCs (alumina-constantan). If there were a temperature difference between this junction and the reference temperature this would create an error in the measurements. The error is easily estimated as this test was done with 21 TCs and only five of hem had this incorrect junction. Therefore if these TCs are ignored in these first tests then the results are still valid. In an attempt to validate this flawed data one of the test was repeated using all the same input parameters but with the correct TC junctions. In this test physical differences could be estimated by comparing the TCs that were already correct in the previous tests. Errors introduced by the different TCs could be seen by comparing the difference in the results of these two sets of tests. What was found was that these differences were all within a degree so the results of these tests were not completely invalid. Although it is not prudent to take direct results of these TCs as actual test data, clear patterns and trends were captured and used to compare the results to other tests using this flawed setup. This assumes that no changes occurred in the junction temperature versus the reference temperature during this period.

During the first casing tests it was obvious that eicosane had leaked from the casing. There was residue found on the insulation material and piles of eicosane around the fill ports and along the weld were also found. The eicosane deposits were also often found on the sticky side of the tapes used to attach the TCs to the casing. Therefore there was some eicosane build-up around the TCs. In the second casing this build-up on the tapes was found again, pointing to some form of contamination. It is unclear if this was eicosane or other residue, from out-gassing Aralidite epoxy for instance. This suggest that some eicosane might have escaped the casing, although it is strange that this residue was not found anywhere on the insulation. A more plausible explanation is that due to the eicosane build-up around the TCs in the tests of the previous casing, there was eicosane on the TCs themselves. And as the TCs were reused for the second casing this residue when heated out-gassed from the TCs onto the tape leaving behind some residue. This would explain why the eicosane was only found locally in this area, although this is by no means proof and therefore would require more rigorous testing to actually detect these small leaks.

The integrated thermal chamber tests were meant to demonstrate the full potential of the TSD casing as it could show how it would store energy in a real thermal environment expected use case. Although the CubeSat casing reached the correct temperatures the subsystem's temperature swings were much larger than expected in orbit. Therefore a lot of energy from the PCB heat source was used to heat the subsystems to the melting temperature before it could be used in the phase change reaction. This can easily be counteracted by repeating the same tests with lower temperature swings in the thermal chamber. However the casing temperature would not have the correct temperature and would therefore absorb more heat than it would in orbit. Although these temperature swings do occur in other CubeSats than the Hiber satellite due to different configurations and orbits. The tests that were performed in the thermal chamber did accurately show the trend of how the heat would distribute itself within the satellite thereby accomplishing the goals of the tests.

Multiple tests that were planned had to be cut short or cancelled due to the Covid-19 outbreak and subsequent shutdown starting in March 2020. The tests that were cancelled are:

- Repeated thermal chamber tests with different configurations and temperature profiles.
- All the tests with the metal foam casing.
- The tests to see how well the pinch seal would work.

9 Conclusions

The PCM TSD is feasible to use as a thermal storage device for CubeSats. The TSD significantly increases in performance while reducing the mass of the thermal control system.

The first casing with the fin filler was not sealed properly, and therefore it started to leak eicosane during the tests. This was likely due at least in part to imperfections in the fabrication of the prototype and the design. The second casing seemed to seal off the PCM well and could be used for further testing.

The predictability of the thermal response of the casing with the FEM software was within the five $^{\circ}C$ accuracy set at the start of the thesis. The model is sufficiently accurate as long as a five $^{\circ}C$ margin is used in the CubeSat thermal design. The model had difficulty predicting the convective cooling effects of the ambient environment, but in space this would be less of an issue and therefore would likely have a higher degree of predictability. However this still needs to be demonstrated in vacuum tests. Other things the model does not predict are cavities and the sloshing of a partially melted PCM in the casing. This could be predicted if an inertial spinning force were applied to the CubeSat, but best practice would be to assume the worst case scenario for the PCM casing.

The tests that were conducted for the casing design to be considered a feasible prototype but are by no means a complete qualification. More testing will be needed before these components can be flown on CubeSats. The main tests are:

- That the casing keeps a proper seal and prevents PCM from leaking after a CubeSat lifetime of heat cycles.
- That the casing is able to keep this seal in a vacuum, even after these large number of cycles.
- That the thermal response of the casing is just as (if not more) predictable in a vacuum as it is outside of it.

9.1. Answers to the Research Questions

The main research question is:
Can a Phase Change Material Thermal Storage Device (TSD) be used as a reliable thermal control system for a CubeSat?
The short answer is yes, PCM TSD show potential to be used as a reliable TCS for a CubeSat. A more detailed answer discussed in the following sub-questions.

Can a CubeSat benefit from a PCM TSD?
Yes, this was clearly demonstrated in the tests results shown in figure 7.27. The CubeSat can benefit from a PCM TSD if the satellite or a subsystem thereof experiences large heat

peaks and valleys that limit its use or could potentially cause damage thereby reducing its operational lifetime. The PCM TSD could potentially reduce the peaks and valleys.

What subsystems would benefit from having a PCM TSD?
The subsystems identified in this thesis where thrusters, radios (especially the power amplifiers), and the batteries. This is of course by no means an exhaustive list and will increase when the power-densities of CubeSats increase.

How could the PCM TSD be implemented?
If a specific subsystem needs thermal stabilization, then the PCM TSD can be directly attached to that component. The TSD would then attempt to balance out the temperature as much as possible, and/or keeping it from reaching extreme temperature peaks or valleys.

What are the design requirements for a CubeSat thermal control system?
The design requirements of a CubeSat thermal control system are to keep the temperatures of the satellite subsystems within their respective operational temperature ranges without exceeding CubeSat requirements. These requirements are listed in the questions below

What are the mass, volume and cost budgets for CubeSats in relation to the thermal control system?
Traditionally TCSs have a mass percentage of 5% of the satellite, leaving about 65 grams per unit CubeSat for the PCM TSD. Although these are just traditional guidelines and are a good starting point for designing the system, they are by no means a hard limit. The volume for the TSD is a bigger issue as this is more limited on a CubeSat, and PCMs often have low mass densities. Therefore a large volume will often be required for the PCM TSD. There are no specific limits to this either but 10% per unit of a CubeSat seems a reasonable upper limit and is much more than is required by the current system. There are multiple places in a CubeSat where there is extra volume that could be utilized by the PCM. This is currently often taken up by electrical harnessing, but some room could be made for a PCM system. The cost of CubeSat components tend to be in the range of \$1000-\$100000. The intent is to make this a cheap and simple component so the limit of the TSD price should be around \$1000. In the end the actual price of the TSD was about €350, but the unit price could be about half of that if a series of 5 or more identical TSDs are made.

What are heat loads a CubeSat can experience that would require thermal control from a TSD?
High power intermittent heat loads from components could be dampened out by the PCM TSD. The energy from these peaks and valleys can also be redistributed to other satellite components adjusting their temperatures to be more favourable as well.

What temperatures need to be maintained by the CubeSat thermal control system for it to be successful?
Temperature needs vary amongst subsystems connected to the TCS. As long as the TSD is able to keep all components attached to it within their own operational temperature ranges it is working successfully. This would only work if the subsystems have operational temperatures in common and if the PCM has a melting point at this temperature.

What other requirements does a CubeSat have for a thermal control system and can all these requirements be met by a PCM TSD?
There are multiple general CubeSat requirements that every component needs to adhere to. These are listed in the CubeSat standard [2]. One particularly critical to PCM TSD is that the PCM has to be non-hazardous. The casing also has to be leak-proof as leakage will render the PCM ineffective and contaminate other satellite subsystems on the CubeSat or any other possible satellite in the vicinity (during ride-shares).

How does a PCM system need to be designed to control the heat load?
The case taken in the thesis was to design the PCM TSD to keep the TXS radio transmitter

power amplifier below its maximum operational temperature of 80 $^{\circ}C$. This is a specific use case that determined the shape and size of the TSD but could in principle be applied to multiple use cases.

What PCM should be used? Paraffins where chosen as the simplest and safest option for use on CubeSats. Although several other possibilities were identified in the event paraffin did not perform as well as required. Eicosane ($C_{20}H_{42}$) was chosen as the best paraffin for this thesis as it has a melting point above expected operational temperature (36.7 $^{\circ}C$) of the Satellite. That way the paraffin would not unintentionally be partially melted by the time it needed to cool the TXS. For other use cases a different paraffin could easily replace the eicosane. Paraffins are fairly similar but differ their melting temperatures and latent heat of fusion. It would be prudent to check other attributes of the material before using them as there are several other minor differences between paraffins.

How much PCM is required to absorb the heat load?
For eicosane about 30.35 grams is sufficient to absorb and release the 8 W emitted for 20 minutes by the TXS. In experiment it could be seen that the TXS was able to run for nearly 60 minutes before the TSD reached 50$^{\circ}C$.

How should the casing be of the PCM TSD be designed?
The casing should be as lightweight as possible while still keeping its structural integrity and ability to withstand the number of heat-cycles it is expected to experience in orbit. By adding fins as filler, allows the heat to penetrate better into the paraffin. Also a threaded bolt hole within the fin allows for components to be clamped directly onto the casing, minimizing the thermal contact resistance. Adding different types of filler materials to the casing can improve the performance, but also increases the mass and complexity of the part. And finally the casing should be sealed so that there is no risk of contamination from the paraffin inside. In this regard, the best performing casing as shown in the tests in this thesis were the machined casing and lid glued together with Aralite epoxy. And the best sealed fill ports were the ones clamped to the casing with a threaded tube connector with an o-ring. The threaded tube connector can later be replaced with a cap or can be sealed using a pinch seal to reduce the space the TSD takes up. Once the casing feasibility has been proven, optimization of the design can start, this can be done by:

- Reducing the mass of the casing as much as possible.
- Optimizing the filler material to have the best heat absorption. Here 3D printed filler material can create the optimal casing structure and filler material geometry.

Where should the PCM system be placed and to which components should it be thermally coupled?
When designing a TCS the subsystems to which it is thermally connected are critical part of the design. Which components should be coupled to the TSD depends on which components need to have their temperature extremes balanced out, and also possibly which components can benefit by being connected to the TSD. This is of course assuming that the components selected have similar temperature ranges and that sharing their heat loads would be beneficial to the component instead of exacerbating existing the thermal issues. Therefore a single TSD can be connected to multiple subsystems with similar thermal requirements. This also works best if there is a hot side and a cold side to the TSD, which is not the case in with the current design of the casing.

How can this system be sized to fit inside a CubeSat?
This thesis focused only on the 1U, 2U and 3U CubeSats. More options for fitting the TSD open up when larger structures are used. The main locations where there is enough room for the TSD is in the stack between the PCBs, in the area in between the CubeSat stacks, (although this is often filled with wire harnessing) and at the top or bottom of the CubeSat. The shape of the TSD should be a rectangle with edges as wide as possible to fit within the CubeSat stack thereby minimizing the thickness it takes up, while maximizing the PCM volume.

This ensures the TSD is efficiently using the volume inside the CubeSat and is not taking up room that is needed for other PCBs, or subsystems. Rounded surfaces might create less stresses in the casing and a more even melting profile of the PCM but would ultimately have less PCM in the casing. Finally by making the casing shape and attachment interfaces to allow placement in multiple possible locations creates flexibility for use in CubeSats.

How can the TSD be made sufficiently reliable so that it can work properly for the entire duration of a CubeSat mission?
This remains an un-answered question as the number of thermal cycles experienced by a CubeSat can vary per mission. To design on the safe side, the casing should be able to withstand fatigue at the higher end of these cycles. This can only be proven by doing tests with large numbers of thermal test cycles in a vacuum environment. There should also be a good way to accurately measure if the casing is emitting paraffin contaminants. The first prototype was not able to withstand the relatively small number of thermal cycles in an ambient environment. This leak was noticed after the cycled durability tests, although it is possible that the leak already occurred earlier. The second casing did very well and did not appear to suffer any paraffin leak, although no test measurements were able to confirm this on a significant level. Although it is critical to prove that a PCM casing can last a larger number of cycles as there is a real risk of fatigue in aluminium and degradation of eicosane over a large number of thermal cycles.

Can the performance of the PCM TSD be predicted accurately, using thermal theory and numerical models?
The FEM model made for this thesis was able to predict the test results within an accuracy of five $^{\circ}C$. The thermal response can properly predict the temperature although it is more difficult to predict exactly when all the PCM has melted. This is a function of the conservation of energy in the casing. The exact accounting of all the heat leaving the system is dependent on convection, conduction and radiation. These are less controlled in an ambient environment then would be in a space environment. The same is true for the effects of cavity formation in a gravity environment which are largely effected by buoyancy. So this could possibly be more predictable in a vacuum micro-gravity environment. The use for this model would mostly be in optimizing the design of the casing, maximizing the heat absorption while minimizing the mass and volume of the casing. Once the thermal response of the casing has been clearly mapped out these profiles can be introduced into models with much less detail.

What properties need to be modelled for an accurate model numerically?
The main way heat travels within the casing is through conduction so the FEM model only takes conduction into account. This is sufficient to predict the heat distribution within the casing. As for calculating the exact heat fluxes in and out of the casing, it is difficult to do this in an ambient environment. If the thermo-optical properties of the casing are accurately mapped then these fluxes can properly be predicted. For the modelling in this thesis the heat fluxes where measured to approximate the heat fluxes to compensate for this. Other things not taken into account when modelling were the expansion of the PCM and the cavity formation. The results of the predictions were close enough to predict the thermal results accurately within five $^{\circ}C$ (although this is only be said for the temperature ranges it was tested. If these casings are to be used in different temperature ranges they will need to be validated for those as well). It is possible that under those circumstances other effects might become dominant.

How can these models be validated so that their results can be relied on?
The validation of the model comes from predicting the thermal response in multiple test configurations and finally from predicting the response for the actual use case in LEO.

10
Recommendations for Future Work

This chapter of the thesis will discuss the opportunities identified that could be of potential be interest for future work. The main goal of this chapter is to summarize some of the work that will need to be done in the future to fully answer the research questions. The following is a list of such work identified during the thesis:

- To create a more exhaustive list of CubeSat subsystems that would benefit from a PCM TSD. The current list consists of thrusters, radios and batteries. Some technologies may have been overlooked in the CubeSat market because of their thermal properties. This would clarify opportunities for PCMs and therefore the CubeSat market.
- To explore the use of different PCMs besides paraffins, for instance fused salt, ionic liquids and eutectics. It would be useful to have a more complete catalogue of these materials and their opportunities versus risks for CubeSats. Also working on engineering solutions to issues that are relevant to those PCMs that were not required for paraffins.
- To model a topology optimization for the filler material on a CubeSat casing. This could be very useful if a casing like this is 3D printed. This would be ideal for getting the best results from the TSD with the least amount of mass.
- The manufacturing of the first casing was done with welds and glues. Both of these seals appeared to not fail after multiple thermal cycles. Although the gluing of the fill ports with such a small surface area was a flawed concept, the welded connection might still be viable option. Mistakes and misalignments in the manufacturing, and by giving correct models to the technician, and by instructing the technicians that the casing had to be helium airtight, it is still possible that the laser welds could be used. Another interesting possibility is if the fill ports were to be attached with laser welds as well. This could be interesting work if the glued connections turn out to not be as airtight as required.
- Future work doing these kinds of thermal response tests would benefit from starting each test at the same temperature. The tests in this thesis were started at slightly different temperatures due to different ambient temperatures and leftover heat from previous tests. The different tests were compared once they reached a common temperature at the thermocouple. In fact this will cause differences in the thermal gradient to become obvious. Most noticeably this can be seen in figure 7.13. Here slightly different starting temperatures caused the solutions of the same casings to diverge into different thermal responses. Some of these effects are due to the difference in orientation of the casing, and some of them are due to the difference in starting temperature.
- The next obvious tests that should be done are those that were planned during this thesis but where unable to continue due to the Covid-19 outbreak. These include the foam casing tests and the thermal chamber tests with smaller temperature swings.

- Also mentioned in the thesis is that the airtight seal of the casing needs to be proven during multiple heat cycles in a vacuum, which should be done sequentially in increasingly better vacuum chambers (as it would be expensive to ruin the very sensitive vacuum chambers on unproven casings). The first steps in doing this would be to increase the number of thermal cycle tests beyond what was done during this thesis. Also a method should be found to measure the paraffin vapor escaping the casing. The amount that was leaked during the first set of tests could not be measured on the scales that were available in the lab. The only reason they were noticed were the paraffin deposits on the casing after multiple tests.
- Once the hermetic seal of the casing has been proven it would be good to test how well the casing would work in a vacuum environment. These tests could also map the best methods for thermally connecting other components to the casing. The reason the casing was not immediately tested in a vacuum environment was because this would risk contaminating sensitive vacuum chambers and other equipment with paraffin, as mentioned in section 4.3.4.
- Finally after the casing has been sufficiently proven not to be a contamination risk to the satellite it should be used in space to fully validate the effectiveness of the device.

Bibliography

[1] Spaceflight101. Flock-2k, 2020.

[2] The CubeSat Program. Cubesat design specification, 2009.

[3] S. Kang and H. Oh. On-orbit thermal design and validation of 1 u standardized cubesat of step cube lab. *International Journal of Aerospace Engineering*, 2016.

[4] KLINT FINLEY. Nasa lets you build your own satellite with phonesat, 2012.

[5] William Graham. Russian dnepr conducts record breaking 32 satellite haul, 2013.

[6] Erik Kulu. Nanosats database, 2019.

[7] A. Golkar A. Poghosyan. Cubesat evolution: Analyzing cubesat capabilities for conducting science missions. *Progress in Aerospace Sciences*, 88(November 2016):59–83, 2017.

[8] Innovative Solutions In Space BV.

[9] Z. de Groot W. Ubbels J. Rotteveel H. Brouwer, L. Teodor. Setting the standard for the 6u internet-of-things cubesat platform: Platform design and in-orbit results. *Proceedings of the International Astronautical Congress, IAC*, 2019-october:21–25, 2019.

[10] Gunther's space page. Hiber 1, 2, 2017.

[11] David G. Gilmore. *Spacecraft Thermal Control Handbook*. The Aerospace Press, 2002.

[12] J. C. Zagal E. Escobar, M. Diaz. Evolutionary design of a satellite thermal control system: Real experiments for a cubesat mission. *Applied Thermal Engineering*, 105:490–500, 2016.

[13] M. Bulut and N. Sozbir. Analytical investigation of a nanosatellite panel surface temperatures for different altitudes and panel combinations. *Applied Thermal Engineering*, 75:1076–1083, 2015.

[14] Y. Nagasaka H. Nagano. Simple deployable radiator with autonomous. *JOURNAL OF THERMOPHYSICS AND HEAT TRANSFER*, 20(4), 2006.

[15] Lynn Jenner. Nasa's new shape-shifting radiator inspired by origami, 2017.

[16] Technology applications inc. Thermal straps, 2016.

[17] R. Dudziak S. L. Tuttle, S. M. Barraclough. Advanced thermal control technologies for nano - satellites. *47th International Conference on Environmental Systems*, (July), 2017.

[18] NASA. `https://sst-soa.arc.nasa.gov/07-thermal`. Accessed: 2019-04-19.

[19] M. Hulse D. Hengeveld P. Hamlington S. A. Isaacs, D. A. Arias. Development of a two-phase heat strap for cubesat applications. *46th International Conference on Environmental Systems*, (July), 2016.

[20] J. Guo H. Brouwer, Z. De Groot. Ssc17-vii-06 solving the thermal challenge in power-dense cubesats with water heat pipes. *31st Annual AIAA/USU Conference on Small Satellites*, 2017.

[21] R. C Van Benthem J. Van Es, H. J. Van Gerner. Component developments in europe for mechanically pumped loop systems (mpls) for cooling applications in space. *46th International Conference on Environmental Systems*, 2016.

[22] K. Mercier P. Guillemot M. Roux, M. Mallah. Designing eclairs and mxt thermal buses for the svom project. *European Space Thermal Engineering Workshop*, 2018.

[23] J. Wertz W. Larson. *Space Mission Analysis & Design*. The Aerospace Press, 2005.

[24] Q. Young D. Homan. The challenges of developing an operational nanosatellite. *22nd Annual AIAA/USU Conference on Small Satellites*, pages 1–7, 2007.

[25] ISISpace BV. Cubesat solar panels.

[26] Panasonic. `https://na.industrial.panasonic.com/sites/default/pidsa/files/ncr18650a.pdf`. Accessed: 2019-04-19.

[27] A. Garzón and Y. Villanueva. Thermal analysis of satellite libertad 2: A guide to cubesat temperature prediction. *Journal of Aerospace Technology and Management*, 10, 2018.

[28] ISISpace BV. Isis high data rate s-band transmitter.

[29] EO portal. Qbito.

[30] R. Peyrou-Lauga O. Pin N. Nutal M. Larnicol J. Crahay J. P. Collette, P. Rochus. Phase change material device for spacecraft thermal control. *62nd International Astronautical Congress*, (January):6020–6031, 2011.

[31] V. Tyagi H. Metselaar S. Sandaran R. Sharma, P. Ganesan. Developments in organic solid–liquid phase change materials and their applications in thermal energy storage. *Energy Conversion and Management*, 95:193–228, 2015.

[32] R. Peyrou-Lauga O. Pin N. Nutal M. Larnicol J. Crahay J. Collette, P. Rochus. Phase change material device for spacecraft thermal control. *62nd International Astronautical Congress*, 2011.

[33] Loura Hall (NASA). Nasa to begin testing next generation of spacecraft heat exchangers.

[34] M. J. O'Neil D. V. Hale, M. J. Hoover. Phase change material handbook, 1971.

[35] S. Sawyer. Using phase change material for thermal control of cubesats with micro-thrusters, 2019.

[36] C. Chen R. Buddhi A. Sharma, V. Tyagi. Review on thermal energy storage with phase change materials and applications. *Renewable and Sustainable Energy Reviews*, 13(2):318–345, 2009.

[37] J. M. Ortiz De Zárate C. Vélez, M. Khayet. Temperature-dependent thermal properties of solid / liquid phase change even-numbered n- alkanes : n- hexadecane , n- octadecane and n- eicosane. *Applied Energy*, 143:383–394, 2015.

[38] R. Kobayashi D. Morgan. Direct vapor pressure measurements of ten n-alkanes m the 10-c28 range. *Fluid Phase Equilibria*, 97:211–242, 1994.

[39] ECHA. Paraffins (petroleum), normal c>10, 2019.

[40] The Good Science Company inc. eicosane.

[41] ISIS. Cubesat structures.

[42] V.V. Tyagi H.S.C Metselaar S.C. Sandaran R.K. Sharma, P. Ganesan. Developments in organic solid–liquid phase change materials and their applications in thermal energy storage. *Energy Conversion and Management*, 95:193–228, 2015.

[43] Ces edupack.

[44] C. G. Marirrodriga O. Mallet, M. Kornman. Development of a paraffin actuator. *7th European Space Mechanisms tribology Symposium*, 1997.

[45] Dr. G. Rogers. Leak detection techniques helium leak testing techniques for industry.

[46] Metal Work Pneumatic. V3v l unidir. Ø 6, 2020.

[47] Swagelok. Tube fittings and tube adapters.

[48] Thorite. Plug hex key bspp thread o-ring seal, 2020.

[49] T. Kinjo M. Saitoh T. Yamamoto R. Hatakenaka, H. Sugita. Heat-transfer characteristics of a light-weight, fin- integrated pcm unit manufactured by additive manufacturing. *47th International Conference on Environmental Systems*, July, 2017.

[50] T. Kinjo M. Saitoh T. Yamamoto R. Hatakenaka, H. Sugita. Heat-transfer characteristics of a light-weight, fin- integrated pcm unit manufactured by additive manufacturing. *47th international conference on environmental Systems*, July, 2017.

[51] E.W.Benilla K. F. Sterret L. E. Karre. Research and development study on thermal control by use of fusible materials, 1966.

[52] Y. Tian C. Y. Zhao, W. Lu. Heat transfer enhancement for thermal energy storage using metal foams embedded within phase change materials (pcms). *Solar Energy*, 84(8):1402–1412, 2010.

[53] J.Klett and O.Ridge. Thermal management solutions utilizing high thermal cunductivity graphite foams. *Bridging the Centuries with SAMPE's Materials and processes Technology*, 45(1933), 2000.

[54] L. Yang C. Guo, X. Ma. Pcm/ graphite foam composite for thermal energy storage device. *IOP Conference Series: Materials Science and Engineering*, 87(1), 2015.

[55] S. Kang and H. Oh. On-orbit thermal design and validation of 1 u standardized cubesat of step cube lab. *International Journal of Aerospace Engineering*, 2016.

[56] F. P. Incropera D. P. Dewitt T. L. Bergman, A. S. Lavine. *Fundamentals of Heat and Mass Transfer*. John Wiley Sons, 2002.

[57] Racemat BV. Cell material engineering.

[58] H. Mohammed P. Nancarrow. Ionic liquids in space technology - current and future trends. *ChemBioEng Reviews*, 4(2):106–119, 2017.

[59] Wikipedia. Eutectic system, 2019.

A

Types of Phase Change Materials

There are many different types of PCMs as can be seen in figure 3.2. An extensive survey of the different PCM types was done in the literature study preceding this thesis in reference [35]. This appendix contains A brief overview of the different types of PCM and their properties that were found. This is done to show the directions in which the design of the PCM device can go if the paraffins ultimately turn out to be problematic. Paraffins have traditionally been the choice of PCM for spacecraft. This is mainly due to the low flammability at low temperatures, low cost, low corrosiveness and high latent per kilogram. But due to their low density and thermal conductivity it is possible they may not be suited for high performance CubeSats. This appendix focuses on the non-paraffin PCMs. Table 3.3 shows the trade-off of all the PCMs discussed in this section.

The chart in figure 3.2 shows a list of different types of PCMs considered. As mentioned in part 3.3.2, the solid-gas and liquid-gas phase changes weren't considered. What remains is the solid-liquid and the solid-solid phase changes. The solid-solid phase change refers to a different stacking of atoms in lattice within a solid. The solid-liquid phase change is categorized into three main parts: organic, inorganic and eutectic. These categories will be discussed in the following section. The information is gathered from these papers [34], [36], [31] and [32].

In general the higher the latent and specific heat of a material the lower the thermal conductivity of the material. This issue can be solved by using filler materials as discussed in section 4.5. Materials that don't have this problem of poor conductivity are metallics and some ionic liquids.

A.1. Organic Phase Change Materials

The first type of PCM seen in figure 3.2 are the organic PCMs. Organic PCMs generally consist of more complex molecules than the inorganics. This causes them to break down at elevated temperatures.

Organic PCMs other than paraffins include:

- Fatty acids
- Sugar alcohols
- Esters
- Poly(ethylene glycol)

These PCMs can be chosen if the paraffins don't meet the design requirements.

A list of non-paraffin organics and their melting points and heat of fusion is shown in table A.1.

The properties of non-paraffin organics are:

- Advantages
  - They provide a wide variety of choices, many of which have convenient melting temperatures
  - they have a high heat of fusion compared to paraffins
  - Some show characteristics of polymorphism (multiple phase changes including solid-solid) which extends their latent heat storage capabilities
- Disadvantages
  - Most are flammable.
  - Some are toxic.
  - Some show characteristics of polymorphism (multiple phase changes) but can therefore be a nuisance when designing a TSD
  - They have a low flash point
  - Their thermal properties are highly sensitive to contamination
  - They tend to decompose at elevated temperatures
  - They have low thermal conductivity

Fatty Acids

The properties of fatty acids are:

- Advantages
  - They have reliable meting and freezing behaviour
  - They are chemically and thermally stable
  - They are non-toxic
  - They do not exhibit supercooling behaviour
- Disadvantages
  - They are relatively expensive compared to paraffins
  - They are mildly corrosive
  - They are highly flammable
  - They have a high surface tension

The properties of sugar alcohols are:

Sugar Alcohols

- Advantages
  - Some show stable thermal properties after thermal cycling
  - They have a small to medium thermal expansion (10 to 15%)
- Disadvantages
  - Most have an inconvenient range of melting temperatures (90 - 200 °C)
  - They exhibit supercooling behaviours
  - Some have poor chemical stability after thermal cycling

Table A.1: Non-paraffin organic PCM properties [36]

Material	Melting point (°C)	Latent heat (kJ/kg)
Formic acid	7.8	247
Caprilic acid	16.3	149
Glycerin	17.9	198.7
D-Lattic acid	26	184
Methyl palmitate	29	205
Camphenilone	39	205
Docasyl bromide	40	201
Caprylone	40	259
Phenol	41	120
Heptadecanone	41	201
1-Cyclohexylooctadecane	41	218
4-Heptadacanone	41	197
p-Joluidine	43.3	167
Cyanamide	44	209
Methyl eicosanate	45	230
3-Heptadecanone	48	218
2-Heptadecanone	48	218
Hydrocinnamic acid	48.0	118
Cetyl alcohol	49.3	141
α-Nepthylamine	50.0	93
Camphene	50	238
O-Nitroaniline	50.0	93
9-Heptadecanone	51	213
Thymol	51.5	115
Methyl behenate	52	234
Diphenyl amine	52.9	107
p-Dichlorobenzene	53.1	121
Oxolate	54.3	178
Hypophosphoric acid	55	213
O-Xylene dichloride	55.0	121
β-Chloroacetic acid	56.0	147
Chloroacetic acid	56	130
Nitro naphthalene	56.7	103
Trimyristin	33–57	201–213
Heptaudecanoic acid	60.6	189
α-Chloroacetic acid	61.2	130
Bee wax	61.8	177
Bees wax	61.8	177
Glyolic acid	63.0	109
Glycolic acid	63	109
p-Bromophenol	63.5	86
Azobenzene	67.1	121
Acrylic acid	68.0	115
Dinto toluent (2,4)	70.0	111
Phenylacetic acid	76.7	102
Thiosinamine	77.0	140
Bromcamphor	77	174
Durene	79.3	156
Benzylamine	78.0	174
Methyl brombrenzoate	81	126
Alpha napthol	96	163
Glautaric acid	97.5	156
p-Xylene dichloride	100	138.7
Catechol	104.3	207
Quinone	115	171
Acetanilide	118.9	222
Succinic anhydride	119	204
Benzoic acid	121.7	142.8
Stibene	124	167
Benzamide	127.2	169.4

Esters

The properties of esters are:

- Advantages
  - They are readily available and cheap
  - They have a narrow melting range
  - They can form eutectics without supercooling
  - They have a good chemical stability
  - They are non-corrosive
- Disadvantages
  - They are flammable to highly flammable
  - They have varying toxicity from mildly to extremely toxic

Polyethelyneglycols

The properties of Polyethelyneglycols are:

- Advantages
  - They are chemically and thermally stable
  - They are non-flammable
  - They are non-toxic
  - They are non-corrosive
  - They are inexpensive
- Disadvantages
  - They have lower heat of fusion at lower melting temperatures

A.2. Inorganic Phase Change Materials

The next class of PCMs are inorganics. These materials generally consist of simpler molecules or are just atoms and ions in a lattice. Inorganics generally have around double the volumetric latent heat storage capacity of organics [36]. This makes them a great candidate for CubeSats, which have limited storage space. Metal PCMs have especially high thermal conductivity which is an excellent quality for a thermal storage device. The main disadvantages are their general corrosiveness to metals.

The first inorganic that is considered here are salts. Salts consist of crystal lattices of positive and negative ions stacked together. These lattices can melt although they generally have a very high melting temperature. Salts are therefore good for high temperature applications. A major drawback to using salts is that they are corrosive.

Salts with a low melting temperature are defined as ionic fluids and are discussed in this paper [58]. These ionic liquids can have very advantageous properties and are also used in thruster systems as green propellants. An advantage is their high latent heat capacity combined with a high thermal conductivity. Their main drawback is that they have to be synthesized and therefore are expensive. The properties of ionic liquids are:

- Advantages
  - They have a high heat of fusion
  - They have high thermal conductivity
  - They have high chemical and thermal stability
  - They have high storage density

  - They have small volume changes when melting
  - They have extremely low vapor pressure

- Disadvantages
  - They are very expensive to synthesize
  - They are corrosive
  - They can be slightly toxic

Salts are soluble in water. In this state they exhibit similar thermodynamic behaviours as melting and freezing within the water, when in fact it is the hydration and dehydration of the salts in the solution. These are referred to as salt hydrates. If the salt is in a solution with enough water then the melting point will be congruent, otherwise not, due to solidification of salts within the solution. The heavier salt will sink to the bottom of the container and will not be able to remix with the rest of the water. This is called stratification. A table of salt hydrate PCMs and their phase change temperatures and heat of fusion are shown in table A.2.

Table A.2: List of Salt Hydrates and their properties [36]

Material	Melting point (°C)	Latent heat (kJ/kg)
$K_2HPO_4 \cdot 6H_2O$	14.0	109
$FeBr_3 \cdot 6H_2O$	21.0	105
$Mn(NO_3)_2 \cdot 6H_2O$	25.5	148
$FeBr_3 \cdot 6H_2O$	27.0	105
$CaCl_2 \cdot 12H_2O$	29.8	174
$LiNO_3 \cdot 2H_2O$	30.0	296
$LiNO_3 \cdot 3H_2O$	30	189
$Na_2CO_3 \cdot 10H_2O$	32.0	267
$Na_2SO_4 \cdot 10H_2O$	32.4	241
$KFe(SO_4)_2 \cdot 12H_2O$	33	173
$CaBr_2 \cdot 6H_2O$	34	138
$LiBr_2 \cdot 2H_2O$	34	124
$Zn(NO_3)_2 \cdot 6H_2O$	36.1	134
$FeCl_3 \cdot 6H_2O$	37.0	223
$Mn(NO_3)_2 \cdot 4H_2O$	37.1	115
$Na_2HPO_4 \cdot 12H_2O$	40.0	279
$CoSO_4 \cdot 7H_2O$	40.7	170
$KF \cdot 2H_2O$	42	162
$MgI_2 \cdot 8H_2O$	42	133
$CaI_2 \cdot 6H_2O$	42	162
$K_2HPO_4 \cdot 7H_2O$	45.0	145
$Zn(NO_3)_2 \cdot 4H_2O$	45	110
$Mg(NO_3) \cdot 4H_2O$	47.0	142
$Ca(NO_3) \cdot 4H_2O$	47.0	153
$Fe(NO_3)_3 \cdot 9H_2O$	47	155
$Na_2SiO_3 \cdot 4H_2O$	48	168
$K_2HPO_4 \cdot 3H_2O$	48	99
$Na_2S_2O_3 \cdot 5H_2O$	48.5	210
$MgSO_4 \cdot 7H_2O$	48.5	202
$Ca(NO_3)_2 \cdot 3H_2O$	51	104
$Zn(NO_3)_2 \cdot 2H_2O$	55	68
$FeCl_3 \cdot 2H_2O$	56	90
$Ni(NO_3)_2 \cdot 6H_2O$	57.0	169
$MnCl_2 \cdot 4H_2O$	58.0	151
$MgCl_2 \cdot 4H_2O$	58.0	178
$CH_3COONa \cdot 3H_2O$	58.0	265
$Fe(NO_3)_2 \cdot 6H_2O$	60.5	126
$NaAl(SO_4)_2 \cdot 10H_2O$	61.0	181
$NaOH \cdot H_2O$	64.3	273
$Na_3PO_4 \cdot 12H_2O$	65.0	190
$LiCH_3COO \cdot 2H_2O$	70	150
$Al(NO_3)_2 \cdot 9H_2O$	72	155
$Ba(OH)_2 \cdot 8H_2O$	78	265
$Mg(NO_3)_2 \cdot 6H_2O$	89.9	167
$KAl\ (SO_4)_2 \cdot 12H_2O$	91	184
$MgCl_2 \cdot 6H_2O$	117	167

The properties of Salt-Hydrates are:

- Advantages
  - They have a high heat of fusion
  - They have relatively high thermal conductivity compared to non-metals
  - They have a small volume change
- Disadvantages
  - They can have incongruent melting points
  - They experience stratification
  - They exhibit supercooling behaviour (without nucleating agents)
  - They can be corrosive to metallic containers
  - Some are slightly toxic

The next class of inorganic PCM are metallics. Metals are known for their high melting temperature and great thermal conductivity. Although there are a large range of metals and alloys to choose from with variable melting points, some metals like mercury are even liquid at room temperature. Metallics are an interesting choice of PCM for CubeSats. This is because metallics are very dense and have thus been avoided in previous missions due to mass penalties. Per volume these PCMs have great properties. If the volume storage for the CubeSats becomes a bottleneck then metallics could be a good solution. Careful selection of the metal and container has to be taken, because the wrong combination can lead to corrosion. A list of metallics is shown with their melting temperature and their heat of fusion in table A.3.

Table A.3: List of metallics and their PCM properties [36]

Material	Melting point (°C)	Latent heat (kJ/kg)
Gallium–gallium antimony eutectic	29.8	–
Gallium	30.0	80.3
Cerrolow eutectic	58	90.9
Bi–Cd–In eutectic	61	25
Cerrobend eutectic	70	32.6
Bi–Pb–In eutectic	70	29
Bi–In eutectic	72	25
Bi–Pb–tin eutectic	96	–
Bi–Pb eutectic	125	–

The properties of metallics are:

- Advantages
  - They have a high heat of fusion per unit volume
  - They have high thermal conductivity
  - They have low vapor pressure
  - They have low volumetric expansion
  - They have high thermal stability
  - They exhibit minimal hazardous behaviour
- Disadvantages
  - They have a low heat of fusion per unit weight
  - They are corrosive to metal containers

  - They have a low specific heat
  - Cadmium has a high vapor pressure and is a serious contaminant
  - Gallium expands when it freezes which makes containment difficult. (Although it is a soft metal)

Water is the most common phase change material. It has the highest latent heat of fusion and has a very large specific heat. Water is generally not used as a PCM but just as a heat sink. This is because when water freezes it expands. Because solids are less mobile than liquids they can be damaging to containers. Water is a great choice for spacecraft carrying humans, as humans need water to survive anyway, serve a dual purpose serving a dual purpose. The properties of water are:

- Advantages
  - It has a high heat of fusion
  - It has a high specific heat
  - It is non-toxic
  - It is non-flammable
  - It is highly stable
  - Pure water is non-corrosive
  - Thermal conductivity is high for a non-metal
- Disadvantages
  - It expands when it freezes (and water ice is very hard)
  - When contaminated with ions water becomes corrosive to metal containers

A.3. Eutectic Phase Change Materials

A eutectic system is a mixture of multiple components that have the same melting temperature at a certain composition that is lower then the melting point of each component individually [59]. Most common eutectic systems are binary alloys (which have similar properties to the metallics) or fused salts. These systems can have great latent heat performances, but they vary greatly depending on the type and concentration of materials used. Therefore it is difficult to make general statements about Eutectic systems.

A list of eutectic systems and their mixing ratio, phase change temperature and heat of fusion is shown in table A.4. The working principles of eutectic systems are shown in figure A.1. The properties of eutectic systems are:

- Advantages
  - They have a wide variety of heat of fusion
  - They have a wide variety of melting temperatures
- Disadvantages
  - They are greatly influenced by moisture
  - They are corrosive to metal containers

Table A.4: List of eutectics and their properties [36]

Material	Composition (wt.%)	Melting point (°C)	Latent heat (kJ/kg)
$CaCl_2 \cdot 6H_2O + CaBr_2 \cdot 6H_2O$	45 + 55	14.7	140
Triethylolethane + water + urea	38.5 + 31.5 + 30	13.4	160
$C_{14}H_{28}O_2 + C_{10}H_{20}O_2$	34 + 66	24	147.7
$CaCl_2 + MgCl_2 \cdot 6H_2O$	50 + 50	25	95
$CH_3CONH_2 + NH_2CONH_2$	50 + 50	27	163
Triethylolethane + urea	62.5 + 37.5	29.8	218
$Ca(NO_3) \cdot 4H_2O + Mg(NO_3)_3 \cdot 6H_2O$	47 + 53	30	136
$CH_3COONa \cdot 3H_2O + NH_2CONH_2$	40 + 60	30	200.5
$NH_2CONH_2 + NH_4NO_3$	53 + 47	46	95
$Mg(NO_3)_3 \cdot 6H_2O + NH_4NO_3$	61.5 + 38.5	52	125.5
$Mg(NO_3)_3 \cdot 6H_2O + MgCl_2 \cdot 6H_2O$	58.7 + 41.3	59	132.2
$Mg(NO_3)_3 \cdot 6H_2O + MgCl_2 \cdot 6H_2O$	50 + 50	59.1	144
$Mg(NO_3)_3 \cdot 6H_2O + Al(NO_3)_2 \cdot 9H_2O$	53 + 47	61	148
$CH_3CONH_2 + C_{17}H_{35}COOH$	50 + 50	65	218
$Mg(NO_3)_2 \cdot 6H_2O + MgBr_2 \cdot 6H_2O$	59 + 41	66	168
Napthalene + benzoic acid	67.1 + 32.9	67	123.4
$NH_2CONH_2 + NH_4Br$	66.6 + 33.4	76	151
$LiNO_3 + NH_4NO_3 + NaNO_3$	25 + 65 + 10	80.5	113
$LiNO_3 + NH_4NO_3 + KNO_3$	26.4 + 58.7 + 14.9	81.5	116
$LiNO_3 + NH_4NO_3 + NH_4Cl$	27 + 68 + 5	81.6	108

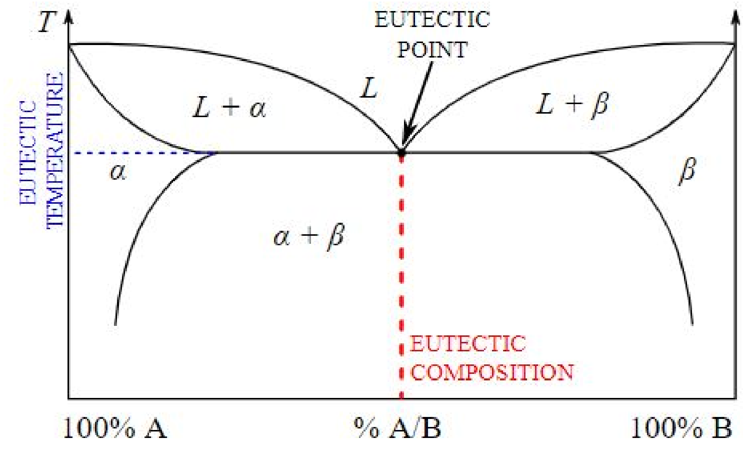

Figure A.1: Working principle of a eutectic system [59]

B

Technical Drawings

This appendix shows the technical drawings that were sent to companies to manufacture the casing prototypes. The fin casing was built internally at ISIS. Its lid was not milled out but laser-cut and is therefore not included in this list of technical drawings.

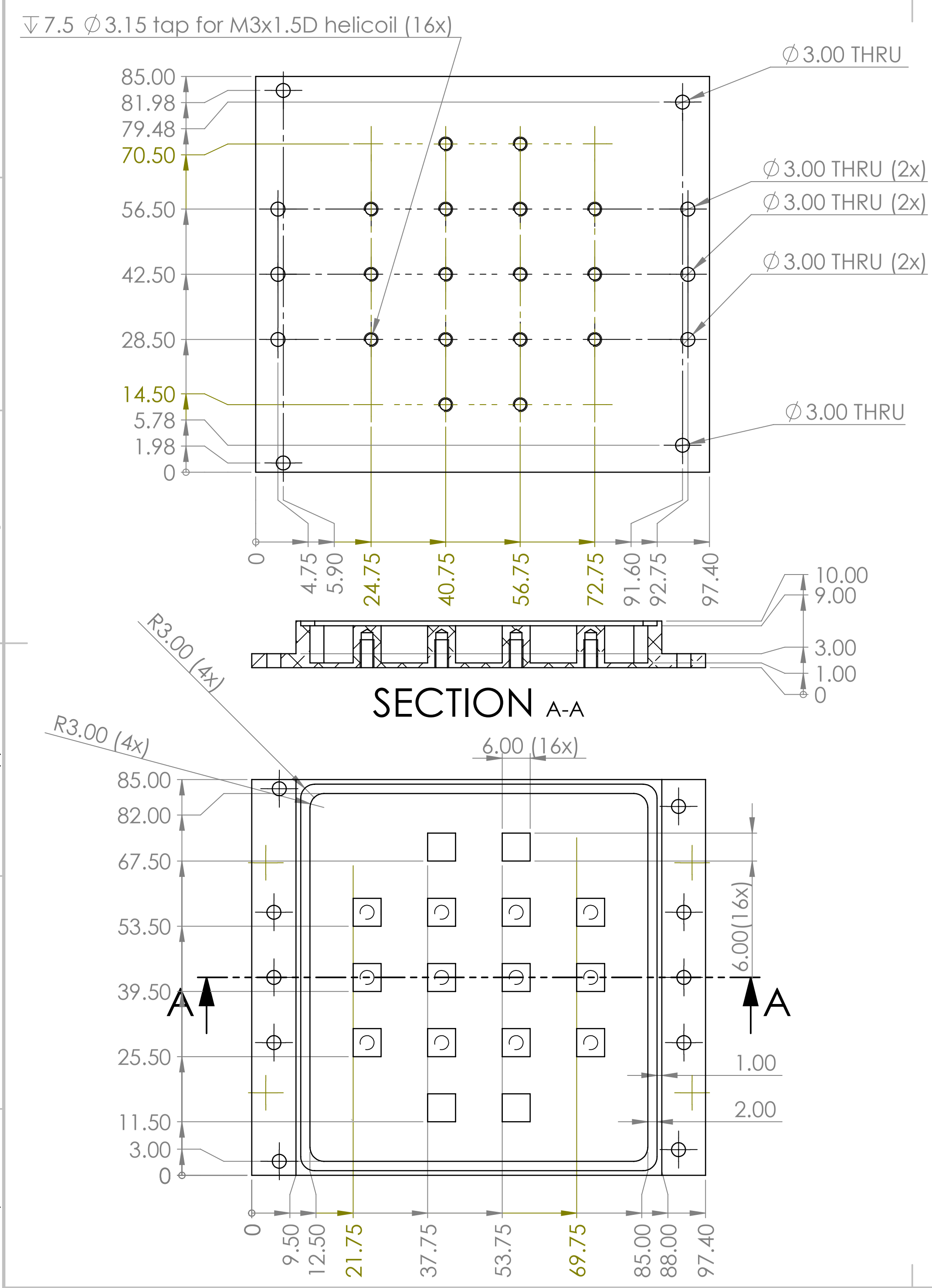

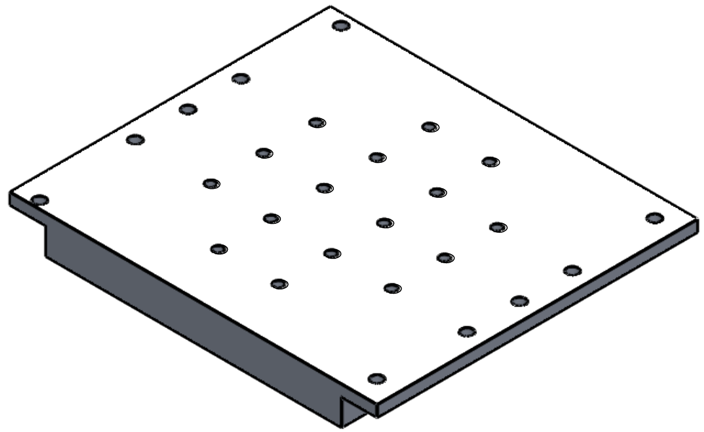

Top ISO view, for reference only

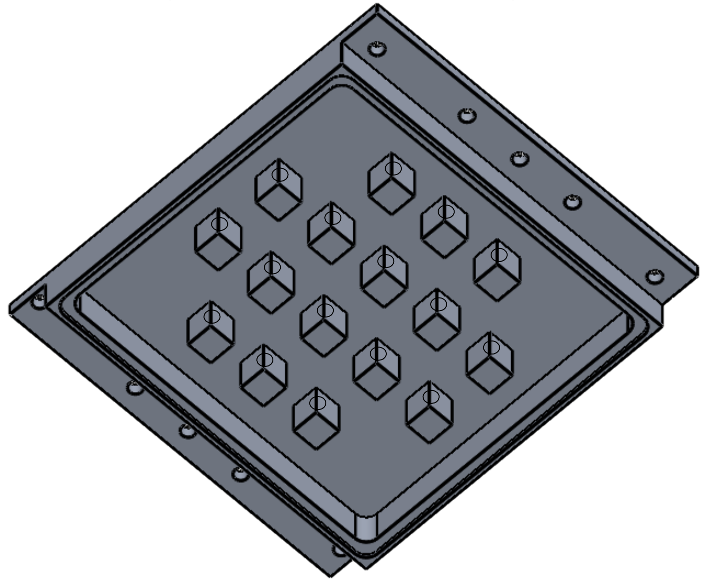

Bottom ISO view, for reference only

UNLESS OTHERWISE SPECIFIED: DIMENSIONS ARE IN MILLIMETERS SURFACE FINISH: TOLERANCES: LINEAR: ANGULAR:	FINISH:	DEBURR AND BREAK SHARP EDGES	DO NOT SCALE DRAWING / REVISION
	NAME / SIGNATURE / DATE		TITLE:
DRAWN			
CHK'D			
APPV'D			
MFG			
Q.A		MATERIAL:	DWG NO. PCM_PCB_fins / A3
		WEIGHT:	SCALE:1:1 / SHEET 1 OF 1

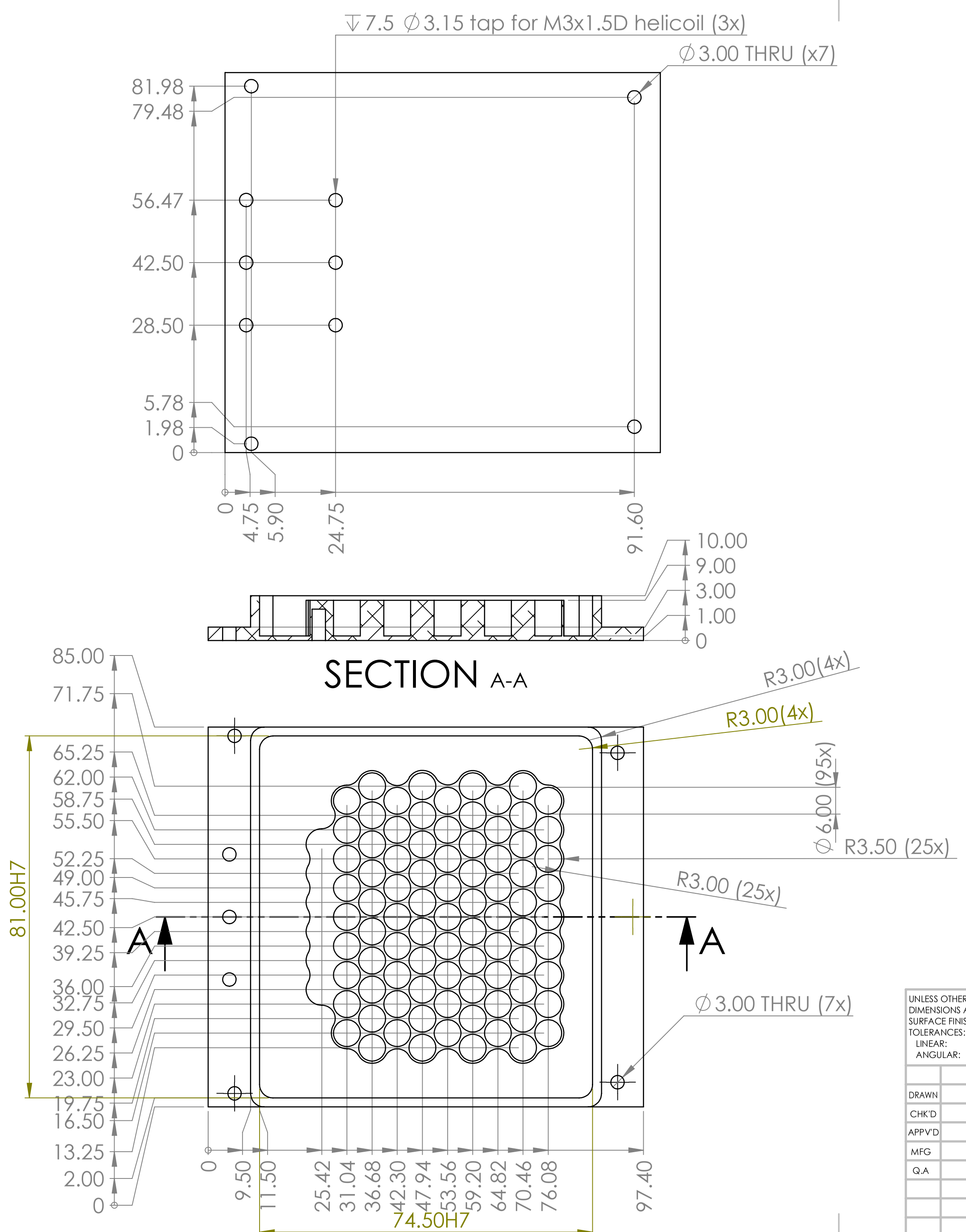

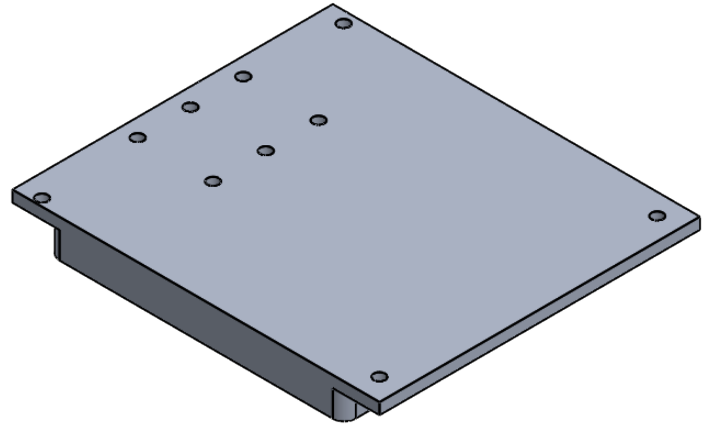

Top ÌSO view for reference only

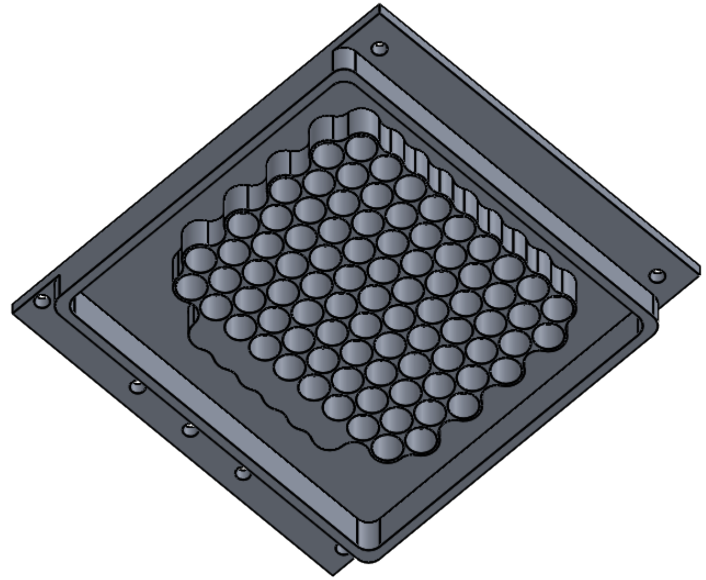

`Bottom ISO view for reference only

UNLESS OTHERWISE SPECIFIED: DIMENSIONS ARE IN MILLIMETERS SURFACE FINISH: TOLERANCES: LINEAR: ANGULAR:	FINISH:	DEBURR AND BREAK SHARP EDGES	DO NOT SCALE DRAWING	REVISION

	NAME	SIGNATURE	DATE		TITLE:
DRAWN					
CHK'D					
APPV'D					
MFG					
Q.A				MATERIAL:	DWG NO. Casing_Honeycomb_CNC A3
				WEIGHT:	SCALE:1:1 SHEET 1 OF 1

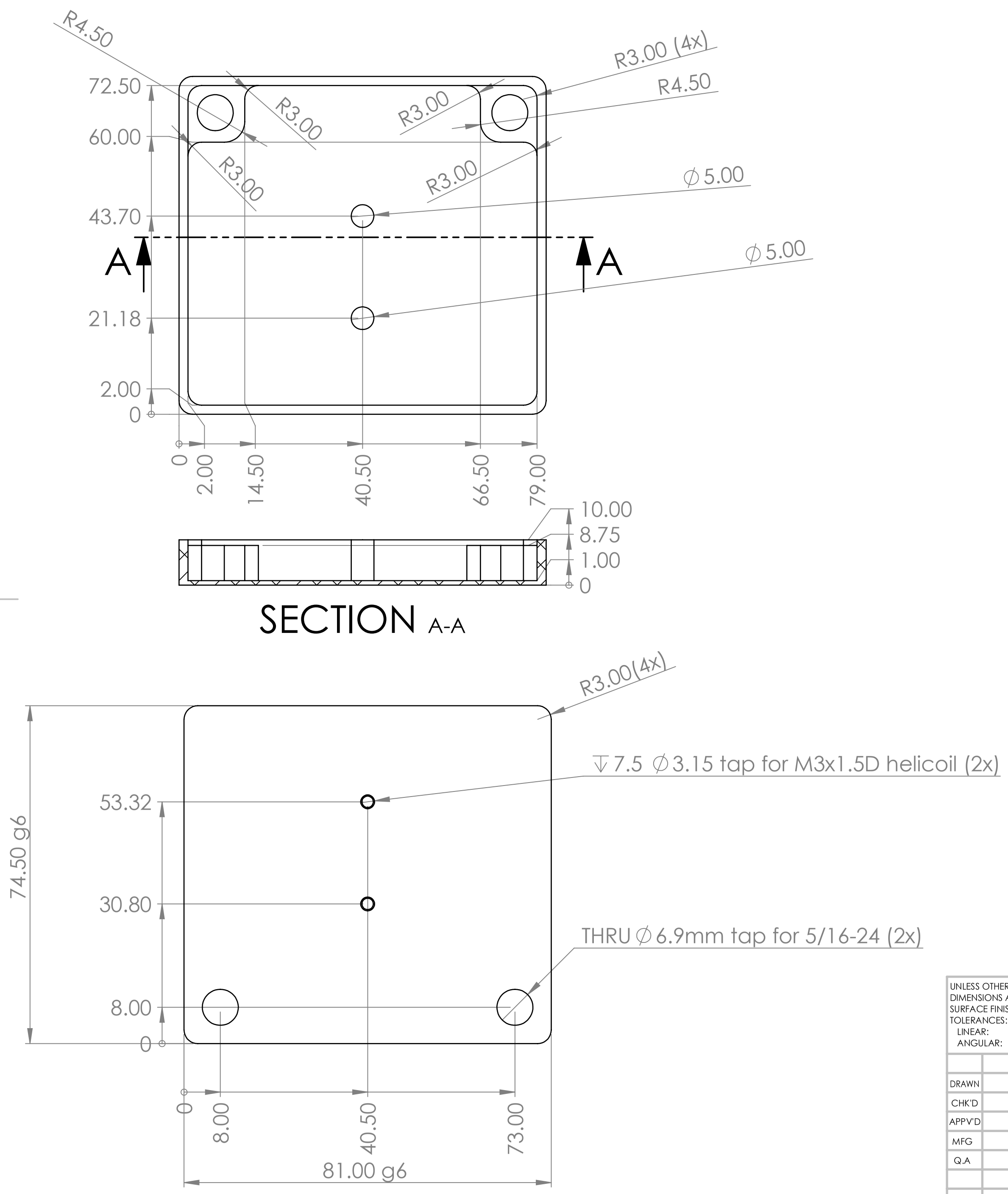

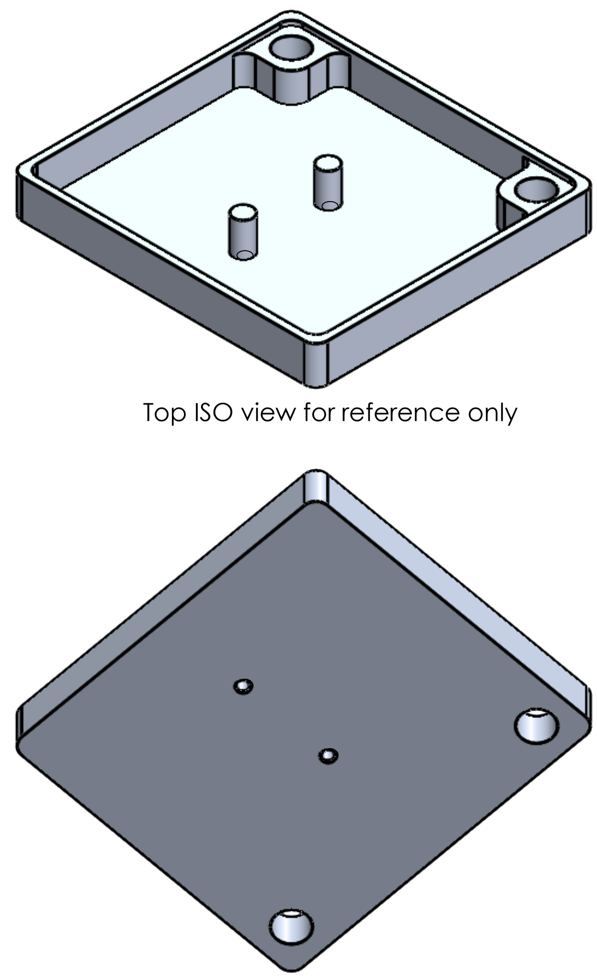

Top ISO view for reference only

Bottom ISO view for reference only

UNLESS OTHERWISE SPECIFIED:
DIMENSIONS ARE IN MILLIMETERS
SURFACE FINISH:
TOLERANCES:
LINEAR:
ANGULAR:

FINISH:

DEBURR AND BREAK SHARP EDGES

DO NOT SCALE DRAWING

REVISION

	NAME	SIGNATURE	DATE
DRAWN			
CHK'D			
APPV'D			
MFG			
Q.A			

TITLE:

MATERIAL:
Aluminium 6082 T6

DWG NO.
Cover_Honeycomb_CNC

A3

WEIGHT:

SCALE:1:1

SHEET 1 OF 1

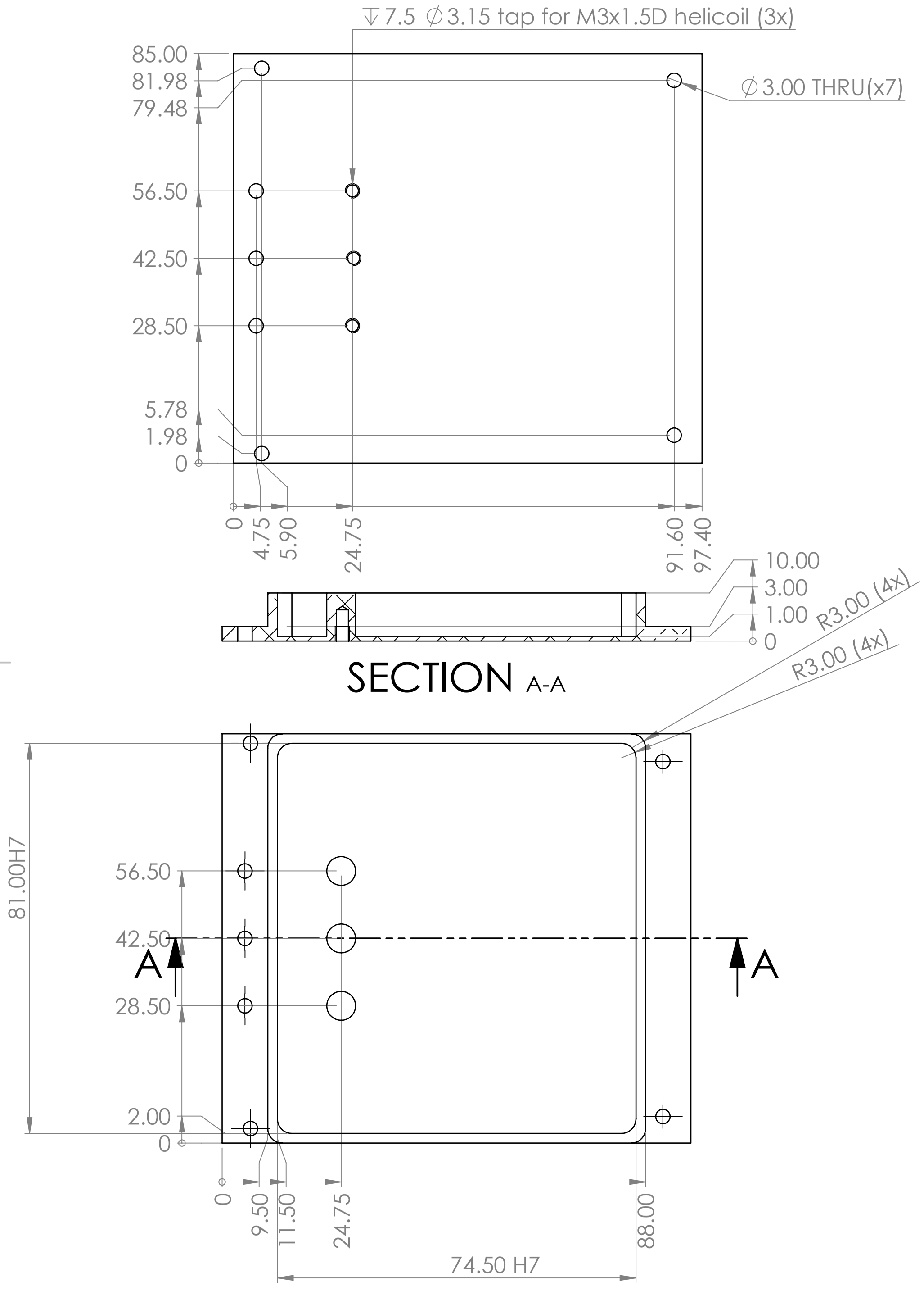

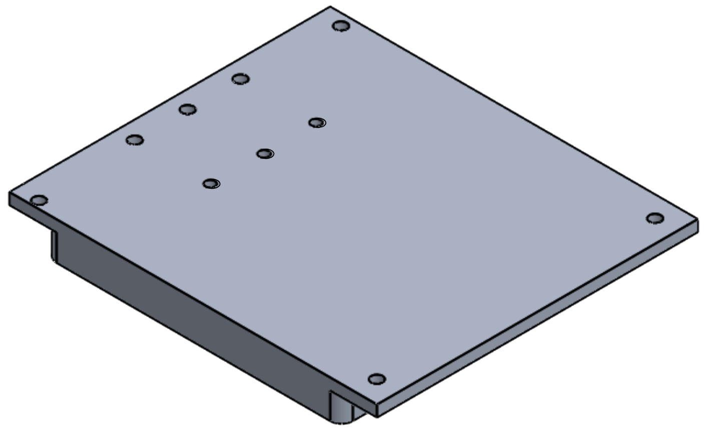

Top ISO view for refference only

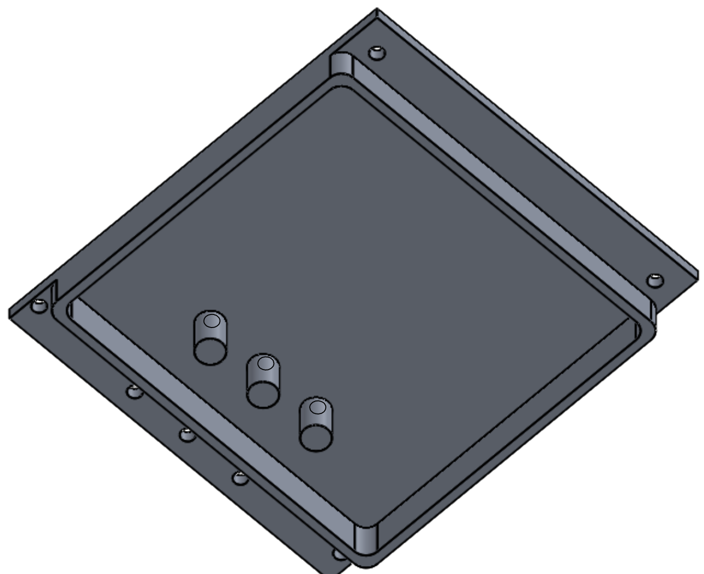

Botton ISO view for refference only

UNLESS OTHERWISE SPECIFIED: DIMENSIONS ARE IN MILLIMETERS SURFACE FINISH: TOLERANCES: LINEAR: ANGULAR:	FINISH:	DEBURR AND BREAK SHARP EDGES	DO NOT SCALE DRAWING	REVISION

	NAME	SIGNATURE	DATE
DRAWN			
CHK'D			
APPV'D			
MFG			
Q.A			

TITLE:

MATERIAL:

DWG NO.

Casing_Foam_CNC

A3

WEIGHT:

SCALE:1:1

SHEET 1 OF 1

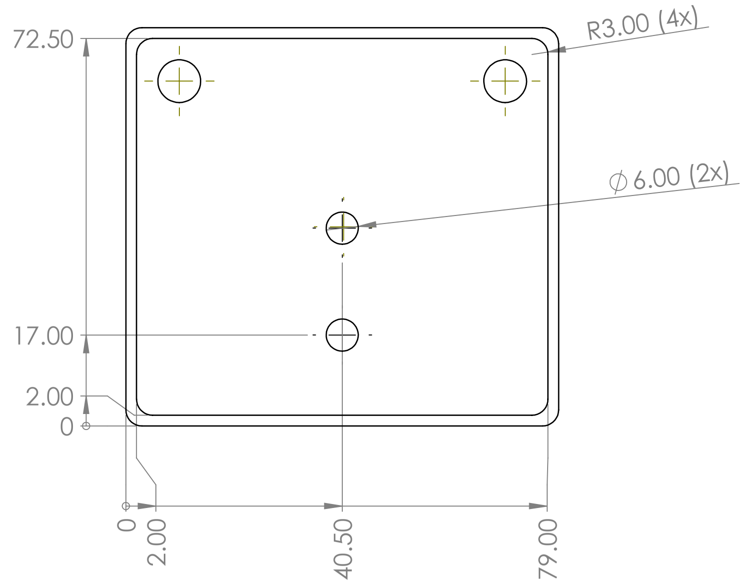

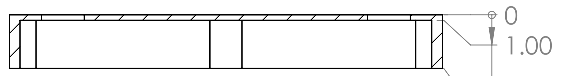

SECTION A-A

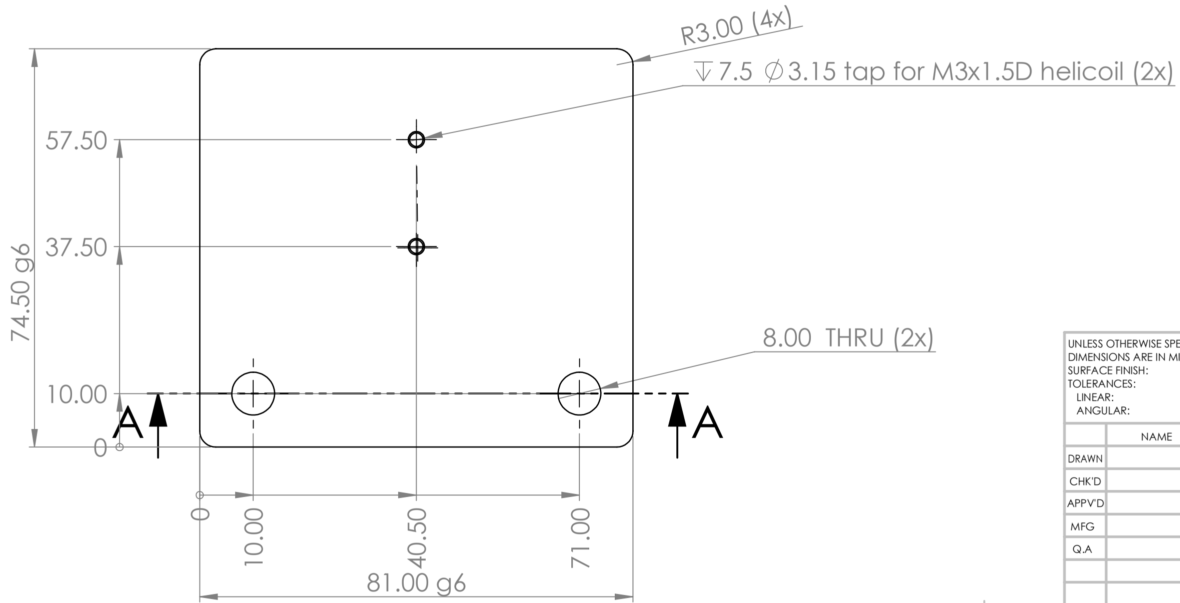

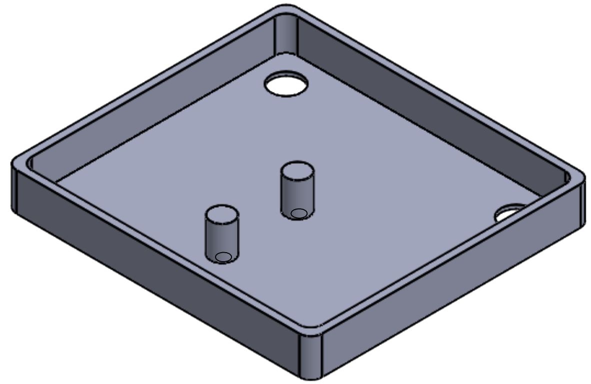

Top ISO view for reference only

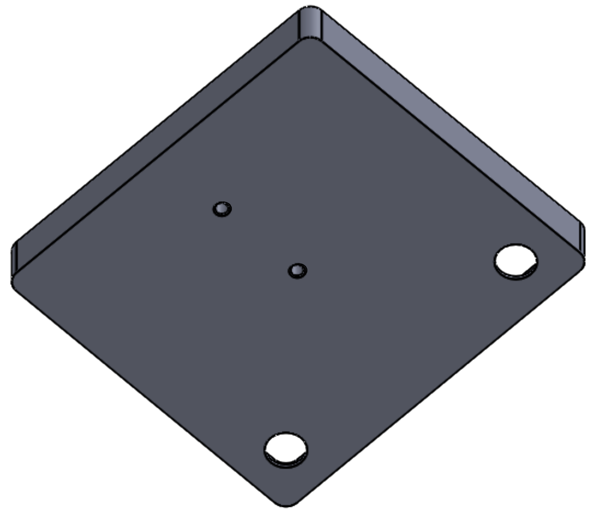

Bottom ISO view for reference only

UNLESS OTHERWISE SPECIFIED: DIMENSIONS ARE IN MILLIMETERS SURFACE FINISH: TOLERANCES: LINEAR: ANGULAR:	FINISH:		DEBURR AND BREAK SHARP EDGES		DO NOT SCALE DRAWING	REVISION
	NAME	SIGNATURE	DATE		TITLE:	
DRAWN						
CHK'D						
APPV'D						
MFG						
Q.A				MATERIAL:	DWG NO. Cover_Foam_CNC	A3
				WEIGHT:	SCALE:1:1	SHEET 1 OF 1

C

FDM simulations

C.1. Matlab Code

```
% written by S. Sawyer
% This script models a 3d PCM heat storage device for a CubeSat

clear frames
close all
clear all
tic
video=1;
fins=1;
loops=10;
sensitivity=1:loops;
TXS_measurements=zeros(1,loops);
thickness=zeros(1,loops);
mass=zeros(1,loops);
for sen=1:loops

    %% Inputs
    %simulation time
    minutes=20;                                          %min
    time=minutes*60;                                     %seconds
    timesteps=0.0025;                                     %seconds
    nsteps=round(time/timesteps);
    discretization=[25 21 8];
    %Contact suface area
    total_width=0.085;
    total_height=0.0785;
    A=total_height*total_width;                          %m^2
    %mass PCM
    %m_paraffin=28.5/1000;
    m_paraffin=(30)/1000;                              %kg
    %phase change temperature range
    pct=6;                                               %Delta K
    %hot plate thickness
    hot_t=0.002;                                         %m
    %cold plate thickness
    cold_t=0.001;                                        %m
    %component wall thickness
    wall_t=0.003;                                        %m
    % starting temperature
```

```
T_0=30;                                                     %C
% PCM melting temperature
T_m=36.7;                                                   %C
percent=0;

%% Fixed values
dissipated_power=8;                                         %W
%power_out=0;
power_out=1.778;
dissipation_time=20*60;
%seconds
%aluminium properties
rho_alu=2700;                                               %kg/m^3
cp_alu=950;                                                 %J/kg/K
k_alu=165;                                                  %W/m/K
%PCM properties
rho_paraffin=910;                                           %kg/m^3
cp_paraffin=1926;                                           %J/kg/K
l_paraffin=248000;                                          %J/kg
k_paraffin=.423;                                           %W/m/K

% liquid PCM properties
rho_paraffin_l=769;                                        %kg/m^3
cp_paraffin_l=2400;                                        %J/kg/K
k_paraffin_l=.146;                                          %W/m/K
%% Allocation
% Allocating the 3d matrixes of 0s and 1s
Allocation=zeros(discretization(1),discretization(2),discretization(3)
    );
Allocation1=ones(discretization(1),discretization(2),discretization(3)
    );
%Temperature
T=Allocation;
%mass
M=Allocation;
%heat capacity
C=Allocation;
%Resistance up
U=Allocation;
%Resistance down
D=Allocation;
%Resistance left
L=Allocation;
%Resistance right
R=Allocation;
%Resistance Forwards
F=Allocation;
%Resistance Backwards
B=Allocation;
%Width
W=Allocation;
%Height
H=Allocation;
%Thermal conductivity
K=Allocation;
%Length
```

```
LEN=Allocation;
% Width coordinates
Width=Allocation;
% Hight coordinates
Height=Allocation;
% Length coordinates
Length=Allocation;
% Total potential latent heat storage capability
Saturation=Allocation;
% Actual stored latent heat
S=Allocation;
% Logic operators
Within_Range=Allocation;
Over_Saturation=Allocation;
Under_Saturation=Allocation;
% TXS temperature over time
T_TXS=zeros(1,round(time/timesteps));
%% Paraffin
% defining praraffin nodes
%paraffin area
paraffin_width=total_width-2*wall_t;
paraffin_height=total_height-2*wall_t;
paraffin_A=paraffin_width*paraffin_height;
fin_frac=(((discretization(1)-5)*(discretization(2)-5))/16)/(
    discretization(1)-2)/(discretization(2)-2);
%PCM thickness
if fins==true
    paraffin_t=m_paraffin/rho_paraffin/(paraffin_A*(1-fin_frac));
else
    paraffin_t=m_paraffin/rho_paraffin/(paraffin_A);
end

gap_t=paraffin_t*(rho_paraffin/rho_paraffin_l-1)+0.001;
                                                    %m
%PCM width
w_para=paraffin_width/(discretization(1)-2);
%PCM hight
h_para=paraffin_height/(discretization(2)-2);
%PCM length
len_para=paraffin_t/(discretization(3)-2);
%PCM without filler
[m_para,C_para,u_para,d_para,l_para,r_para,f_para,b_para]...
    =Properties(w_para,h_para,len_para,rho_paraffin,cp_paraffin,
        k_paraffin);
M(2:end-1,2:end-1,2:end-1)=m_para;
C(2:end-1,2:end-1,2:end-1)=C_para;
U(2:end-1,2:end-1,2:end-1)=u_para;
D(2:end-1,2:end-1,2:end-1)=d_para;
L(2:end-1,2:end-1,2:end-1)=l_para;
R(2:end-1,2:end-1,2:end-1)=r_para;
F(2:end-1,2:end-1,2:end-1)=f_para;
B(2:end-1,2:end-1,2:end-1)=b_para;
W(2:end-1,2:end-1,2:end-1)=w_para;
H(2:end-1,2:end-1,2:end-1)=h_para;
K(2:end-1,2:end-1,2:end-1)=k_paraffin;
LEN(2:end-1,2:end-1,2:end-1)=len_para;
```

```
    Saturation(2:end-1,2:end-1,2:end-1)=l_paraffin*m_para;
    % rate of change of properties due to melted fraction
    drho=(rho_paraffin_l-rho_paraffin)/(l_paraffin*m_para);
    dcp=(cp_paraffin_l-cp_paraffin)/(l_paraffin);
    dk=(k_paraffin_l-k_paraffin)/(l_paraffin*m_para);
    dlen=(len_para*rho_paraffin/rho_paraffin_l-len_para)/(l_paraffin*
        m_para);

    %% Casing
    %properties of the casing nodes
    %properties of the hot plate nodes
    w_hot=paraffin_width/(discretization(1)-2);
    h_hot=paraffin_height/(discretization(2)-2);
    %connector range
    wrange_start=round((29.5/1000-wall_t)/w_hot);
    wrange_end=wrange_start+round(((29.5)/1000-wall_t)/w_hot);
    hrange_start=2;
    hrange_end=hrange_start+round((16.5/1000-wall_t)/h_hot);

    w_hoths=w_hot*(wrange_end-wrange_start+1);
    h_hoths=h_hot*(hrange_end-hrange_start+1);
    len_hot=hot_t;
    [m_hoths,C_hoths,u_hoths,d_hoths,l_hoths,r_hoths,f_hoths,b_hoths]...
        =Properties(w_hoths,h_hoths,len_hot,rho_alu,cp_alu,k_alu);
    [m_hot,C_hot,u_hot,d_hot,l_hot,r_hot,f_hot,b_hot]...
        =Properties(w_hot,h_hot,len_hot,rho_alu,cp_alu,k_alu);
    M(2:end-1,2:end-1,1)=m_hot;
    C(2:end-1,2:end-1,1)=C_hot;
    U(2:end-1,2:end-1,1)=u_hot;
    D(2:end-1,2:end-1,1)=d_hot;
    L(2:end-1,2:end-1,1)=l_hot;
    R(2:end-1,2:end-1,1)=r_hot;
    F(2:end-1,2:end-1,1)=f_hot;
    B(2:end-1,2:end-1,1)=b_hot;
    W(2:end-1,2:end-1,1)=w_hot;
    H(2:end-1,2:end-1,1)=h_hot;
    K(2:end-1,2:end-1,1)=k_alu;

    LEN(2:end-1,2:end-1,1)=len_hot;
    Saturation(2:end-1,2:end-1,1)=0;

    % properties of the cold plate nodes
    w_cold=paraffin_width/(discretization(1)-2);
    h_cold=paraffin_height/(discretization(2)-2);
    len_cold=cold_t;
    [m_cold,C_cold,u_cold,d_cold,l_cold,r_cold,f_cold,b_cold]...
        =Properties(w_cold,h_cold,len_cold,rho_alu,cp_alu,k_alu);
    M(2:end-1,2:end-1,end)=m_cold;
    C(2:end-1,2:end-1,end)=C_cold;
    U(2:end-1,2:end-1,end)=u_cold;
    D(2:end-1,2:end-1,end)=d_cold;
    L(2:end-1,2:end-1,end)=l_cold;
    R(2:end-1,2:end-1,end)=r_cold;
    F(2:end-1,2:end-1,end)=f_cold;
    B(2:end-1,2:end-1,end)=b_cold;
    W(2:end-1,2:end-1,end)=w_cold;
```

```
H(2:end-1,2:end-1,end)=h_cold;
K(2:end-1,2:end-1,end)=k_alu;
LEN(2:end-1,2:end-1,end)=len_cold;
Saturation(2:end-1,2:end-1,end)=0;


%properies of the horizontal wall nodes
w_hwall=total_width./(discretization(1));
h_hwall=wall_t;
len_hwall=(paraffin_t+hot_t+cold_t)./(discretization(3));
[m_hwall,C_hwall,u_hwall,d_hwall,l_hwall,r_hwall,f_hwall,b_hwall]...
    =Properties(w_hwall,h_hwall,len_hwall,rho_alu,cp_alu,k_alu);
M(1:end,[1 end],1:end)=m_hwall;
C(1:end,[1 end],1:end)=C_hwall;
U(1:end,[1 end],1:end)=u_hwall;
D(1:end,[1 end],1:end)=d_hwall;
L(1:end,[1 end],1:end)=l_hwall;
R(1:end,[1 end],1:end)=r_hwall;
F(1:end,[1 end],1:end)=f_hwall;
B(1:end,[1 end],1:end)=b_hwall;
W(1:end,[1 end],1:end)=w_hwall;
H(1:end,[1 end],1:end)=h_hwall;
K(1:end,[1 end],1:end)=k_alu;
LEN(1:end,[1 end],1:end)=(len_hwall);
Saturation(1:end,[1 end],1:end)=0;

%properties of the vertical wall nodes
w_vwall=wall_t;
h_vwall=paraffin_height./(discretization(2)-2);
len_vwall=(paraffin_t+hot_t+cold_t)./(discretization(3));
[m_vwall,C_vwall,u_vwall,d_vwall,l_vwall,r_vwall,f_vwall,b_vwall]...
    =Properties(w_vwall,h_vwall,len_vwall,rho_alu,cp_alu,k_alu);
M([1 end],2:end-1,1:end)=m_vwall;
C([1 end],2:end-1,1:end)=C_vwall;
U([1 end],2:end-1,1:end)=u_vwall;
D([1 end],2:end-1,1:end)=d_vwall;
L([1 end],2:end-1,1:end)=l_vwall;
R([1 end],2:end-1,1:end)=r_vwall;
F([1 end],2:end-1,1:end)=f_vwall;
B([1 end],2:end-1,1:end)=b_vwall;
W([1 end],2:end-1,1:end)=w_vwall;
H([1 end],2:end-1,1:end)=h_vwall;
K([1 end],2:end-1,1:end)=k_alu;
LEN([1 end],2:end-1,1:end)=(len_vwall);
Saturation([1 end],2:end-1,2:end)=0;
% properties of the fins
if fins==true;
    w_filler=w_para;

    h_filler=h_para;

    len_filler=paraffin_t/(discretization(3)-2);
    [m_filler,C_filler,u_filler,d_filler,l_filler,r_filler,f_filler,
        b_filler]...
        =Properties(w_filler,h_filler,len_filler,rho_alu,cp_alu,k_alu)
            ;
```

```
        M(5:4:end-4,5:4:end-4,2:end-1)=m_filler;
        C(5:4:end-4,5:4:end-4,2:end-1)=C_filler;
        U(5:4:end-4,5:4:end-4,2:end-1)=u_filler;
        D(5:4:end-4,5:4:end-4,2:end-1)=d_filler;
        L(5:4:end-4,5:4:end-4,2:end-1)=l_filler;
        R(5:4:end-4,5:4:end-4,2:end-1)=r_filler;
        F(5:4:end-4,5:4:end-4,2:end-1)=f_filler;
        B(5:4:end-4,5:4:end-4,2:end-1)=b_filler;
        W(5:4:end-4,5:4:end-4,2:end-1)=w_filler;
        H(5:4:end-4,5:4:end-4,2:end-1)=h_filler;
        K(5:4:end-4,5:4:end-4,2:end-1)=k_alu;
        LEN(5:4:end-4,5:4:end-4,2:end-1)=len_filler;
        Saturation(5:4:end-4,5:4:end-4,2:end-1)=0;
    end
    %% model setup
    if mod(discretization(1),2)<=0.01
        halfw=round(length(Allocation(1,:,1))/2)+2;
    else
        halfw=round((length(Allocation(1,:,1)))/2)+2;
    end

    if mod(discretization(2),2)<=0.01
        halfh=round(length(Allocation(:,1,1))/2);
    else
        halfh=round((length(Allocation(:,1,1)))/2);
    end

    % power leaving the cold plate
    Q_out=zeros(discretization(1),discretization(2),discretization(3));
    Q_out(:,:,end)=power_out/discretization(1)/discretization(2);
    %
    % q_input=dissipated_power/A_TXS;
    % allocation of the matrix for the power entering the PCB
    Q_in=zeros(discretization(1),discretization(2),discretization(3));
    %
    % l_A=paraffin_A/(discretization(1)-2);
    % input_number=(paraffin_A-mod(paraffin_A,(discretization(1)-2)^2))/(discretization(1)-2)^2;
    %

    %Setup of the starting temperatures
    T0=ones(discretization(1),discretization(2),discretization(3))*T_0;
    T(:,:,:)=T0;
    %Setup of the input power in the TXS amplifier
    prev_seconds=1;
    %% Model
    for i=1:time/timesteps
        for j=1:discretization(1)
            Width(j,:,1)=sum(W(1:j,:,1),1);
            Width(j,:,2:end)=sum(W(1:j,:,2:end),1);
        end
        for j=1:discretization(2)
            Height(:,j,1)=sum(H(:,1:j,1),2);
            Height(:,j,2:end)=sum(H(:,1:j,2:end),2);
        end
        %setup of the length coordinates
```

```matlab
        for j=1:discretization(3)
            Length(:,:,j)=sum(LEN(:,:,1:j),3);
        end

        %display the current minute
        seconds=round(i*timesteps/60);
        if seconds ~= prev_seconds
            clc
            disp([num2str(seconds),' minutes'])
            disp(['loop ',num2str(sen)])
        end
        prev_seconds=seconds;

        %switch off input power after set time
        if abs(i*timesteps-dissipation_time)<=timesteps;
            Q_in=zeros(discretization(1),discretization(2),discretization(3));
            percent=100*sum(sum(sum(S(:,:,:),3),2),1)/sum(sum(sum(Saturation(:,:,:),3),2),1);
        end
        %measure TXS temperature
        T_TXS(:,i)=T(round((wrange_start+wrange_end)/2),round((hrange_start+hrange_end)/2),1);
        % conductive couplings up down
        UD=(U(:,1:end-1,:).^-1+D(:,2:end,:).^-1).^-1;
        % conductive couplings left right
        LR=(L(2:end,:,:).^-1+R(1:end-1,:,:).^-1).^-1;
        % conductive couplings forward backwards
        FB=(F(:,:,1:end-1).^-1+B(:,:,2:end).^-1).^-1;

        %Temperature differences between nodes
        T_UD=T(:,1:end-1,:)-T(:,2:end,:);
        T_LR=T(1:end-1,:,:)-T(2:end,:,:);
        T_FB=T(:,:,1:end-1)-T(:,:,2:end);
        % energy transfers between nodes
        Q_UD=T_UD.*UD;
        Q_LR=T_LR.*LR;
        Q_FB=T_FB.*FB;
        % Acual change in energy per node
        %forward Euler moddel
        dQ_UD=cat(2,zeros(discretization(1),1,discretization(3)),Q_UD)...
            -cat(2,Q_UD,zeros(discretization(1),1,discretization(3)));
        dQ_LR=cat(1,zeros(1,discretization(2),discretization(3)),Q_LR)...
            -cat(1,Q_LR,zeros(1,discretization(2),discretization(3)));
        dQ_FB=cat(3,zeros(discretization(1),discretization(2),1),Q_FB)...
            -cat(3,Q_FB,zeros(discretization(1),discretization(2),1));
        dQ=(Q_in+dQ_UD+dQ_LR+dQ_FB-Q_out)*timesteps;

        % determine which nodes are within melting temperature and saturation range
        Within_Range=(S>=0).*(S<=Saturation).*(abs(T(:,:,:)-T_m)<=pct/2);
        % determine which nodes will absorb more energy than the total amount
        % of saturation
        Devision=Saturation./(C.*pct+Saturation);
        Over_Saturation=(S+dQ.*Devision>Saturation);
```

```
        % determine which nodes will loose more energy than is available
            in the
        % saturation
        Under_Saturation=(S+dQ.*Devision<0);
        % Define the change in saturation
        dS=Devision.*Within_Range.*((Allocation1−Over_Saturation).*(
            Allocation1−Under_Saturation).*dQ...
             +(Saturation−S).*Over_Saturation+Under_Saturation.*(−S));
        % Determine the new saturation level
        S=S+dS;
        % Determine the new temperature
        T=T+(dQ−dS)./C;
        % Define the new heat capacities of the PCM
        C=C+dS.*dcp;
        % previous length
        prev_LEN=LEN;
        % previous thermal conductivity
        prev_K=K;
        % define new thermal conductivity
        K=K+dS.*dk;
        % define new PCM lenght
        LEN(2:end−1,2:end−1,2:end−1)=LEN(2:end−1,2:end−1,2:end−1)+dS(2:end
            −1,2:end−1,2:end−1).*dlen;

        % change conductive couplings
        U=U.*LEN.*K./prev_LEN./prev_K;
        D=D.*LEN.*K./prev_LEN./prev_K;
        L=L.*LEN.*K./prev_LEN./prev_K;
        R=R.*LEN.*K./prev_LEN./prev_K;

        F=F.*prev_LEN.*K./LEN./prev_K;
        B=B.*prev_LEN.*K./LEN./prev_K;
    end

plot(1:length(T_TXS),T_TXS)
thickness(sen)=hot_t+cold_t+paraffin_t;
TXS_measurements(sen)=T_TXS(end);
mass(sen)= sum(sum(sum(M)));
end
```

```
function [ mass,C,up,down,left,right,front,back ] = Properties( w,h,l,rho,
    cp,k )
%This function determines the mass, sensible heat, and thermal
    conductivity
%of a node based on its shape and material input

mass=w*h*l*rho;
C=mass*cp;
up=w*l*k/(h/2);
down=up;
left=h*l*k/(w/2);
right=left;
front=h*w*k/(l/2);
back=front;

```

```
end
```

C.2. FDM model Sensitivity

The following figures show the sensitivity of the final TXS temperature to mass or thickness increase with a changing casing parameter, after 20 minutes with an input power of 8 Watts. The parameters are:

- Casing wall thickness (figures C.1 and C.2)
- PCM mass (figures C.3 and C.4)
- Casing base plate thickness (figures C.5 and C.6)
- Casing lid thickness (figures C.7 and C.8)

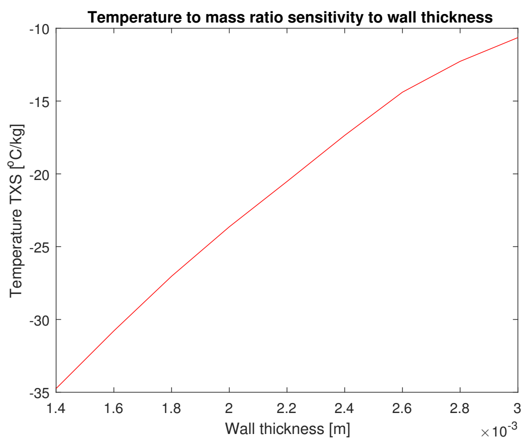

Figure C.1: Derivative of the maximum temperature of the thermal response to mass by changing the wall thickness

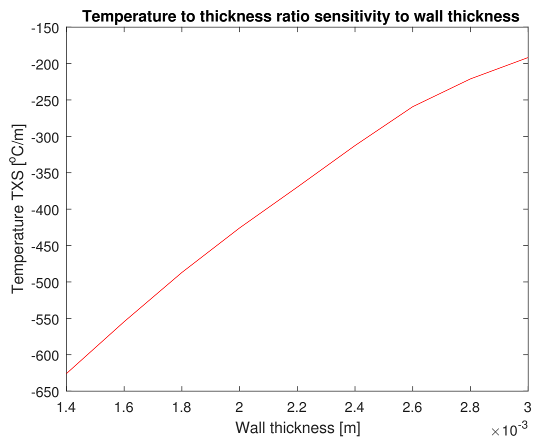

Figure C.2: Derivative of the maximum temperature of the thermal response to thickness casing by changing the wall thickness

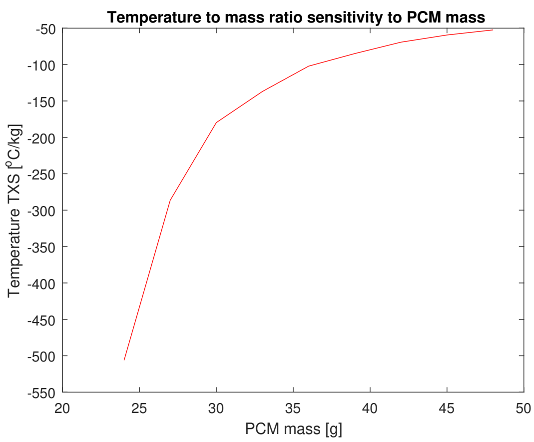

Figure C.3: Derivative of the maximum temperature of the thermal response to mass by changing the PCM mass

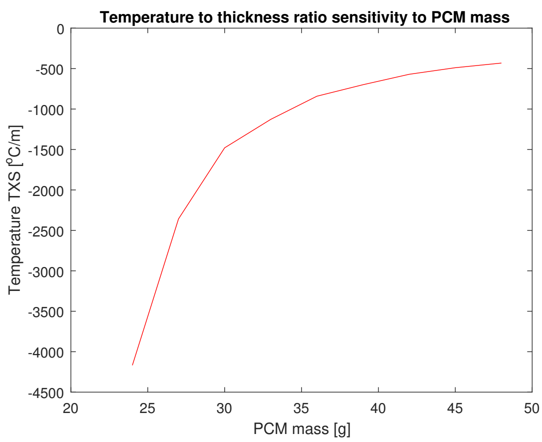

Figure C.4: Derivative of the maximum temperature of the thermal response to thickness by changing the PCM mass

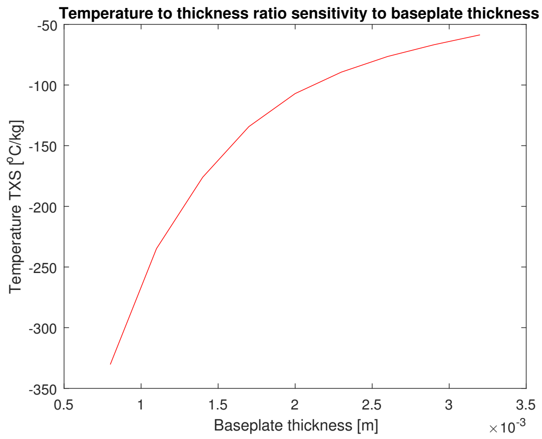

Figure C.5: Derivative of the maximum temperature of the thermal response to mass by changing the base plate thickness

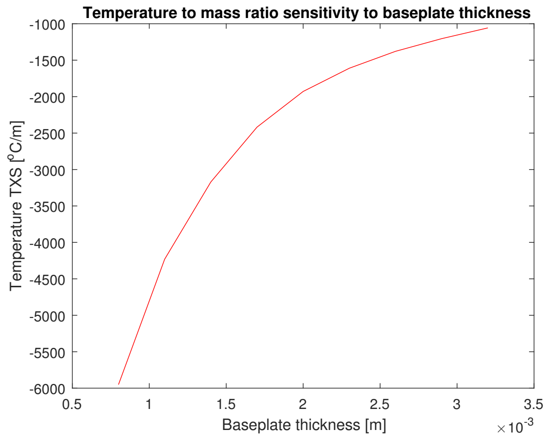

Figure C.6: Derivative of the maximum temperature of the thermal response to thickness by changing the base plate thickness

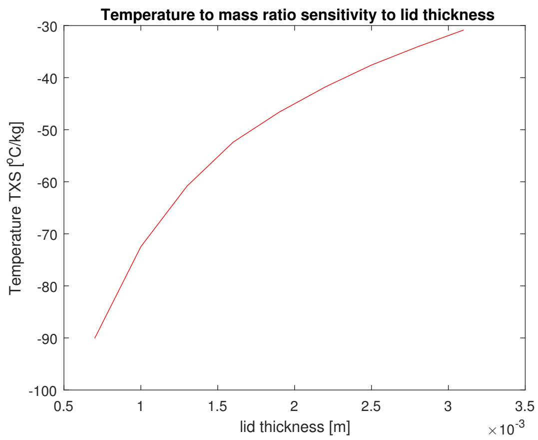

Figure C.7: Derivative of the maximum temperature of the thermal response to thickness by changing the casing lid thickness

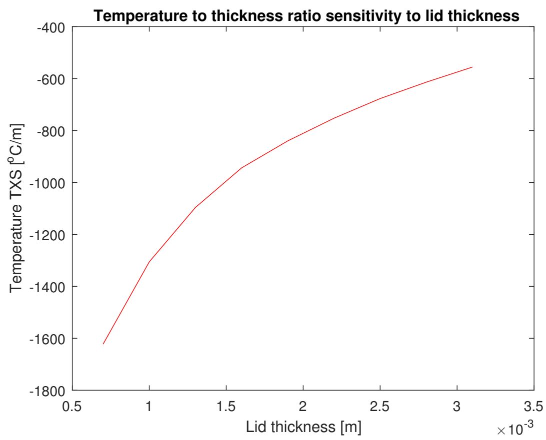

Figure C.8: Derivative of the maximum temperature of the thermal response to mass by changing the casing lid thickness

D
Test plan

This appendix shows the test plan that was followed.

Experiment		Input	Output	Success criteria
A1: Proper thermal response: Baseline test of empty casing		Thermocouples, 8W of input power, heating wire, empty casing, TXS device	Temperature measurements of TXS and casing	Thermal response within 5 degrees of simulated results
A2: Proper thermal Response: Test casing with PCM and filler material	A2_1: With fins A2_2: With honeycomb A2_3: With foam	Thermocouples, 6, 8, 10 and 12 W of input power, heating wire, filled casing with filler, TXS device	Temperature measurements of TXS and casing	Thermal response within 5 degrees of simulated results
A3: Proper thermal Response: Test the PCM device in different orientations.		Thermocouples, 8W of input power, Heating wire, filled casing with filler, TXS device	Temperature measurements of TXS and casing	Thermal response within 5 degrees of simulated results AND clear difference in measurements of different orientations
A4: Measure the thermal response: Measure the thermal response of a melted PCM in the device while cooling down		Thermocouples, heat sink (dummy batteries), filled casing with filler material	Temperature measurements of casing and the heat sink	Thermal response within 5 degrees of simulated results
B1: Effective cooling: What is the temperature response of the TXS without a heat sink?		Thermocouples, 8W of input power, Heating wire, TXS device	Temperature measurements of TXS	Set a baseline for the next measurements
B2: Effective cooling: How does the TXS respond with a heat sink of the same weight as the PCM device		Thermocouples, 8W of input power, Heating wire, TXS device, copper heat sink	Temperature measurements of TXS and copper heat sink	Set a benchmark beyond which the PCM has to perform better than
B3: Effective cooling: Can the TXS be kept below a certain temperature, and is this a better response then the heat sink at B2.	B3_1: With fins B3_2: With honeycomb B3_3: With foam	Thermocouples, 8W of input power, Heating wire, filled casing with filler, TXS device	Temperature measurements of TXS and casing	TXS is kept below a certain temperature. The heat sink has performed better than the heat sink in B2

B4: Effective cooling: How long will a saturated PCM keep battery temperatures above 0 degrees (eclipse period)		Thermocouples, Filled casing with filler, dummy batteries	Temperature measurements of TXS and casing	Keep the battery hot long enough to survive an eclipse period
C1: Durability: Measure the thermal response of the PCM device with multiple thermal cycles	C1_1: With fins C1_2: With honeycomb C1_3: With foam	Thermocouples, 8W of input power, Heating wire, filled casing with filler, TXS device	Temperature measurements of TXS and casing AND Observations of the physical effects on the casing and the filler material	Measure the effect of multiple heat cycles on the performance of the device. AND Determine the physical effects on the casing and the filler material
C2: Durability: Measure the effect of different manufacturing methods on the filler materials	C2_1: Mill out C2_2: Glue on	Thermocouples, 8W of input power, Heating wire, filled casing with filler	Temperature measurements casing AND Observations of the physical effects on the casing and the filler material	Determine the physical effects of melting and freezing cycles on the casing and the filler material
D1: Integrated: Measure the thermal response of the PCM device integrated into a CubeSat stack and with another heat sink like the frame or a battery pack		Thermocouples, 8W of input power, Heating wire, filled casing with filler, TXS device, CubeSat frame, heat sink	Temperature measurements of TXS, casing CubeSat frame and heat sink	Measure the thermal response of the TXS, casing frame and heat sink with an accuracy of 5 degrees
D2: Integrated: Measure the thermal response of the integrated system in multiple thermal cycles		Thermocouples, 8W of input power, Heating wire, filled casing with filler, TXS device, CubeSat frame, heat sink	Temperature measurements of TXS, casing CubeSat frame and heat sink	Measure the thermal response of the TXS, casing frame and heat sink with an accuracy of 5 degrees
D3: Integrated: Measure the thermal response of the integrated system with a similar heat profile as the one it would experience in LEO		Thermocouples, 8W of input power, Heating wire, filled casing with filler, TXS device, CubeSat frame, heat sink, thermal chamber	Temperature measurements of TXS, casing CubeSat frame and heat sink	Measure the thermal response of the TXS, and see if it is able to keep the subsystems within their operating temperatures

E

Model inputs

This section shows the model inputs that were used for the Comsol FEM models and how they were derived.

E.1. Ambient Cooling

In the first step, the steady state heat-losses are measured at increments of $10\ ^{\circ}C$. This is done before the casing is filled as the phase change would greatly increase the heat-up time and could interfere with the measurements. This allows the heat-losses of the casings to be estimated to ensure an accurate prediction of the thermal response of the model. In a vacuum the casing would not suffer any ambient convection and therefore could be predicted more accurately as only the radiation heat transfers would need to be calculated. The steady state heat-losses are plotted in figures E.1 and E.2. A curve fit was done through these heat-losses which led to the following equation:

$$P \approx 0.072 \cdot (T - 21) + 0.074 \tag{E.1}$$

In this equation P is power in W, T is temperature in C.

One issue with these measurements is that the casing has a thermal gradient throughout and the total average temperature is lower than the measured temperature. This does not change the effect of the heat-loss at the temperature at the specific location of the TC, therefore it is valid to say that a certain amount of heat was lost when the connecting piece was at specific temperatures. In the transient case the thermal gradient through the casing will be less linear and therefore have an even lower average temperature. To attempt to cancel these effects out the curve-fitted heat-loss is modelled over the entire surface of the casing; doing this will decrease heat loss of the casing model.

E.2. Contact resistance

The thermal resistance over the interface between the connector piece and the casing is also an unknown and is therefore something that must be measured. The thermal resistance was determined by measuring the difference in temperature between the connector and the casing. As the input power is and shape of the connector is known, the heat flux can be calculated using the equations in section 5.1.1.

Next the contact heat resistance can be measured by taking the difference in the measured temperature of the connector piece and the casing. These measurements are shown in figures E.4 and E.3. These measurements were mapped and the equation showing the contact resistance is shown in equation E.2. TCs are not able to be placed exactly at the contact interface, but are placed close by. The thermal gradient through the aluminium between the TC and the interface gives a small error. It is not obvious how the thermal gradient can easily be calculated using analytical equations. Therefore the FEM model is used to calculate this

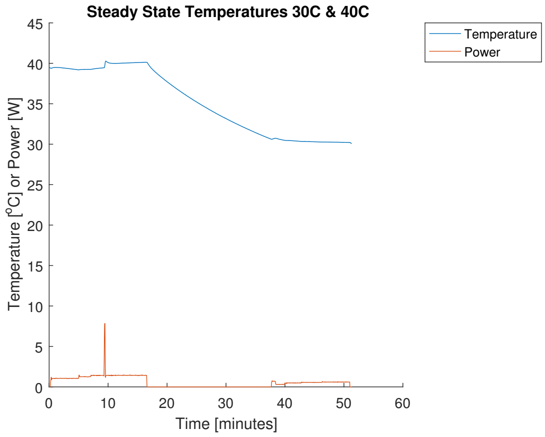

Figure E.1: Steady state heat loss at 30C and 40C

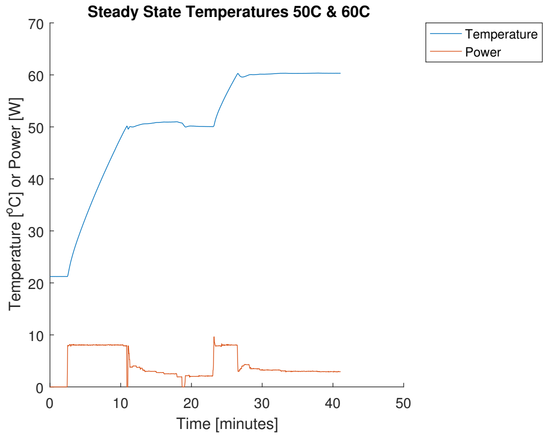

Figure E.2: Steady state heat loss at 50C and 60C

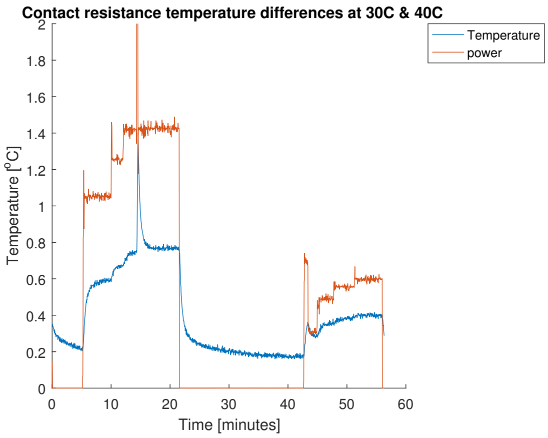

Figure E.3: Contact temperature difference at 30C and 40C

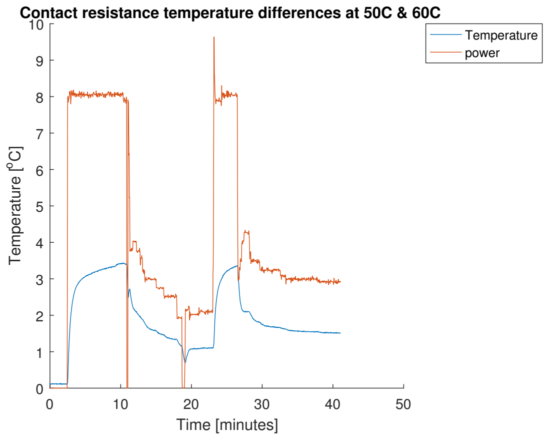

Figure E.4: Contact temperature difference at 50C and 60C

temperature difference numerically. The thermal gradient scales with the heat flux which scales with the input power. This calculation is repeated for all the steady state heat losses. These values where interpolated to calculate the relationship between input power and the ΔT, these relationships are shown in equation E.3.

$$\Delta T \approx 4.4 \cdot 10^{-4} \cdot q + 0.12 \tag{E.2}$$

$$\Delta T \approx 2.5 \cdot 10^{-4} \cdot q + 0.13 \tag{E.3}$$

In this equation q is heat flux in $\frac{W}{m^2}$, T is temperature in K.

There is no guarantee that these values can be extrapolated. Therefore an extra measurement was done with the thermal response of 8 Watts of input power. The same TCs where measured and their temperatures extracted. The thermal response difference of these TCs is plotted in figure E.5. The thermal gradient is around 4 $°C$, adjusted is 2.36 $°C$. These are close to the predicted values by equations E.2 and E.3 as 3.89 $°C$ and 2.28 $°C$. These same steps were repeated for the honeycomb casing.

E.3. Aluminium Foam

It is not obvious how the foam can properly be modelled without creating extremely fine discretization for the foam filler. The aggregate thermal properties were used to model the

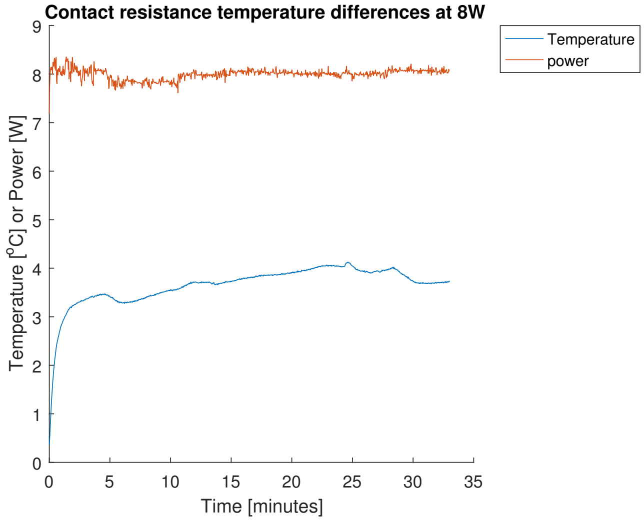

Figure E.5: Contact Resistance at 8W

Table E.1: Model inputs at different temperatures

Temperature $[^\circ C]$	power $[W]$	Contact ΔT $[K]$	Adjusted contact ΔT $[K]$
30	0.6	0.4	0.29
40	1.4	0.8	0.52
50	2.1	1.1	0.68
60	2.9	1.5	0.91

foam. The foam that was planned to be used had a volume fraction of about 25%. The effective heat capacity and density can be calculated. In an attempt to calculate the effective thermal conductivity can be done using equation E.4.

$$k_{eff} = \epsilon \cdot k_{aluminum} + (1-\epsilon) \cdot k_{PCM} \tag{E.4}$$

In this equation k is the thermal conductivity of a material in $\frac{W}{m \cdot K}$, ϵ is the porosity of the foam.

Calculating the effective thermal conductivity is not as simple as doing so for the mass or heat capacity. Using equation E.4 a value of 42.5 $\frac{W}{m \cdot K}$ is calculated. This value is optimistic as it doesn't take account of the distinct structural features of the foam-paraffin aggregate, or the fact that this property is not determined by mass-fractions. The exact properties of the foam could be calculated if the properties of the foam were known although they would still be difficult to model. But as it was not, a conservative estimate of $k_{eff} = 10\frac{W}{m \cdot K}$ was made.